

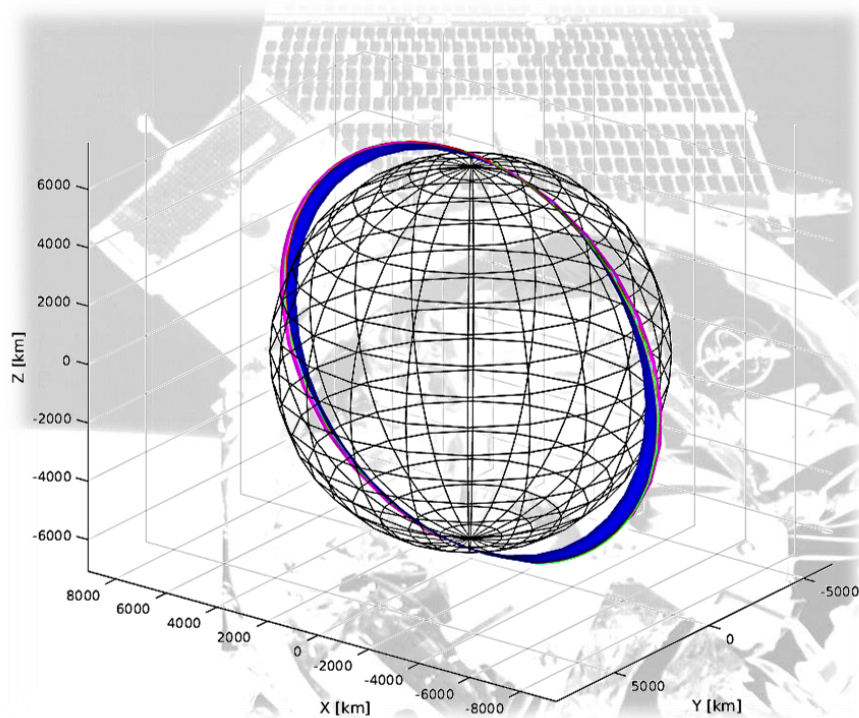
Master Thesis

Investigation of Earth-Bound Low-Thrust Trajectories for Mission Analysis of Multiple Target On-Orbit Servicing

RT-MA 2015/16

Author:

Yuval Porat



Betreuer:

Dr. -Ing. Jan Harder

Lehrstuhl für Raumfahrttechnik / Institute of Astronautics
Technische Universität München



To my parents and to my partner in life

*„We want to open up space for humanity, and in order to do that, space must be **affordable**.”*

– Elon Musk, The Independent

Figure on the title page: several color-coded transfer trajectories, representing multi-target on-orbit servicing, on the background of the Orbital Express spacecraft – the first successful autonomous on-orbit servicing demonstration mission.



Acknowledgments

First and foremost, I would like to express my outmost gratitude to Dr. Ralph Kahle for his guidance, support and invaluable advices throughout the work on the project and for taking the time to review this thesis. Special thanks are also directed to Dr. Andreas Ohndorf for kindly taking the time to teach me how to use InTrance, and for helping me with the definition and troubleshooting of the various scenarios investigated in this thesis. I also very much thank Sofya Spiridonova for kindly assisting me by running the reference scenario in GESOP which was a vital contribution to my work.

Last but not least, I would like to express my thanks and appreciation to my supervisor Dr. –Ing. Jan Harder, particularly for assisting me in all organizational matters and for always providing me with prompt and succinct answers to every inquiry, request or problem I had.

Zusammenfassung

In den letzten Jahren hat das Thema „On-Orbit-Servicing“ an wesentliche Aufmerksamkeit gewonnen. On-Orbit-Servicing bezieht sich auf alle Vorgänge, die auf einem Raumfahrzeug im Orbit durchgeführt werden, wie Reparatur, Betankung, Montage etc. Bisher haben sich die meisten Studien über dieses Thema auf das Vervollkommen autonomer Rendezvous- und Andockmanöver eines Servicers fokussiert, der einen einzelnen Satelliten bedienen soll.

Um jedoch die Effizienz einer künftigen On-Orbit-Servicing-Mission zu steigern und die Kosten zu reduzieren, sollte ein Servicer mehrere Clients bedienen können. Darüber hinaus sind hocheffiziente Niedrigschubantriebssysteme, die bisher nur für Deep-Space-Missionen oder Stationkeeping von geostationären Satelliten verwendet wurden, in der Lage große Δv -Anforderungen für viel weniger Treibstoffmasse im Vergleich zu herkömmlichen chemischen Antriebe bereitzustellen. Das Ziel dieser Forschung ist es, einen grundlegenden Rahmen für Multi-Ziel On-Orbit-Servicing Mission Analyse mit Niedrigschubantriebe zu schaffen.

Diese Arbeit untersucht drei Szenarien, die repräsentativ sind, für einleuchtende zukünftige On-Orbit-Servicing-Missionen. Das erste Szenario befasst sich mit der aktiven Entfernung von 5 hohes-Risiko Weltraumschrott-Objekte aus einem stark überlasteten erdnahen Orbit in einem Zeitraum von einem Jahr. Für dieses Szenario wurde ein neuartiges Programm für Bahnoptimierung namens InTrance verwendet. Dieses Programm nutzt künstliche neuronale Netze mitsamt einem evolutionären Algorithmus um Niedrigschubbahnen zu optimieren. Die Simulationen dieses Szenarios bestätigen die Machbarkeit dieses Szenarios. Jedoch erfordert die Verwendung von InTrance für Bahnoptimierung eine erhebliche Menge an Zeit, die seine Verwendung in einer Konzeptionsphase einer Mission unpraktisch machen würde. Das zweite Szenario befasst sich mit der Wartung von geostationären Satelliten und ist in zwei Subsznarien unterteilt. Im ersten SubszENARIO werden 10 Kundensatelliten von ihrer Umlaufbahn zu einer Entsorgungsumlaufbahn 350 km oberhalb der geostationären Umlaufbahn entsorgt. Im zweiten SubszENARIO tankt ein Servicer 24 operativen Satelliten in der geostationären Umlaufbahn im Ablauf von vier Touren. Jede Tour beginnt und endet in einer Depot-Station, die 150 km über der geostationären Umlaufbahn gebracht wird, und die das Reservoir von Kraftstoff sowohl für die Kunden als auch für den Servicer hält. Beide Subsznarien basieren auf ähnlichen Referenzmissionen, die von der NASA untersucht wurden. Die Ergebnisse der Simulationen sind mit den Referenzergebnissen verglichen und bestätigen die Vorteile der Niedrigschubantriebe gegenüber chemischem Antrieb sowohl in Bezug auf Treibstoffmasseverbrauch als auch auf der gesamten Missionszeit. Das dritte Szenario untersucht eine Mission, in der ein Servicer mit der Zustellung einer Nutzlast von einem erdnahen Orbit auf die geostationäre Umlaufbahn zugeordnet ist. Die Nutzlast in dieser Untersuchung wird als Ersatzteile angenommen, die in geostationären Satelliten ausgetauscht werden sollten.

Das Framework in dieser These schließt der Verfahren, Strategien und Werkzeuge ein, die für die Beurteilung der Machbarkeit eines On-Orbit-Servicing Szenarios in Bezug auf die erforderlichen Treibstoffmasse und Gesamtmissionszeit notwendig sind. Die Szenarien, die in dieser Studie untersucht worden sind, dienen als beispielhafte, jedoch archetypische Implementierungen des Rahmens auf plausible Szenarien.

Abstract

In recent years, the topic of on-orbit servicing has been gaining growing attention. On-orbit servicing relates to all operations carried out in orbit on a spacecraft such as repair, refueling, assembly, transport etc. Most studies done so far on this topic have focused mainly on perfecting autonomous rendezvous and docking maneuvers of a servicer attending a single cooperative or non-cooperative target.

However, in order to increase efficiency and reduce costs future on-orbit servicing missions will have to be able to attend multiple clients using a single servicer. Also, highly efficient low-thrust propulsion systems, which have been used until now only for deep-space missions or station-keeping of geostationary satellites, are capable of providing large Δv requirements for much lower propellant mass in comparison to conventional chemical propulsion. The goal of this research is to provide a foundational framework for multi-target on-orbit servicing mission analysis using low-thrust propulsion.

This thesis investigates three scenarios, which are representative of plausible future on-orbit servicing missions. The first scenario deals with the active removal of 5 high-risk debris objects from a highly congested low-Earth orbit within a timeframe of one year. For this scenario, a novel trajectory optimization program called InTrance is used. This program utilizes an artificial neural network together with an evolutionary algorithm to optimize low-thrust Earth-bound transfer trajectories. The simulations of this scenario confirm the feasibility of this scenario. However, the use of InTrance for trajectory optimization requires a substantial amount of time which might render its use in a conceptual phase of a mission impractical. The second scenario deals with servicing of geostationary satellites and is divided to two sub-scenarios. In the first sub-scenario 10 client satellites are removed from their orbit to a disposal orbit 350 km above the geostationary orbit. In the second sub-scenario a servicer refuels 24 operational satellites in the geostationary orbit in the course of 4 different tours. Each tour begins and ends in a depot station that is placed 150 km above the geostationary orbit and which holds the reservoir of fuel for both the clients and the servicer itself. Both sub-scenarios are based on similar reference missions investigated by NASA. The results of the simulations are compared to the reference results and provide confirmation of the advantages of low-thrust propulsion over chemical propulsion both in terms of propellant mass consumption and total mission time. The third scenario investigates a notional mission in which a servicer is assigned with delivering a payload from low-Earth orbit to the geostationary orbit. The payload in this investigation is assumed to be hardware components intended for replacement in satellites in the geostationary orbit.

The inaugural work done in this thesis offers a framework for the analysis of low-thrust multi-target on-orbit servicing missions including procedures, strategies and tools, which are essential for assessing the feasibility of a scenario in terms of required propellant mass and total mission time. The scenarios investigated in this study serve as exemplary, albeit archetypal, implementations of the framework on plausible scenarios.

Table of Contents

1	INTRODUCTION	13
1.1	Motivation and Background	13
1.2	State of the Art	14
1.2.1	Past Completed Missions	14
1.2.2	Past Planned Missions	15
1.2.3	Future Planned Missions	16
1.2.4	Current Studies on Multiple Targets OOS	17
1.3	Problem Definition	20
1.4	Materials and Methods	21
1.5	Thesis Outline	22
2	SCENARIOS CONFIGURATION	23
2.1	Scenario 1: LEO – LEO	23
2.1.1	Mission Architecture	24
2.1.2	Target and Launcher Selection	25
2.1.3	Target Sequence Selection	26
2.1.4	Servicer Design	31
2.2	Scenario 2: GTO – GEO – GEO/GYO	34
2.2.1	Sub-scenario 2.1: Satellite removal from GEO	34
2.2.2	Sub-scenario 2.2: Satellite refueling in GEO	38
2.3	Scenario 3: LEO – GEO	40
2.3.1	Mission Architecture	41
2.3.2	Servicer Design	41
3	APPLIED TOOLS	42
3.1	Trajectory Analysis Using InTrance	42
3.1.1	Trajectory Optimization	42
3.1.2	Spacecraft Steering Using Evolutionary Neurocontrollers	45
3.1.3	Extension to a Multiphase Non-Heliocentric Framework	47
3.2	Coplanar Low-Thrust Multi-Target Analysis Tool (Matlab)	49
3.2.1	General Description	49
3.2.2	Assumptions and Restrictions	49
3.2.3	Functional Description	49
3.2.4	Program Modules	51
3.2.5	Program Validation	57

4	RESULTS AND DISCUSSION	65
4.1	Scenario 1: LEO – LEO	65
4.1.1	Transfer 1: From Injection Orbit to Client #5	65
4.1.2	Transfer 2: From Client #5 to Client #1	68
4.1.3	Transfer 3: From Client #1 to Client #3	70
4.1.4	Transfer 4: From Client #3 to Client #4	72
4.1.5	Transfer 5: From Client #4 to Client #2	74
4.1.6	Discussion	76
4.2	Scenario 2: GTO – GEO – GEO/GYO	77
4.2.1	Transfer GTO to GEO	77
4.2.2	Validation with GESOP	79
4.2.3	Sub-scenario 2.1	80
4.2.4	Sub-scenario 2.2	82
4.3	Scenario 3: LEO – GEO	84
5	CONCLUSIONS AND FUTURE WORK	85
6	REFERENCES	88
	APPENDICES	92
A.	REFINED LIST OF CURRENT SATELLITES IN GEO	92
B.	MATLAB INPUT SPACECRAFT CONFIGURATION FILE	96
C.	MATLAB OUTPUT FILES	97
C1.	GTO-GEO Satellite Removal Module	97
C2.	GTO-GEO Satellite Refueling Module	100
C3.	LEO-GEO Satellite Repair Module	104
D.	INTRANCE INPUT FILES	106
D1.	Evolutionary Algorithm Parameter File – coldstart.eap	106
D2.	Neurocontoroller Parameter File – ctrl.ncp	106
E.	COMPUTER SPECIFICATIONS	107
E1.	InTrance Simulations	107
E2.	Matlab Simulations	107

List of Figures

Fig. 1-1: EPOS Test Facility in Oberpfaffenhofen, Germany	16
Fig. 1-2: Astroscale Mission Architecture. Figure adapted from [10].	17
Fig. 1-3: ADRaS-A mission architecture. Figure adapted from [15].....	18
Fig. 2-1: Predictions of growth of the LEO space debris environment. Figure adapted from [21].	23
Fig. 2-2: Top 500 R/Bs and S/C for removal, as of 2010. Figure adapted from [21].	26
Fig. 2-3: Optimal configuration of targets in LEO	27
Fig. 2-4: RAAN Drift-rate of selected targets	28
Fig. 2-5: RAAN angle propagation during 1 st transfer	30
Fig. 2-6: Targets' RAAN angle at beginning of 1 st transfer	30
Fig. 2-7: Targets' RAAN angle at end of 1 st transfer	30
Fig. 2-8: Required propellant mass and transfer time for a phase change of 180° with a 1.5 kW thruster. Figure modified from [33].....	34
Fig. 2-9: NASA GEO satellite removal architecture. Figure adapted from [1]	35
Fig. 3-1: Layered artificial neural network. Adapted from [37].....	44
Fig. 3-2: General Evolutionary Algorithm structure. Adapted from [20].....	45
Fig. 3-3: An EA individual consisting of ANN parameters. w_{ij} – neurons' weight factors, γ_i and θ_i – neurons' transfer function parameters. Adapted from [20].....	46
Fig. 3-4: InTrance Functionality Layout. Adapted from [37]	46
Fig. 3-5: Finding optimal trajectory from an EA individual using a neurocontroller. Adapted from [37].....	46
Fig. 3-6: InTrance Multiphase Framework. Adapted from [20].....	48
Fig. 3-7: Target rendezvous selection	50
Fig. 3-8: GEO satellite removal program structure	54
Fig. 3-9: GEO satellite refueling program structure	57
Fig. 3-10: GMAT mission configuration.....	60
Fig. 3-11: GMAT results: Servicer longitude in deg vs. MET in sec.....	61
Fig. 3-12: GMAT results: Servicer altitude in km vs. MET in sec	61
Fig. 3-13: GMAT results: Propellant mass consumption in kg vs MET in sec. Left – Propellant mass. Right – Servicer dry mass in red and total mass in green.....	64
Fig. 4-1: Transfer 1 isometric projection	67
Fig. 4-2: Transfer 1 polar view	67
Fig. 4-3: Transfer 1 equatorial view	67
Fig. 4-4: Transfers 1 (blue) and 2 (red) isometric projection	69
Fig. 4-5: Transfer 2 front view	69
Fig. 4-6: Transfer 2 side view	69



Fig. 4-7: Transfers 2 (red) and 3 (green) isometric projection.....	71
Fig. 4-8: Transfer 3 front view.....	71
Fig. 4-9: Transfer 3 side view	71
Fig. 4-10: Transfers 3 (green) and 4 (cyan) isometric projection	73
Fig. 4-11: Transfer 4 front view.....	73
Fig. 4-12: Transfer 4 side view	73
Fig. 4-13: Transfers 4 (cyan) and 5 (magenta) isometric projection	75
Fig. 4-14: Transfer 5 front view.....	75
Fig. 4-15: Transfer 5 side view	75
Fig. 4-16: GTO to GEO transfer isometric view	78
Fig. 4-17: GTO to GEO polar view.....	78
Fig. 4-18: GTO to GEO equatorial view	78
Fig. 4-19: Total mission time and total propellant mass as function of servicing time	81
Fig. 4-20: Objective function Vs. servicing time	82
Fig. 4-21: Histogram of servicer's total required propellant mass from 150 simulation runs	83
Fig. 4-22: Histogram of total servicing time from 150 simulation runs	83



List of Tables

Tab. 2-1: Classical orbital elements of selected LEO deorbit targets, on 01.11.2015	26
Tab. 2-2: Servicer's injection orbit parameters	26
Tab. 2-3: Nodal regression rate of targets and injection orbit	29
Tab. 2-4: Spacecraft design parameters of reference missions.....	31
Tab. 2-5: Comparison of flight-proven SEP thrusters	32
Tab. 2-6 : Assembly Node Trade-Off.....	37
Tab. 2-7: LEO-GEO Transfer. Data taken from [20]	41
Tab. 3-1: LTOMs - GTOMs comparison based on [20] and [38].....	43
Tab. 3-2: Longitude accuracy validation	63
Tab. 4-1: Transfer 1 initial and final states.....	66
Tab. 4-2: Transfer 2 initial and final states.....	68
Tab. 4-3: Transfer 3 initial and final states.....	70
Tab. 4-4: Transfer 4 initial and final states.....	72
Tab. 4-5: Transfer 5 initial and final states.....	74
Tab. 4-6: Scenario 1 simulation results	76
Tab. 4-7: GTO to GEO initial and final states	79
Tab. 4-8: Sub-scenario 2.1 Matlab results	80
Tab. 4-9: Scenario 3 Matlab results.....	84



Symbols and Constants

Space-related Constants:

g_0	9.81	$\frac{m}{s^2}$	Earth's gravitational acceleration	μ	3.986×10^{14}	$\frac{km^3}{s^2}$	Earth's gravitational constant
R_E	6378.43495	km	Earth's radius	J_2	0.0010826		Orbital perturbation due to Earth's oblateness

Symbols:

a	km	Semi-major axis
i	rad	Orbit inclination
e		Eccentricity
Ω	rad	Right Ascension of the ascending node
ω	rad	Argument of periapsis
ν	rad	True anomaly
n	$\frac{rad}{sec}$	Mean motion
P	W	Power
F	N	Force/Thrust
\dot{m}	$\frac{kg}{sec}$	Fuel mass flow

Abbreviations

ADR	Active Debris Removal	i.g.	Initial guess
AN	Assembly Node	IOD	In-Orbit Demonstration
ANN	Artificial Neural Network	ISS	International Space Station
DARPA	Defense Advanced Research Project Agency	LEO	Low Earth Orbit
DLR	German Space Agency	LTOM	Local Trajectory Optimization Method
DOF	Degrees Of Freedom	MEO	Middle Earth Orbit
EA	Evolutionary Algorithm	MEV	Mission Extension Vehicle
EMR	Energy to Mass Ratio	MJD	Modified Julian Date
ENC	Evolutionary Neurocontroller	NC	Neurocontroller
EOL	End Of Life	NLP	Non-Linear Programming
EP(S)	Electric Propulsion (System)	OOS	On-Orbit Servicing
EPOS	European Proximity Operations Simulator	PGS	Power Generation System
ESA	European Space Agency	PMD	Post Mission Disposal
EVA	Extra Vehicular Activity	R/B	Rocket Body
GEO	Geo-Stationary Orbit	RAAN	Right Ascension of the Ascending Node
GMAT	General Mission Analysis Tool	RnD	Rendezvous and Docking
GTO	GEO Transfer Orbit	S/C	Spacecraft
GTOM	Global Trajectory Optimization Method	SEP	Solar Electric Propulsion
GYO	Graveyard Orbit	SIS	Space Infrastructure Servicing
HEO	High Elliptical Orbit	SMA	Semi-Major Axis
HST	Hubble Space Telescope	SSO	Sun Synchronous Orbit

1 Introduction

1.1 Motivation and Background

A key design driver in current satellite design methodologies is the “Launch and Forget” approach. This approach generally considers the design and manufacture of a satellite as a one-track process, in which the spacecraft, once in space, cannot be attended or sent back to the factory for repair (unlike the production of automobiles or aircrafts, for example). One of the problems associated with this approach is that once a space vehicle is launched into space and a hardware problem occurs, it is a very complicated and expensive procedure to send a replace/repair mission to fix the malfunctioning satellite in orbit. Therefore, a large portion of the design financial and time budgets must be allocated for extensive tests and validation processes prior to launch in order to increase the satellite’s reliability to an acceptable value. Keeping satellite hardware up-to-date is yet another challenging feat often encountered by satellite manufacturers. The time that elapses from the beginning of the design process until the satellite is launched can last from several years in simple projects to several decades in the more complicated deep-space missions. During that time, some of the hardware that was incorporated in the initial design might already be obsolete, or become obsolete during the operational period of the satellite due to rapid improvements in technology.

An obvious and practical solution that can address both issues is the introduction and acceptance of a paradigm shift in space design philosophies that allows for regular maintenance of satellites in orbit by a servicer satellite. The robotic servicer will be able to carry out missions, which in the prospect of this thesis will be collectively referred to as On-Orbit Servicing (OOS) missions. These missions will include such tasks as satellite repair, satellite refueling, replacement of hardware components as required and collection and removal (e.g. deorbit or reorbit) of space debris and decommissioned satellites from congested orbits.

To allow for cost-effective missions the servicer should be able to attend multiple targets in each tour, either for performing similar tasks (i.e. only refueling, only deorbiting etc.) or for combined mission types. Apart from reducing mission costs, launching one servicer capable of attending multiple targets also reduces the amount of new debris that is generated as a result of launching the servicer spacecraft (S/C).

Further, this thesis does not restrict itself to only co-planar OOS missions. Therefore, the servicer might also need to perform several fuel-expensive orbital maneuvers (e.g. inclination changes), which render conventional chemical propulsion impractical on grounds of too large fuel mass requirements. Instead, this thesis explores the use of continuous low-thrust propulsion by means of Solar Electrical Propulsion (SEP). This type of propulsion can achieve very high exhaust velocities, which can in turn significantly reduce the required propellant mass. Indeed, such continuous low-thrust propulsion systems require longer operation times to achieve the required Δv , which in turn poses a challenge in terms of trajectory optimization. This issue is also addressed in this thesis.

1.2 State of the Art

The concept of OOS is not new. In fact, several OOS missions have already been conducted in the past. Generally speaking, there are two types of OOS missions; One type is manned OOS, where there is direct human authority and interaction with the serviced client. Such OOS missions are often carried out in the International Space Station (ISS), for example. The second type is fully autonomous OOS missions, where the servicing platform has the capacity to autonomously approach, rendezvous, dock and service the client. Between those two extremes there exists, of course, a range of other mission architectures with varying human interactivity in the servicing process.

In the following, several examples of famous past missions and interesting future concepts for on-orbit servicing mission are listed.

1.2.1 Past Completed Missions

Manned OOS:

The first On-Orbit Servicing mission was the construction of the 1st American space outpost – Skylab, in 1973 [1]. About 10 days after the launch of Skylab, problems occurred with the thermal shielding of the space station which required human intervention through an Extra Vehicular Activity (EVA) to replace the thermal shielding. This marked the first manned on-orbit repair mission.

Like the Skylab space station, also the Russian space station Salyut-7, which was launched in 1982, experienced several problems that required human intervention. One of them was a fuel leak from one of the fuel tanks that was discovered in 1983, and necessitated a 4-hour EVA to fix it.

Later, in 1984, another remarkable OOS mission was carried out for the retrieval, repair and redeployment of the Solar Maximum Mission (SMM) satellite, which experienced failures in its attitude control system. What was remarkable about this mission, was that the SMM was one of the few missions, where a spacecraft was designed and built using a modular design that facilitated OOS. This design approach is still controversial today, but the SMM mission proved the advantages of modular satellite designs. Astronauts from the Challenger Space Shuttle went on an EVA, successfully captured the defunct satellite, repaired and redeployed it.

The second, and probably most famous, manned OOS using the Space Shuttle was that of the Hubble Space Telescope (HST). In fact, repairing the Hubble telescope required no less than 5 manned servicing missions [1]. The HST, like the SMM satellite, was designed to allow for regular servicing and refurbishment. The HST servicing missions proved useful and advantageous not only by repairing a US\$10 billion spacecraft, which would otherwise have been deemed non-operational, it also allowed for upgrades to be integrated in the S/C after launch, making it current and up-to-date even 20 years after its launch.

Currently, regular manned on-orbit servicing is being done on the International Space Station. As of February 2016, 193 EVAs have been carried out on the ISS [2] for assembly and regular maintenance of the space station. Of course, some of the maintenance of the ISS can be done from inside the station and does not require an EVA, but it can still be considered as On-Orbit Servicing. These servicing missions guarantee the seamless operation of the continuously populated space station from

the arrival of the first resident crew in November 2000 until today, with end of mission expected to occur in the 2020's.

Robotic OOS:

Orbital Express [3]: Orbital Express was a joint American mission between U.S. Defense Advanced Research Projects Agency (DARPA) and NASA. The mission consisted of two spacecraft that were intended to demonstrate on-orbit servicing mission scenarios. The mission was launched on March 8, 2007 and concluded in July 22nd, 2007 with the deactivation of both satellites in orbits that will decay within 25 years. The mission achieved for the first time in history important milestones in OOS including: autonomous rendezvous and docking between servicer and client using a robotic arm, fuel transfer between servicer and client, hardware installation by the servicer on the client, health monitoring and functionality verification of hardware by the servicer.

1.2.2 Past Planned Missions

MDA – Space Infrastructure Servicing (SIS) is a Canadian aerospace company who planned during the early 2010's a geosynchronous refueling project titled Space Infrastructure Servicing. The idea for the SIS spacecraft was that it would attach to the apogee motor of an operational telecommunication satellite in Geostationary Orbit (GEO), and transfer fuel to it through a fuel pressure line. In 2012, MDA decided to put the project on hold, since it reportedly could not find enough clients to sign up a service agreement with the company [4].

ConeXpress/SMART-OLEV project started out as a cooperation between Dutsch Space, Orbital Recovery Corp. and DLR [5] to provide life extension services to GEO satellites. The novelty about this project was that the servicing S/C would use electric propulsion based on the design of the successful European Space Agency (ESA) mission SMART-1. In addition, to save costs the ConeXpress S/C would use the otherwise empty unused space in the Ariane 5 payload adapter. This conic shaped adapter is what gave ConeXpress its name. This S/C was initially designed to be small and light-weight (~1200 kg) and to be built mainly for Off-The-Shelf products to reduce its construction price. It was designed to extend the lives of GEO satellites up to 12 years beyond their original operational lifetime. Similar to other OOS initiative ConeXpress would also dock to the client satellite by inserting and locking a probe into the client's apogee motor's nozzle. This should have also allowed ConeXpress to dock with uncooperative targets. Later on, the UK based aerospace company Orbital Satellites Services Ltd., with the help of a European industrial consortium of aerospace companies and national space agencies, took on the ConeXpress design and developed the SMART-OLEV mission which now not only used the propulsion system heritage from SMART-1, but also based its structure completely on that of the SMART-1 spacecraft. Currently the SMART-OLEV project is on hold.

DEOS, which stands for DEutsche Orbitale Servicing mission, is a German project led by the German Space Agency (DLR). This project includes an IOD for a rendezvous, docking and servicing of both a controlled and an uncooperative tumbling target [5]. The mission would include two S/C; a servicer and client, which would be able to emulate both types of target behavior (i.e. controlled and uncontrolled). The servicer will implement a robotic arm to rigidly grasp and dock with the target spacecraft.

Simulations of the rigid grasping of a tumbling target have been carried out in the European Proximity Operations Simulator (EPOS) test facility, in Oberpfaffenhofen, using two 6 Degrees-Of-Freedom (DOF) robots, that can translate w.r.t each other on a 25 m rail (see Fig. 1-1). The DEOS project included two phases: Phase A was dedicated to the conceptual design of the servicing platform, whereas Phase B concentrated on the design of the client satellite [6]. After the successful completion of the Phase B study, the DEOS project is currently on hold.



Fig. 1-1: EPOS Test Facility in Oberpfaffenhofen, Germany

1.2.3 Future Planned Missions

ViviSat [7] is a joint venture between Orbital ATK and U.S. Space LLC. to provide In-Orbit satellite life extensions services. As of today, *ViviSat* plans to launch their first Mission Extension Vehicle (MEV) in 2018. They claim to have already signed with 4 clients that would use their services. The MEV is reported to have a lifespan of 15 to 20 years. It would dock to a GEO client satellite's apogee motor to run its services. These services could include station-keeping, inclination reduction, satellite relocation, repair and potentially even in-orbit assembly. It is estimated that each MEV could perform 3 – 4 missions during its operational lifetime [8].

E.Deorbit [9] is an on-going ESA Active Debris Removal (ADR) project which is planned to launch in 2021 on board a Vega launcher. The mission is targeted at removing a large ESA-owned uncooperative space debris object from the 800-1000 km SSO region. ESA has awarded in September 2015 two parallel contracts to Airbus Defense and Space and the company OHB to come up with a detailed design of a capture mechanism required for ADR. In addition and as part of the *E.Deorbit* project, in December 2014, ESA signed a Memorandum of Understanding with DLR for a joint IOD mission of ADR, taking advantage of DLR's already acquired knowledge on robotic autonomous rendezvous maneuvers through their DEOS program. The new ESA-DLR joint mission, named CAPTARE, will be jointly and equally financed by ESA and DLR, it will implement a robotic arm (as done in the DEOS program) and it is scheduled to be launched in 2020, to comply with the general *E.Deorbit* timeline.

Astroscale is a Singapore-based private satellite services company that develops missions that will: 1. provide End-Of-Life/Deorbit services for large space debris objects and 2. Provide orbital debris monitoring and characterization of small size debris objects in congested Low Earth Orbits (LEO) regions [10]. The ADR mission will consist of a micro-satellite based on the heritage of the Hodoyoshi spacecraft bus, where a mothership S/C, using electrical propulsion system, will carry a deorbit S/C, using a clustered solid rocket booster. The mothership will approach a tumbling satellite, de-tumble it, then release the deorbiting S/C which will attach itself to the de-tumbled target using adhesives and deorbit it using its own clustered solid rocket booster (see Fig. 1-2) [11]. The mission is currently in its development phase and a 2018 IOD mission is in the planning.

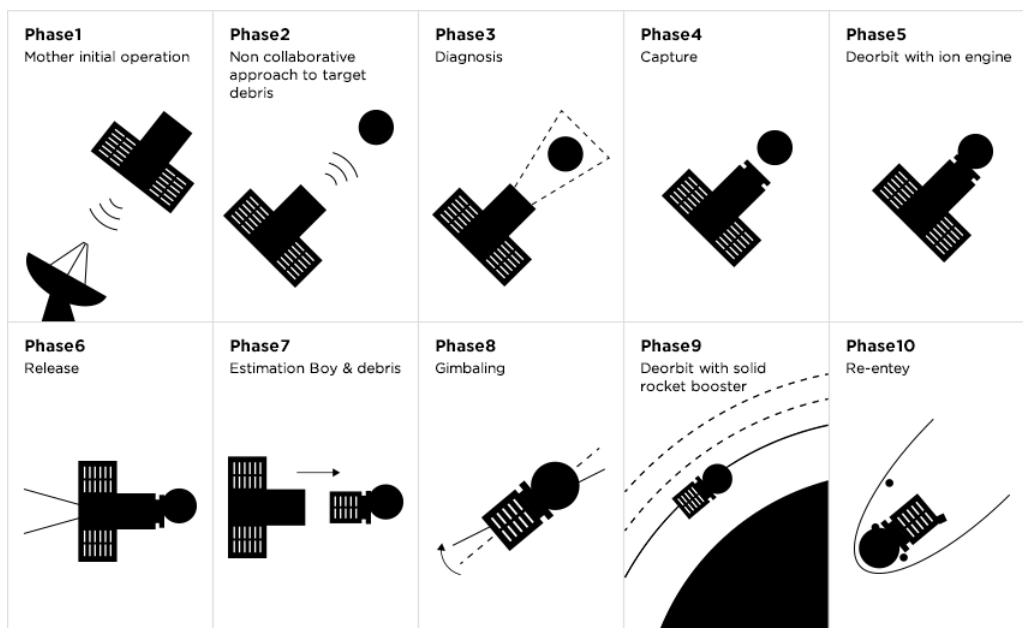


Fig. 1-2: Astroscale Mission Architecture. Figure adapted from [10].

Effective Space Solutions is another private space services company, based in Israel. Not a lot of information can be freely found about the company, however, similar to other OOS companies, they too intend to use low-thrust electric engines for their servicing S/C. Their business model is to provide station-keeping as well as removal services for GEO satellites [12]. The capturing mechanism suggested for the Effective Space Solutions Servicer will use 4 rigid robotic arms that would grasp and hold the adapter ring of the target satellite. Then, after rigid connection has been established, the servicer will use its own electric propulsion to provide station-keeping and removal from orbit services.

1.2.4 Current Studies on Multiple Targets OOS

It is worth noting that all of the aforementioned OOS mission examples deal primarily with the operation or In-Orbit Demonstration (IOD) of a servicer attending a single client. To date, not a lot of study has been done regarding multiple-target OOS.

In 2013, S. Peters et al. [13] published their study on autonomous ADR methods for multiple targets removal and identification of those targets. They identified orbits with high concentration of high-risk targets, and looked for clusters of high-risk targets in

those orbits that would facilitate removing as many targets as possible at the shortest time and for the least amount of fuel. Later, in 2014 [14] and 2015 [15, 16] they extended their study to include a notional mission architecture for the removal of 5 SL-8 rocket bodies. This notional mission described the design of a servicer satellite with a launch mass of 1025 kg, as well as of a deorbit kit with a mass of 414 kg that would be attached by the servicer to a target by means of a robotic arm. The servicer and all of the deorbit kits would be launched together in a single launch (Fig. 1-3a). However, the deorbit kits will not be integrated in the servicer's S/C design. Instead, all of the deorbit kits will be launched to a parking orbit beneath the targets orbits. Consequently, the servicer would rendezvous and dock with one deorbit kit at a time (Fig. 1-3b), and then transport it and attach it to a target (Fig. 1-3c). The attached kit would then autonomously deorbit the target (Fig. 1-3d) while the servicer transfers back to the parking orbit to retrieve the next deorbit kit in preparation for the next target deorbit maneuver (Fig. 1-3e). This architecture is schematically displayed in Fig. 1-3. According to the preliminary spacecraft design, both the servicer and the deorbit kit would use chemical propulsion resulting in a total Δv of 400 m/s for the entire mission, equivalent to about 190 kg of hydrazine as propellant, an almost fifth of the total servicer launch mass. However, it is important to note that, in their simulation, Peters et al. assumed all targets to share the same inclination. This resulted in a lower Δv budget than that of the more realistic case of different target's inclinations, since out-of-plane orbital changes require much more Δv than in-plane orbital changes.

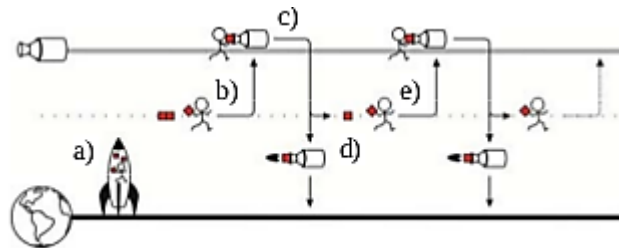


Fig. 1-3: ADRoS-A mission architecture. Figure adapted from [15]

Another conceptual mission was proposed by Bombardelli et al. [17], where the Ion Beam Shepherd method was utilized for the removal of multiple spent rocket upper stages. In this method, ejecta of ionized particles imparts a momentum change on a target in space by pointing the jet of ions towards the body, thereby generating an action force on the it without any mechanical contact between the servicer and the target. Bombardelli et al. ran a preliminary analysis to estimate the total mission time and S/C mass required for the removal of multiple targets. Similar to the work of Peters et al. they also ran an identification analysis of potential high-risk targets for removal. Their analysis, however, resulted with the upper stages of the Zenit-2 family as ideal candidates for removal. In addition, instead of completely deorbiting the Zenit upper stages, they proposed repositioning the debris objects to uncrowded orbital regions, which will both significantly reduce the risk of collisions as well as reduce the required servicer propellant mass. The preliminary analysis of Bombardelli et al. included, for simplification purposes, the removal, or repositioning, of only 2 Zenit upper stages from an orbit of approximately 825 km to a "LEO graveyard orbit" at an altitude of 725 km. This mission architecture resulted in a servicer mass of 400 kg, of which only about 40 kg was allocated for propellant, using a pair of 75 mN RIT-22 ion thrusters with 3400 sec specific impulse and 4 kW total power consumption. The analysis showed

that using the ion beam shepherd method and the above-mentioned S/C design, the 2 debris targets could be repositioned within a one-year timeframe.

A different approach for multiple target rendezvous maneuvers was offered in 2008 by Bevilacqua and Romano [18]. In their work, they used differential drag between several spacecraft to control the respective orbits. By using on-off air drag devices on each spacecraft a relative differential acceleration could be generated and the respective orbits controlled. The obvious advantage of this method is its capability to provide long term propellant-free multiple target rendezvous maneuvers. However, since this method relies on residual atmosphere, it can obviously only be applicable to LEOs. In addition, Bevilacqua and Romano devised their algorithm for an exemplary on-orbit assembly mission, where 4 chaser satellites were to rendezvous with one target. Rendezvous between 2 satellites (i.e. servicer and target) is of course also possible using this method. However, to make it a viable and efficient alternative to other forms of propulsion both S/C should have the air drag device to be able to better control the relative acceleration between the two S/C. While this is of course possible for on-orbit assembly missions, where the S/C are designed accordingly in advance, it is less attractive for OOS missions such as active removal of uncontrolled targets, where the targets do not have the possibilities to actively change their drag acceleration.

In 2010, the American National Aeronautics and Space Administration (NASA) compiled an internal report [1] that assessed the feasibility of various in-orbit servicing mission architectures. Among other things, the report presented results of assessment studies of feasibility and practicality of OOS, identification and assessment of existent technologies that are required for OOS as well as key technologies that should be developed for future servicing missions and an outline for decision making on matters regarding ground and flight servicing techniques. The report culminated in the development of six notional mission architectures pertaining to the six most profitable or attractive OOS architectures: Removal of GEO satellites to graveyard orbit, Refueling of GEO satellites, Upgrade and refurbishment of a serviceable LEO satellite, Space Assembly missions – for example the assembly of a 30 m space telescope in the Earth-Moon Lagrange Point 1, a Human-Robotic servicing mission in an HEO and a Human-Robotic assembly mission at the Sun-Earth Lagrange Point 2. Each of these notional mission included a detailed mechanical design of the spacecraft involved as well as cost and mission timeline estimations.

In another study for the removal of multiple targets from a Sun Synchronous Orbit (SSO), B. Chamot investigated 3 different OOS architectures and compared them in terms of mission cost per mass removed [19]. The three architectures were, a so-called “Picker” which involved launching several servicers, each one responsible for deorbiting a single target, the second architecture included a “Mothership” that visited several targets and attached an autonomous deorbit kit to each one, and the third scenario was that of a “Shuttle Servicer” that would dock and deorbit each target by itself. The results of this analysis showed that the Picker architecture was the most cost efficient alternative. While this study provides useful tools for future analysis of ADR missions, these results are mission-architecture dependent, and it is hard to draw a general conclusion on which architecture is the best. For example, the “Mothership” scenario assumes a specific design of the mothership and deorbit spacecraft. In addition, it is assumed that each Mothership can hold up to 3 deorbit kits, and that additional launches of Mothership S/C (equipped with additional deorbit kits) are required for the continuation of the mission. Alternatively, other configurations might

be considered, where the Mothership can hold more than 3 deorbit kits, and where additional deorbit kits can be later supplied in separate launches without having to launch new Mothership S/C as well. The Mothership would subsequently rendezvous with the resupplied deorbit kits and continue its mission. Such a configuration could reduce the number of required launches and greatly reduce the overall cost of the mission.

A detailed investigation from an economical point of view of various satellite servicing markets was conducted in 2005 by B. Sullivan. This study thoroughly examined market trends in the space industry, opportunities for lifetime extension missions as well as economic feasibility of retirement services for geosynchronous satellites and relatively accurate cost and profit estimations of different servicing architectures. The main result of this study showed that there are tens of servicing opportunities per year (considering all types of servicing missions, e.g. refueling, removal, repair, health-monitoring etc.) each of which totaling in over \$100M annual market value. Further, this study also proposed a servicer design, which would attend multiple targets, based on the cost evaluation method used in the work. This servicer design was found to break-even in terms of costs after providing retirement services to 8 targets.

1.3 Problem Definition

As described in Section 1.2, most studies and missions done so far on OOS were mainly focused on maturing the technology needed for servicing a single target. On a technological level, this is an obvious and necessary first step for future OOS missions. However, since the underlying objective of OOS is to reduce space-flight costs and associated space debris growth, it is important to consider from a mission design and mission planning point of view, what requirements and constraints should be considered when dealing with multiple target OOS missions. In addition, as explained in Section 1.1, in order to minimize propellant mass consumption required for the transfers, continuous low-thrust SEP will be used for the trajectory simulations.

Therefore, the aim of this thesis is to answer the following question:

Which multiple-target On-Orbit Servicing transfer scenarios are feasible by means of low-thrust propulsion?

It is stressed at this point, that the work done in this thesis is proposed as a conceptual study that should help in decision-making at the very early stages of an OOS mission analysis and design. The deliverables of this thesis will be orders of magnitude of total mission time and required total fuel mass, depending on mission architecture. More accurate and rigorous figures of those deliverables are out of the scope of this thesis, as these are usually needed at later stages of the mission design process.

1.4 Materials and Methods

The variety of scenarios that could be considered for simulations of OOS operations can be generally divided according to Type of Orbit (LEO, GEO, etc.) and Type of Mission (Active Debris Removal, Refueling, Repair, etc.).

The type of orbit affects what perturbations are to be included in the simulation. For example, while in LEO atmospheric drag is quite a substantial perturbation, it becomes negligible relative to solar radiation pressure and third-body perturbations in GEO missions. In addition, the types of maneuvers are also affected by the Orbit type; LEO missions may, in general, include fuel-exhaustive maneuvers such as changes of the inclination or Right Ascension of the Ascending Node (RAAN) angle, whereas in GEO the maneuvers will be mostly phasing maneuvers or changes to the semi-major axis (e.g. re-orbiting) within the orbital plane.

The type of mission also influences the configuration of the simulation; different types of mission may include different payloads with different masses. For Active Debris Removal mission, for example, the payload may include a de-orbiting kit and a robotic arm or some other mechanisms for capturing and docking. Refueling missions may include as payload the refueling mechanism and the liquid fuel itself that should be transferred to the client satellite. Furthermore, the mission type also defines the method of encounter between the chaser and the target which is important for the configuration of the simulation. An OOS mission can include a rendezvous where the servicer itself docks to the target and attaches a deorbiting device to it, or alternatively the servicer could perform a fly-by maneuver, during which it releases a self-navigating deorbiting device in the vicinity of the target that attaches autonomously to the target.

This thesis will focus on the following OOS scenarios of interest:

1. LEO-LEO missions: This scenario includes servicing tours for active debris removal from LEOs, or rendezvousing with LEO satellites for refueling or attaching a removal package (payload, hardware, engine etc.)
2. GTO-GEO(-Graveyard): Here the servicer will transfer from a GTO insertion orbit to GEO. Once in GEO two possible scenarios are examined; one in which the servicer removes satellites approaching their End-Of-Life (EOL) from GEO to a graveyard orbit (GYO), and one in which the servicer refuels client GEO satellites to extend their operational lifetime.
3. LEO-GEO mission: In this scenario the servicer should bring required payload from LEO (for instance from the ISS or from the servicer depot) to several client satellites in GEO and then return to LEO to resupply in preparation for the next round.

Note that in each of the aforementioned scenarios the servicer tour includes multiple targets in each of the respective orbits. In addition, reasonable target candidates for each scenario and their orbit characteristics will be taken from appropriate source (such as online satellite catalogues or relevant literature).

Since the purpose of this work is to identify feasible OOS scenarios for general low-thrust OOS missions, and not for a specific mission, different S/C designs may be applied to each scenario according to the specific mission being simulated.

The investigation metrics and methods required for answering the research question will be:

1. Computation run-time. Note that this metric would only serve as a measure for the feasibility of the investigated scenario. Since using different trajectory optimization programs or improving the efficiency of the optimization program used in this thesis is out of the scope of this thesis, this metric will not be subjected to optimization.
2. Time scales of transfer trajectories in OOS missions using SEP
3. Amount of consumed propellant mass by using SEP compared to conventional propulsion systems.
4. Critical evaluation of the results in comparison to existing results from study cases found in the literature.

The minimization of metrics 2 and/or 3 will, in turn, allow the maximization of the number of targets attended by a servicer in a single tour.

For the optimization process an optimization program called InTrance will be used. This program implements an optimization method that includes an Artificial Neural Network (ANN) for determining the optimal steering strategy of the spacecraft (S/C) and an Evolutionary Algorithm (EA) for training the ANN.

While the current version of InTrance allows for the optimization of multiphase missions including optimization of the mission as a whole and optimization of the individual phases [20], it does not allow for optimization of the sequence of the targets, i.e. the order in which the servicer will visit its targets. That means that the target sequence must be determined a-priori and given to InTrance as a boundary condition. Therefore, before setting up the different scenarios, first the sequence of targets to be visited should be determined.

Also, for coplanar multi-target transfers, which will be required for several of the scenarios investigated here (see Sections 2.2 and 2.3) a new Matlab tool will be developed utilizing analytical optimal low-thrust transfer solutions.

1.5 Thesis Outline

The introduction to the thesis, provided in this chapter, is followed in Chapter 2 by a comprehensive description of all the scenarios and sub-scenarios that are investigated in the scope of this thesis. Chapter 3 provides a detailed account of the tools used for the simulation of the scenarios described in Chapter 2. Section 3.1 introduces the optimization program InTrance which was mainly used for the calculation of Scenario 1 (described in Section 2.1). Section 3.2 describes the development of the Matlab tool that was specially developed for the work on this thesis, and which was primarily used for the simulation of Scenario 2 (Section 2.2) and Scenario 3 (Section 2.3). The implementation of the tools described in Chapter 3 on the scenarios described in Chapter 2 and the results of those simulations are described in Chapter 4 together with a discussion on the results. Finally, Chapter 5 draws conclusions about the investigated scenarios and the simulation results and provides suggestions for future follow-up work on this topic.

2 Scenarios Configuration

In this chapter, a general description is given for the three main scenarios investigated in this thesis (see Section 1.4).

2.1 Scenario 1: LEO – LEO

For this scenario, the OOS mission is assumed to include ADR only. In his study from 2011 [21] J. –C. Liou showed that with no active debris removal of objects from LEO (a case commonly known as “Business As Usual”) and assuming 90% success rate of Post Mission Disposal (PMD) of launched S/C, the number of objects in LEO larger than 10 cm will increase by 70% in the next 200 years. Liou suggested that at least 5 large objects will have to be removed from LEO every year starting from the year 2020 in order to stabilize the LEO debris environment. Fig. 2-1 shows results of the computation of 3 different ADR scenarios, all of which include 90% success rate of PMD; The red line – corresponds to the business as usual case, the blue line corresponds to the removal of 2 objects/year starting from 2020 and the green line corresponds to the removal of 5 objects/year starting from 2020. These results are today widely accepted within the scientific community and are therefore used in this work as a design driver for the baseline mission simulation of this scenario. Here, the servicer will have to sequentially rendezvous with 5 clients within a year, and attach a deorbit kit to each of them. In this scenario, the mission is considered to start at orbit insertion of the servicer, and end when the last deorbit kit is attached to the last target (i.e. excluding the launch phase and the time it takes for the targets to re-enter the atmosphere).

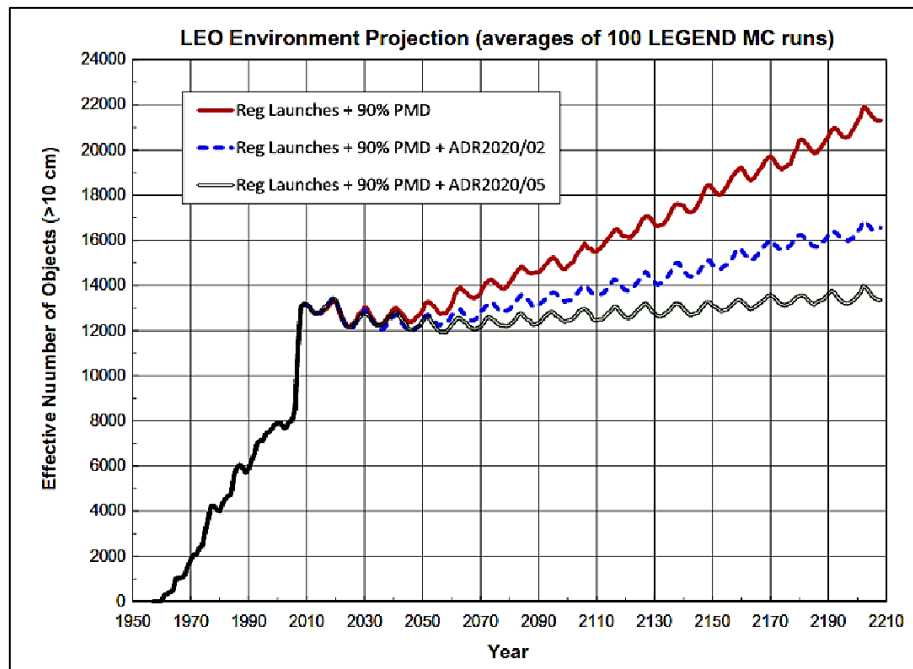


Fig. 2-1: Predictions of growth of the LEO space debris environment. Figure adapted from [21].

2.1.1 Mission Architecture

For an ADR mission, several concepts exist for the docking and removal of a debris object from an overcrowded orbit. These concepts may defer in several ways:

1. How a target is removed from its orbit: space tug vs. pull and mechanical vs. non-mechanical removal. Different combinations of these four elements may be conceived; A space-tug, mechanical docking solution may involve a rigid arm that attaches to the target and then “pushes” it to a different orbit using the servicer’s own propulsion system or the propulsion of a deorbit kit. A space-tug non-mechanical solution may involve, for instance, an ion thruster that uses an ejecta of ions to push the target to a different orbit. A pulling mechanical solution may involve a net that would be deployed to capture a debris object, which will then be pulled to its final orbital destination. A pulling non-mechanical solution might involve magnetic interaction between the servicer and target to pull the target to a different orbit.
2. The final destination orbit of the target: A target might be placed in a low orbit from which it will quickly enter the atmosphere and disintegrate or it might be relocated to another orbital location, which is less crowded and poses lower risk of collisions than the original target’s orbit.
3. How a servicer attends multiple targets: In [19] B. Chamot provided a detailed analysis of three types of ADR missions: “Picker” – separate servicer for each target, “Mothership” – one servicer carrying multiple deorbit kits and “Shuttle” – one servicer deorbiting by itself several targets. In [16], S. Peters et al. considered a fourth alternative, which is a combination of the “Mothership” scenario and “Shuttle” scenario (see Subsection 1.2.4). The advantage of this solution is that it simplifies the design of the servicer, since it does not require to carry multiple deorbit kits at one time. However, this poses other problems which become significant in the case of low-thrust transfers. Commuting back and forth from the parking orbit to the targets’ orbits doubles the number of required transfers and increases the required propellant mass and total mission time. In addition, since the parking orbit of the deorbit kits is in a lower orbit than the targets, its RAAN angle will drift during the mission. This will necessitate the servicer to either spend even more time in drift orbits or more fuel to correct the servicer’s RAAN angle to match these RAAN angle changes.

For this LEO-LEO scenario, the servicer assumes to carry all of the deorbit kits on-board, and transfers directly from one target to the next after the current target has been serviced. The mission ends after the last deorbit kit has been attached to the last target. Whether the deorbit kit transfers the target to a reentry trajectory or to another orbital location is not addressed in this study and does not influence in any way the results of this study. In addition, it is assumed that the servicer would mechanically attach to the target in order to deliver the deorbit kit to it. However, the close proximity operations and docking mechanisms are not simulated in detail, but are considered only in terms of the additional time (and fuel) that will be required for docking and servicing.

After the end of a mission, the servicer could potentially be resupplied with additional deorbit kits that would be sent separately to a parking orbit. The servicer would then have to reach the parking orbit only once in order to pick up all of the new kits in preparation for the next route.

2.1.2 Target and Launcher Selection

In [13, 15, 16, 22], S. Peters et al. laid out guidelines for selection of potential targets for deorbiting from LEO. According to these guidelines, and in order to minimize operation costs, the potential targets should be clustered, i.e. the maximal separation between their orbital elements should be minimal. A “cluster” is defined as a collection of satellites that share the same semi-major axis to within 50 km and whose inclination and RAAN angles all fall within 2° of each other. The investigation and identification of possible candidates for deorbiting carried out in [13] yielded a few clusters of SL-8 and SL-16 Rocket Bodies (R/B), most of which in near polar orbits at altitudes between 900 km and 1000 km. Using these guidelines, a similar selection process was done in this work. The SL-8 R/B were the second stage of the Kosmos 3M launcher, now retired. They have a dry mass of 1400 kg, length of 6 m and a diameter of 2.4 m [21]. According to space debris mitigation guidelines set by ESA in [23] every collision involving energy-to-mass ratio (EMR) larger than 40 J/kg will be a catastrophic event, which will cause the break-up and total fragmentation of the target objects. The EMR is calculated as the ratio between the kinetic energy of the debris object divided by the mass of the target:

$$EMR = \frac{\frac{1}{2}M_D V_{imp}^2}{M_T} \quad (2-1)$$

where, M_D is the mass of the Debris object, V_{imp} is the impact velocity, which for a circular orbit is calculated for the worst case scenario (head-on collision) as twice the orbital velocity, and M_T is the mass of the target. One can rearrange equation (2-1) to express the limit in terms of the target’s mass. Doing this for a typical SL-8 R/B results in the following condition for a catastrophic collision: $M_T < 3,796$ ton. This means that practically every object currently in orbit, that will collide with an SL-8 R/B will completely break up and create large amount of fragments. In addition, the orbital region, in which the SL-8 R/B are concentrated (polar region, between 900-1000 km) is a highly congested LEO region which should be prioritized for ADR. Liou prioritized in [21] the top 500 R/Bs and S/Cs for ADR according to highest mass and collision probabilities. Fig. 2-2 shows the top 500 R/Bs and S/Cs where the different families of objects are marked.

Using updated data from the NORAD catalog [24] a cluster of SL-8 R/B was selected. The orbital elements of the selected targets, as of 01.11.2015, are summarized in Tab. 2-1, where each target satellite is identified by its NORAD catalog satellite ID. For this scenario, the launch is assumed to be carried out by a DNEPR launcher. The reason is that the DNEPR launcher is a light-weight launcher that can bring payloads up to 2500 kg to high-inclination orbits with relatively good injection accuracy¹. According to the DNEPR user’s manual [25] the launcher can transport payloads to orbits in discrete inclinations: 50.5°, 64.5°, 87.3° and 98°. The altitude of an insertion orbit for a 2000 kg spacecraft launched into an 87.3° inclined orbit lies at 500 km, and this is the orbit that has been selected as the insertion orbit to start the simulation (and the servicing route) of this scenario. Tab. 2-2 summarizes the servicer’s injection orbital parameters. Further discussion about the injection orbit parameters is provided in Subsection 4.1.1.

¹ Altitude: $\sim\pm 4.5$ km, Inclination: $\sim\pm 0.045^\circ$, RAAN: $\sim 0.06^\circ$ [25]

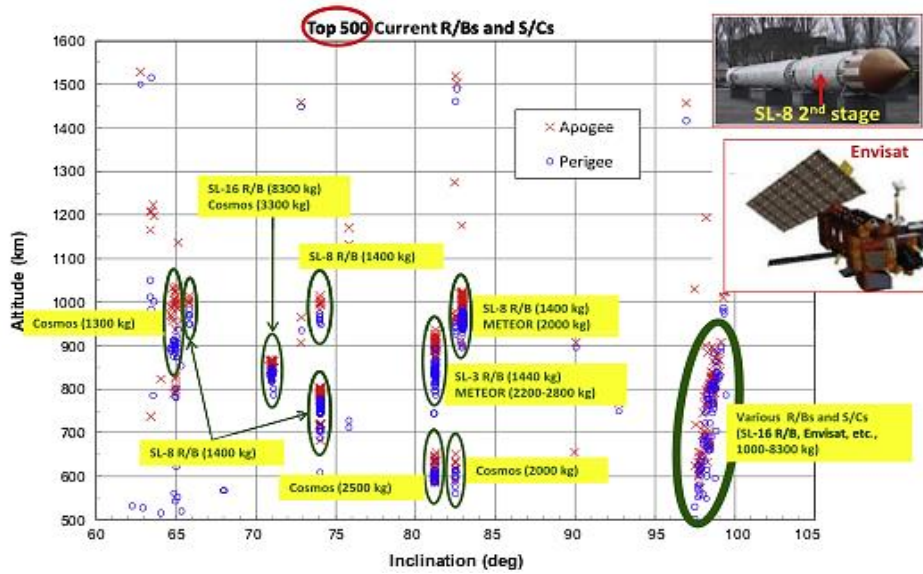


Fig. 2-2: Top 500 R/Bs and S/C for removal, as of 2010. Figure adapted from [21].

Tab. 2-1: Classical orbital elements of selected LEO deorbit targets, on 01.11.2015

Target Number	NORAD – ID	a [km]	i [deg]	e	Ω [deg]	ω [deg]	ν [deg]
1	10020	7,349.314	82.94	0.00315	84.934	171.11	N/A
2	14625	7,362.345	82.92	0.00206	87.142	300.01	N/A
3	16292	7,353.071	82.93	0.00293	85.52	310.17	N/A
4	15399	7,356.223	82.94	0.0034	85.433	15.36	N/A
5	28522	7,308.669	82.94	0.0046	86.97	167.56	N/A

Tab. 2-2: Servicer's injection orbit parameters

	a [km]	i [deg]	e	Ω [deg]	ω [deg]	ν [deg]
servicer	6,878.14	87.3	0.001	54.29	0	0

2.1.3 Target Sequence Selection

InTrance, in its current version, cannot optimize the order in which targets have to be visited by the servicer. Therefore, a different method for choosing the sequence has to be implemented.

As the selected targets are clustered, they obviously share similar orbital elements. Nevertheless, they still have small differences in their orbital elements that can be used to optimize the sequence of visits. The elements that exhibit the largest differences between the different targets are the Semi-Major Axis (SMA) and the RAAN angle (the true anomaly, which is a fast changing element, and the argument of periapsis, which is irrelevant for near-circular orbits, are not considered here).

One way of using the dynamic nature of the problem to save fuel is by exploiting the natural RAAN drift of the orbit for changing the servicer's RAAN angle w.r.t that of the target. To this end, before each transfer, the servicer would have to wait in a parking orbit (which might be, for instance, the orbit of the previous client). During the wait, the RAAN angles of the servicer and target will move w.r.t each other, and the wait duration would have to be long enough such that by the time the servicer reaches the target their RAAN angles will be equal. However, since low-thrust engines require long operation times, minimizing mission duration outweighs minimizing propellant mass consumption and such potentially long drift maneuvers should be avoided. Since the RAAN angle naturally drifts westwards (for all orbits with inclination smaller than 90° as in our case), long drift durations could be avoided if certain conditions are met. If the targets happen to be organized in such a way, that the target with the easternmost RAAN angle also has the highest RAAN angle rate of change, and the rest of the targets are organized such that the further eastwards a target is located, the smaller its RAAN drift-rate is, than the servicer could move from west to east, from one target to the next, potentially without having to correct its RAAN angle. This optimal configuration is displayed schematically in Fig. 2-3. In this configuration the servicer would visit the westernmost target first (target number 1 in Fig. 2-3). During the transfer and service time of target 1, the RAAN angle of the servicer (and target 1) will drift westwards, closing the gap to the RAAN angle of target number 2. If in addition, the targets are organized such that the drift-rate difference between two successive targets decreases the further east a target is (as shown in Fig. 2-3) this could ensure favorable configuration of the last targets to be visited (namely targets 4 and 5). This means that the RAAN angle of target 4 remains west to that of target 5 even after the servicer has visited clients 1 – 3, since the RAAN drift-rate of target 4 is only slightly larger than that of target 5, meaning that target 4 moves relatively **slowly** towards target 5.

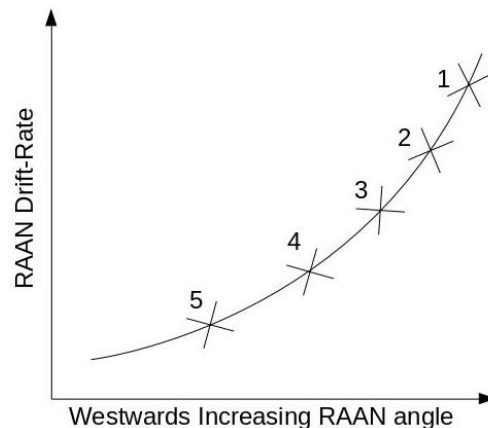


Fig. 2-3: Optimal configuration of targets in LEO

From the last discussion it is evident that an optimal constellation of the targets is quite a unique occurrence, and indeed, in this investigation that is unfortunately not the case. Fig. 2-4 displays the distribution of RAAN angles of the 5 targets listed in Tab. 2-1 and their respective RAAN drift-rates. The targets in the figure are identified as (T1...T5) and their drift-rates are calculated with equation (2-2) [26],

$$\dot{\Omega}_{J_2} = -1.5nJ_2 \left(\frac{R_E}{a(1-e^2)} \right)^2 \cos(i) \quad (2-2)$$

where $\dot{\Omega}_{J_2}$ refers to the RAAN drift-rate in [deg/day] due to the J_2 perturbation, n is mean motion in [deg/day], $J_2 = 0.0010826$ is the orbital perturbation due to Earth's oblateness, R_E is Earth's radius, a is the satellites semi-major axis, e is the orbit eccentricity and i is the orbit inclination.

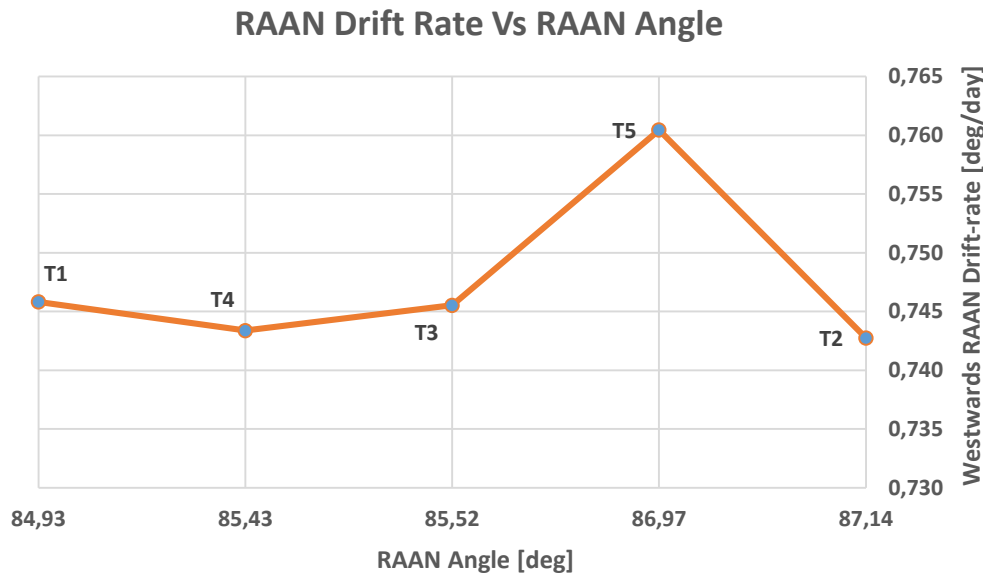


Fig. 2-4: RAAN Drift-rate of selected targets

As shown in Fig. 2-4, there is no correlation between the RAAN angle of the targets at the beginning of the mission and their respective RAAN drift-rates. The constellation of targets, as depicted in Fig. 2-4, means that if the servicer were to attend the westernmost target first (i.e target number 2), during the transfer to and servicing of this target, the servicer would have actually been drifting **away** (i.e. eastwards) from the rest of the targets, since the RAAN drift-rate of target 2 is smaller than that of all the rest. In addition, one has to bear in mind, that in the course of the mission the relative separation of RAAN angles between the different targets will change, meaning that the constellation of the targets depicted in Fig. 2-4 is a temporary one which corresponds to the targets constellation at the **beginning** of the mission. Therefore, the dynamic nature of the problem must be considered in the determination process of the visiting sequence. Finding an optimal (or near-optimal) visiting sequence requires solving a dynamic travelling salesman problem, which is out of the scope of this work. Instead, a simple local optimization method using the following algorithm was realized:

1. Choose first target
2. Calculate transfer time and fuel mass consumption from injection orbit to first target
3. Propagate all other targets through transfer duration calculated in previous step
4. Find which target's RAAN angle is closest to that of the servicer at the end of the transfer maneuver

5. Calculate transfer time and fuel mass consumption from current servicer location to the target found in step 4.
6. Repeat steps 3-5 until all targets are attended.

Choosing the first target to be visited requires analyzing the specific problem at hand. Using equation (2-2) the RAAN drift-rate of the injection orbit is calculated. The drift-rates of all targets as well as that of the injection orbit are summarized in Tab. 2-3.

Tab. 2-3: Nodal regression rate of targets and injection orbit

	T1	T2	T3	T4	T5	Injection Orbit
$\dot{\Omega}_{J_2} \left[\frac{deg}{day} \right]$	-0.7458	-0.7427	-0.7455	-0.7434	-0.7604	-0.3604

Tab. 2-3 clearly shows that the injection orbit is subjected to a much slower nodal regression than the rest of the targets. Therefore, since the injection orbit's RAAN angle can be freely determined by the designer, by selection of the launch epoch, it will be wise to select the injection orbit's RAAN angle to be further west to that of the westernmost target. That way, during the long transfer of the servicer from its 500 km injection orbit to the higher orbits of the targets (900 – 1000km) the faster westwards moving RAAN angles of the targets will close the gap to the RAAN angle of the servicer. If chosen properly, by the end of the transfer maneuver the servicer's RAAN angle will be equal to that of the target without additional corrections. However, the proper selection of the initial RAAN angle of the injection orbit depends on the duration of the transfer trajectory between the injection orbit and the first target, since this transfer duration determines how much the RAAN angle of the target will move w.r.t that of the servicer. Examining Tab. 2-1 we see that target 5 has the lowest altitude of all the targets, meaning that as the servicer ascends towards the targets from its injection orbit, it will encounter the orbit of target 5 first (in terms of altitude). Since we can also observe by examining Tab. 2-3, that target number 5 is subjected to the highest nodal regression rate of all targets, it is safe to assume that during the long transfer of the servicer, the "fast-moving" RAAN angle of target 5 will "overtake" the other targets RAAN angle, and will become the westernmost target by the end of the servicer's transfer maneuver. An initial simulation of the servicer's transfer from its injection orbit to the orbit of target 5 resulted in 158 days (including 10 days for docking, see Chapter 4). Fig. 2-5 shows the propagation of the RAAN angle of all targets throughout the 158 days of the first transfer. Fig. 2-6 and Fig. 2-7 show the RAAN angles of the targets at the beginning and at the end of the transfer, respectively. As expected, these figures confirm that target 5, which started at the 2nd easternmost location (i.e. 2nd from the top Fig. 2-6), became the westernmost target by the end of the transfer (i.e. bottom line in Fig. 2-7) due to its rapid nodal regression. Therefore, target 5 was chosen to be the first client to be visited. Subsequently, the rest of the clients were chosen according to the algorithm previously outlined and the final sequence of targets has resulted in (see Chapter 4 for description of the simulation and the results):

Injection Orbit → 5 → 1 → 3 → 4 → 2

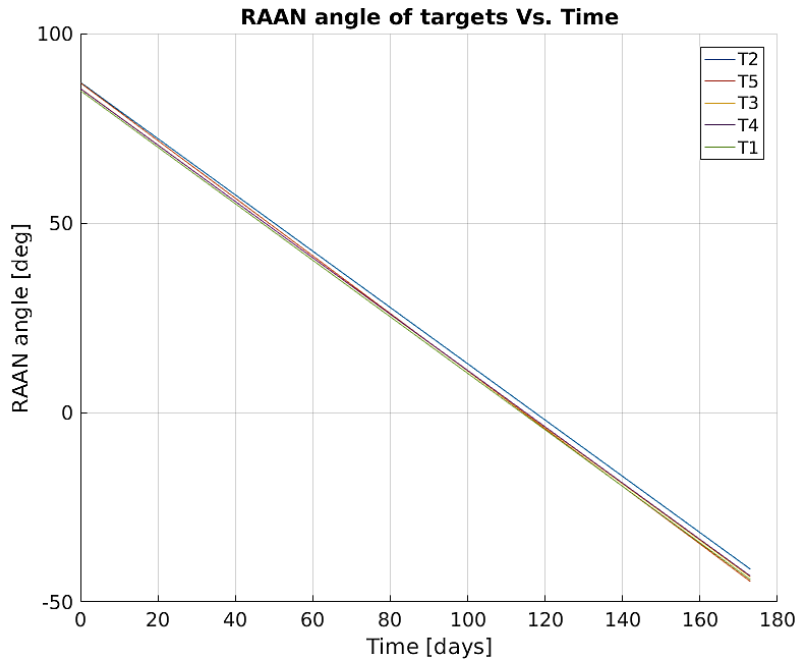


Fig. 2-5: RAAN angle propagation during 1st transfer

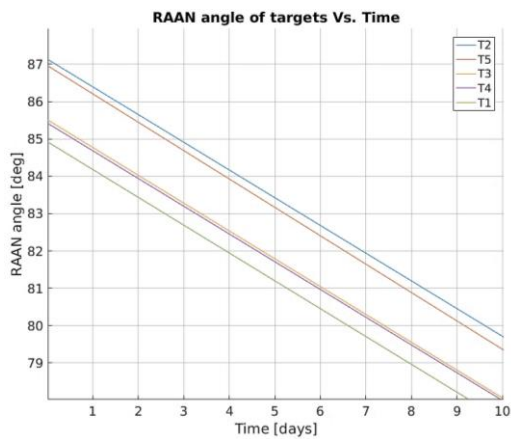


Fig. 2-6: Targets' RAAN angle at beginning of 1st transfer

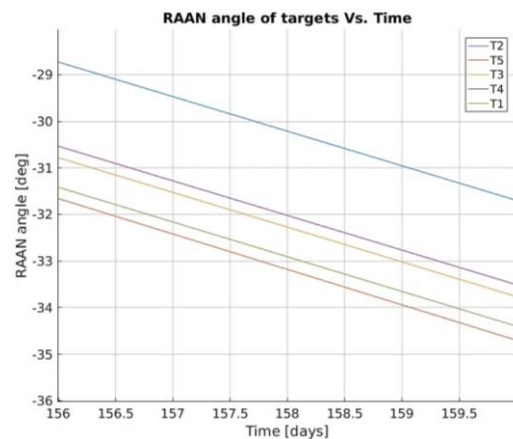


Fig. 2-7: Targets' RAAN angle at end of 1st transfer

With the knowledge of the first transfer duration, one can now calculate the required initial RAAN angle of the injection orbit. For that, the nodal regression rate is integrated over the transfer duration. It is stressed, that since the nodal regression rate is dependent on the SMA, eccentricity and inclination (cf. equation (2-2)), which change during the transfer, the nodal regression rate is in itself time-dependent over the integration period,

$$\Delta\Omega = \int_{t=t_0}^{t=t_1} \dot{\Omega}_{J_2}(t) dt = - \int_{t=t_0}^{t=t_1} 1.5nJ_2 \left(\frac{R_E}{a(t)[1 - e(t)^2]} \right)^2 \cos(i(t)) dt \quad (2-3)$$

where, $\Delta\Omega$ is the change in RAAN angle of the servicer during the transfer in [deg], $t_0=0$ is the start time of the first transfer and $t_1=148$ days is the end time of the first transfer.

Finally, the initial injection orbits' RAAN angle is calculated by,

$$\Omega_{\text{injection}} = \Omega_{\text{end}}^5 - \Delta\Omega \quad (2-4)$$

where, Ω_{end}^5 is the RAAN angle of target 5 at the end of the transfer maneuver (but before the servicing period begins), which should be equal to that of the servicer at that time. For the first transfer $\Delta\Omega$ is calculated to be $\Delta\Omega = -79.86^\circ$ and $\Omega_{\text{end}}^5 = -25.57^\circ$ which gives for the injection orbit RAAN angle: $\Omega_{\text{injection}} = 54.23^\circ$ (see Tab. 2-2).

2.1.4 Servicer Design

The time of the first transfer depends on the spacecraft design, which can also be optimized. Shorter transfer times will require more thrust, which will increase the demand on power which in turn will require bigger solar panels and heavier S/C. Therefore, a compromise has to be made between having smaller solar panels and having longer transfer times. A detailed design of the spacecraft is out of the scope of this work, however, the key design parameters of the S/C must be determined prior to being inputted into the simulation. Several S/C designs for ADR missions have been found in the literature and are compared in Tab. 2-4, where m_0 refers to the servicer S/C dry mass, the second column refers to the characteristic power of the solar array and m_{DK} refers to the total mass of one Deorbit Kit.

Tab. 2-4: Spacecraft design parameters of reference missions

S/C	m_0 [kg]	Solar Char. Power [kw]	m_{DK} [kg]
Agora [27]	1452	1.703	100
Astroscale ADRS-1 [11]	90	0.1 ²	30
ADReS – A [15]	1025	N/A	414

The missions in Tab. 2-4 describe different concepts of ADR missions. Based on the reference missions S/C designs, first the servicer S/C dry mass was selected to be 1500 kg which corresponds to the upper limit of servicer dry mass in Tab. 2-4 and thereby constitutes the worst case scenario. In addition, a dedicated launch would be required to meet the specific injection orbit requirement, which means that the entire launcher capacity could be used. Next, the deorbit kit design was addressed. While both the Astroscale mission and ADReS-A use their own design for a specialized deorbit kit, the Agora mission uses an “off-the-shelf” deorbit kit from the company D-Orbit. For generalization purposes this work also assumes the use of the D3-LEO deorbit kit from D-Orbit [29]. Note, that the mass of the D3-LE0 device at the time the simulation parameters were set, was approximated at 100 kg by extrapolating the device mass of the existing device to meet the orbit requirement of the target in this scenario, and this is the mass that was taken for one deorbit kit in the simulation.

² No information on power generation was available in [11]. Instead the value for the Hodoyoshi-4 S/C, on which ADRS-1 is based was taken from [28]

Current design of the D3-LEO [30] now features different configurations of the device with varying capabilities and masses, depending on the orbit and mass of the target that should be deorbited. According to the new design, the appropriate configuration of the D3-LEO would weigh approximately 150 kg which exceeds the first estimation by 50 kg. This added mass is within acceptable margins for the servicer and does not require recalculation of the scenario. An electric propulsion system was selected next for the servicer. For the selection of the EP system the following equation was used [31]:

$$\frac{P_e}{F} = \frac{1}{2} g_0 I_{sp} \quad (2-5)$$

where P_e is thruster power in [W], F is the thrust force in [N], g_0 is Earth's gravitational acceleration in [m/s^2] and I_{sp} is the thruster's specific impulse in [sec].

Equation (2-5) facilitates carrying out a trade-off study for the selection an SEP: Maximizing the I_{sp} of the SEP would increase its efficiency which translates to less propellant needed for a given maneuver. On the other hand, this would also translate to a higher power requirement on the S/C which means larger, heavier solar panels, or lower thrust of the S/C which means longer transfer times.

Tab. 2-5 compares several flight-proven SEP thrusters. The data in Tab. 2-5 was taken from [20]. Tab. 2-5 lists only flight proven SEP thrusters, although other, more advanced, thrusters exist in different phases of development. However, for this thesis it was decided to limit the selection to available flight-proven hardware as much as possible.

Tab. 2-5: Comparison of flight-proven SEP thrusters

Thruster	F [mN]	P_e^* [W]	I_{sp} [sec]	Mission Applied
NSTAR	93	2567	3127	DS1, Dawn (NASA)
PPS-1350-G	88	1500	1650	Smart1 (ESA)
T5	18	476	3200	GOCE (ESA)

Note, that in Tab. 2-5, P_e^* refers to the maximum electrical thruster input power, whereas P_e in equation (2-5) refers to the ion jet power, i.e. the power actually used by the ions to propel the S/C. The transformation between the two can be achieved using the total power efficiency η_t :

$$P_e = \eta_t P_e^* \quad (2-6)$$

For this scenario, since 5 targets are to be attended within a limited time of 1 year, the thrust level of the thruster was given more weight than the required Power. Also, current advancements in Solar Array technology allow for high power generation for lower mass and low stowing volume. For example, the UltraFlex Solar Array manufactured by Orbital ATK and already used twice on the Cygnus S/C in resupply missions to the ISS, have a power-to-mass ration of 150 [W/kg] [32]. With this ratio, which is at the time of writing these lines the highest in the market, the required solar array mass for one NSTAR thruster is approximately 17 kg. Therefore, to maximize S/C acceleration and minimize transfer times, 3 NSTAR thrusters will be used and

6 kW will have to be generated by the Power Generation System (PGS), resulting in a solar array mass of 40 kg.

Finally, the S/C design parameters assumed for the simulation of this scenario are:

Isp [sec]	3100
Thruster Type	NSTAR
Max. Thrust [mN]	93
No. of Thrusters	3
Efficiency η	0.56
Propellant gas	Xenon
Total Mass [kg]	2000 (including 5 deorbit kits)
Deorbit Kit Mass [kg]	100 per unit
Power [w]	6000

Remarks about Phasing, Closing-in and Final Approach

After the servicer has raised its orbit to less than a predefined distance from the target (say 3 km) it needs to perform a phasing maneuver that will bring it close enough to the target to perform the final approach and docking maneuver. Usually this distance for final approach is a couple of hundreds of meters from the target [26].

S. T. King et al. analyzed in [33] maneuvers of satellites using EP in near-Earth orbits. One of the analyzed scenarios included a worst-case scenario phasing maneuver (i.e. 180° phasing) of a satellite in LEO with a mass of 500 kg and for a range of I_{sp} values between 1000 sec and 3000 sec, and input power range between 100 W and 1.5 kW. In this thesis, the servicer's mass is 4 times larger than that of the reference case in [33]. However, from Newton's second law ($F = ma$) it is obvious that in order to get similar acceleration for a servicer with a mass 4 times larger, one needs 4 times the thrust. From equation (2-5) we see that for a given I_{sp} there is a linear proportionality between thrust and power, i.e. 4 times more thrust requires 4 times more power. Therefore, since for the S/C simulated in this work the power input is taken to be 6 kW which is 4 times the maximum input power of the reference S/C, it can be assumed that the transfer times and propellant mass consumption found in [33] for the maximum values of I_{sp} and input power correspond to those of the S/C design used in this work.

Fig. 2-8 shows the results found in [33] for a phasing maneuver of 180° using a 1.5 kW thruster. As can be seen, for a thruster with $I_{sp} = 3000$ sec and for a reasonable amount of propellant mass between 1 and 3 kg, the phasing maneuver will take between 3 days and 20 hours, respectively.

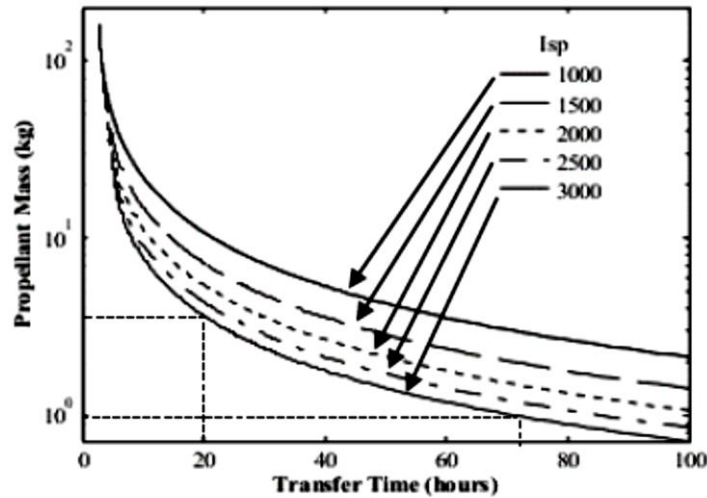


Fig. 2-8: Required propellant mass and transfer time for a phase change of 180° with a 1.5 kW thruster. Figure modified from [33]

These phasing times which are measured in hours or days are much shorter than the transfer maneuvers themselves between the orbits, which are measured in weeks or months. Therefore, the phasing maneuvers themselves are not simulated, but instead a fixed time for the approaching, docking and servicing is added to the simulated results. That is, the simulations give the results for transfer times and propellant fuel consumptions for the transfer between orbits with free true anomaly, on top of which a fixed time is added to account for matching the true anomalies and for servicing.

2.2 Scenario 2: GTO – GEO – GEO/GYO

The purpose of this scenario is to investigate OOS missions within the GEO/Graveyard belt. However, since the servicer first has to reach GEO orbit, this scenario assumes the servicer is delivered to a GTO by the launcher, and from there it assumes control and transfers itself to GEO. In the following, two sub-scenarios will be explored: one, in which the servicer is tasked with removing decommissioned satellites from GEO to specific location in the Graveyard orbit, and in the other, the servicer will have to refuel several client satellites with intermediate rendezvous with a depot station, near the GEO belt, for self-refueling of the servicer and resupply of fuel for the clients.

2.2.1 Sub-scenario 2.1: Satellite removal from GEO

2.2.1.1 Mission Architecture

This sub-scenario is intended to provide a general idea of fuel and total mission duration requirements for a multiple target GEO satellite removal mission.

The mission consists of a servicer satellite capable of capturing (docking and undocking) multiple cooperative satellites after reaching their EOL and transferring them to dedicated assembly positions (assembly nodes) in a graveyard orbit, 350 km altitude above GEO.

In their OOS study report from 2010 [1], NASA investigated a multiple target GEO satellite removal scenario, in which a servicer would remove 10 communication satellites from GEO to a graveyard orbit 350 km above GEO within a mission life-time of 5 years.

Fig. 2-9 depicts the architecture suggested in [1] for the removal of one client satellite from GEO to a graveyard (disposable) orbit. A similar scenario will be investigated here with the following differences to the NASA reference scenario:

- The servicer S/C will use EP instead of chemical propulsion as in [1]. Therefore, the transfer maneuvers will be continuous and not Hohman transfers.
- The S/C will be injected into a GTO and will transfer from there to the geostationary orbit, contrary to [1] where the servicer is assumed to be delivered directly to GEO.
- The reference servicer utilizes a drift orbit (at an altitude of GEO+300 km) where it will drift as long as required to close the angular gap to the next client. The servicer in this work could either use a drift orbit, or a direct transfer to the next target, whichever is faster (see Chapter 3.2).
- The serviced client satellite will be removed to a specific location within the graveyard orbit and will be attached there to an assembly node. In the reference scenario, the clients are removed to a random location within the graveyard orbit.

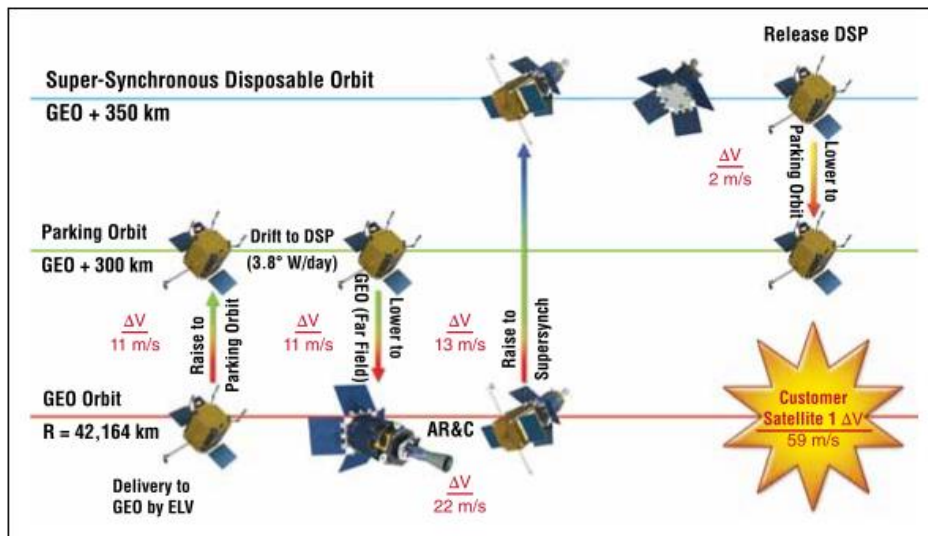


Fig. 2-9: NASA GEO satellite removal architecture. Figure adapted from [1]

2.2.1.2 Assembly Nodes (AN)

The idea of the dedicated assembly nodes comes from long-term considerations of debris growth in the graveyard orbit. Currently, retired communication satellites in GEO are removed to a random position in the graveyard orbit, where they remain for the rest of their lives. In the future, as more and more retired satellites will be brought to the graveyard orbit, the risk for collision between decommissioned satellites in the graveyard orbit will increase. These collisions pose the risk of creating large amounts of debris which will not necessarily be contained in the graveyard orbit. Different perturbations like solar radiation pressure or third-body perturbations, which are significant in the graveyard orbit, may alter a debris object's orbit in such a way that it

could eventually find its way back to the GEO belt, endangering the operational satellites there. Therefore, this scenario investigates a potential solution to the problem, where decommissioned satellites are brought to dedicated assembly nodes evenly distributed around the graveyard orbit. These assembly nodes are assumed to be rigid structures to which the client satellites can be firmly attached, thus minimizing the risk of in-orbit collisions between satellites in graveyard orbit. Detailed design of the assembly nodes is not part of this study, and it is also assumed that the assembly nodes are already in place at the beginning of the mission (i.e. they are not part of the payload to be launched with the servicer). It is, however, assumed that the AN will have several docking ports, to which the discarded satellite could be firmly attached. This assumption is incorporated in the simulation by adding a fixed time for the attachment of the client satellite to an AN, which is similar to the time required for the docking process of the servicer with the client satellite.

2.2.1.3 Target Selection

As this sub-scenario deals with servicing the GEO belt, the target candidates will obviously be communication satellites, as this is the predominant type of S/C in GEO.

For simplifications reasons, all client satellites are assumed to have similar mass. In “Space Mission Analysis and Design”, by Wertz and Larson [34], characteristic mass budgets for different types of S/C are presented. An averaged dry mass of communication satellites is calculated at 815 kg. This averaged value is taken as the clients’ mass, since they are assumed to be at their EOL and thus they have used up all or most of their propellant.

2.2.1.4 Key Assumptions

This sub-scenario assumes all client satellites as well as all assembly nodes are evenly distributed around their respective orbits. Further, it is assumed that all satellites and nodes are coplanar with inclination 0.

With regards to the client satellites it is also assumed that the satellites are cooperative, i.e. they have reached their EOL with enough fuel to perform small correction maneuvers to stay within their allocated slot. This assumption eliminates the East-West drift of the client satellites which means that they remain in the vicinity of their operational longitude until their disposal. Making this assumption can be justified by properly timing the servicer transfer maneuvers such that it always reaches a client satellite before the client completely depletes its own fuel (or in case of fuel depletion – before the client satellite drifts outside its allocated slot).

2.2.1.5 Assembly Nodes setup and configuration

Exact description of the assembly node mechanical design is out of the scope of this work. However, it is assumed that these rigid structures will be simple constructions, whose sole intention is to provide a rigid link between decommissioned satellites, i.e. they don't have subsystems like power generation or propulsion so their position is not corrected or controlled. However, to facilitate attaching a satellite to the node, it is assumed the nodes are passively stabilized (e.g. spin stabilization).

It is important to identify key characteristics of the assembly nodes such as their numbers and locations within the graveyard orbit. Here, a trade-off should be made on the number of nodes, since having too many nodes will incur possibly unnecessary additional costs (mainly due to construction and launches) whereas having too little nodes will necessitate longer transfers from GEO to graveyard orbit, thereby rendering the disposal process inefficient.

To find the optimal number of assembly nodes, first the transfer time and propellant mass consumption is calculated for a single transfer of a servicer with a docked client from a location in GEO to a location in GYO. The calculation is done for an even distribution of the client's location around the GEO orbit with 10° longitude intervals. This is then repeated for different number of assembly nodes in GYO: 3, 6, 8, 10, 12, 14 and 16. That is, for each number of ANs in GYO, 36 transfers of a servicer + client are computed, where each transfer starts from a different GEO location (longitude 0° , longitude 10° etc.)

Then, for each case (e.g. 3 assembly nodes, 6 assembly nodes etc.) the maximal amount of fuel mass as well as the maximal transfer time from all 36 transfers is computed. The results of the maximal propellant mass and transfer times are summarized in Tab. 2-6.

As could be expected, Tab. 2-6 shows that the more assembly nodes are in use, the less time and less fuel mass is required to transfer a client from GEO to GYO. If there was a single assembly node in use, the worst case transfer scenario would be one, where the client satellite is exactly 180° opposite to the assembly node location resulting in the longest (and most fuel expensive) transfer. The more assembly nodes are in use the smaller the angular difference between the client satellite and the next closet assembly node is, resulting in shorter transfer times.

Tab. 2-6 : Assembly Node Trade-Off

No. of Assembly Nodes	Max. Propellant Mass [kg] (Improvement w.r.t previous case)	Max. Transfer Time [days] (Improvement w.r.t previous case)
3	7.906 (--)	16.758 (--)
6	5.784 (27 %)	9.502 (43 %)
8	5.303 (8 %)	8.711 (8 %)
10	4.996 (6 %)	8.207 (6 %)
12	4.776 (4 %)	7.845 (4 %)
14	4.434 (7 %)	7.283 (7 %)
16	4.150 (6 %)	6.817 (6 %)

For this work, the service time is assumed to be 7 days (i.e. time required for close approach navigation and docking). Therefore, the maximal cut-off value for transfer time is also taken to be 7 days, i.e. we require that the maximum time it takes for the

servicer to transfer a client from GEO to GYO will not exceed 7 days. From examination of Tab. 2-6 we see that this condition is first met when 16 assembly nodes are in use.

Consequently, the configuration of the simulation of this sub-scenario will be the removal of 10 client satellites to any of 16 assembly nodes evenly distributed in graveyard orbit.

2.2.1.6 Servicer Design

Since the task of the servicer in this sub-scenario is similar to the task of the servicer in Scenario 1: LEO-LEO (see Subsection 2.1.4), i.e. docking and removal of a target, the design used for both S/C will be similar but not identical. As will be discussed in Subsection 4.2.1, the first transfer of the S/C from GTO to GEO is carried out using InTrance, and the subsequent transfers between clients and ANs using Matlab. To guaranty a seamless simulation of the mission the same S/C design parameters were used in both the InTrance part and the Matlab part. In its current version, InTrance cannot calculate Earth-bound transfer trajectories terminating at a certain location in the target orbit, but only transfers to a target orbit with undefined true anomaly. Therefore, it was assumed in the simulation that the phasing time required to bring the servicer to a specific location in the target orbit is only a small fraction of the entire GTO to GEO transfer duration. To validate this assumption, the InTrance simulation was designed based on a similar simulation which was run with the commercial orbit optimization software GESOP [35]. The GESOP simulation included two runs; one in which the target orbit was chosen with a free true anomaly, and one in which a specific target true anomaly constraint was predefined. The results of this validation are presented in Section 4.2. To accommodate the S/C design change to match that of the GESOP reference case, the following S/C design parameters of the servicer have been used in this sub-scenario. Design parameters not listed here are similar to those used in Scenario 1:

Isp [sec]	1700
Thrust [mN]	440
Dry Mass [kg]	2000
Efficiency η	0.612

2.2.2 Sub-scenario 2.2: Satellite refueling in GEO

This sub-scenario is intended to provide a general idea of fuel and total mission duration requirements for a multiple target GEO satellite refueling mission.

2.2.2.1 Mission Architecture

As in the previous sub-scenario, also here the simulation is based on a proposed GEO refueling scenario, described in the NASA OOS study report [1] (Notional Mission 2).

The mission here consists of 2 elements: 1. A servicer satellite capable of sequentially capturing multiple cooperative client satellites, who have all but depleted their fuel supply, and replenishing their fuel supply in order to extend their operational lifetime.

2. A depot station positioned 100 km above GEO that will hold enough fuel supply for the servicer to refuel up to 24 clients over the course of 10 years.

Both the depot and the servicer will be initially brought to the depot operational orbit. Three possibilities exist for bringing the servicer and the depot to their initial orbit:

1. Launching the coupled servicer-depot duo to a GTO and from there, using its own electric propulsion subsystem, the servicer will raise the orbit altitude of the servicer-depot duo to their initial operational (Depot) orbit.
2. Launching the servicer to GTO and letting it raise its own orbit to the depot operational orbit, while the depot will be inserted directly to its operational orbit (using the upper stage of the launching rocket)
3. Launching both the servicer and the depot directly to the depot operational orbit using the launcher's upper stage

After initially reaching the depot operational orbit (and after completing the commissioning phase) the servicer will embark on its first sortie to deliver fuel to the client satellites in GEO.

The servicer would perform 4 sorties, servicing up to 6 clients in each sortie, after which it will rendezvous with the depot station to replenish both its own fuel supply as well as the fuel packages intended for the client satellites.

Following differences are introduced in this work w.r.t the reference scenario in [1]:

- The servicer S/C will use EP instead of chemical propulsion. Therefore, the transfer maneuvers will be continuous and not Hohman transfers.
- The servicer S/C together with the fuel depot will be injected into a GTO and will transfer from there to the depot orbit 100 km above geostationary orbit, whereas the reference scenario assumed a launch of the servicer and depot directly to GEO.
- The reference servicer utilizes a drift orbit (at an altitude of GEO+300 km) where it will drift as long as required to close the angular gap to the next client. The servicer in this work utilizes a direct transfer to the next target, which, in this case, will be faster than a drift orbit transfer (see Chapter 3.2).

2.2.2.2 Target Selection

The client satellites for this sub-scenario are communication satellites located around the GEO belt. The clients for the simulation are chosen randomly from a database of currently active satellites in GEO, updated on 15th, November 2015 [36].

For the client selection the complete GEO satellite database was refined to include only satellite whose inclination is smaller than 1.0° and who are positioned in a unique location, i.e. if two satellites are positioned in the same slot, they are considered as one satellite (see Appendix 0 for the refined list). For every sortie, 6 unique clients are sampled uniformly at random, without replacement, from the refined database, i.e. in the entire mission all 24 satellites will be different, such that no satellite would be refueled twice during one mission.

2.2.2.3 Key Assumptions

Servicing (i.e. refueling) duration is assumed to be 7 days (including automated RnD maneuver and the refueling of the client).

Resupply at the Depot station is assumed to last 10 days. With regards to the client satellites, it is assumed that the satellites are cooperative, i.e. they have not completely depleted their fuel supply to the point where they can no longer be actively controlled.

2.2.2.4 Spacecraft Design

The servicer S/C design assumed for this sub-scenario is similar to the one described in Subsection 2.2.1:

Isp [sec]	1700
Thrust [mN]	440
Total Mass [kg]	2000
Propellant Mass [kg]	30
plus 30% margin [kg]	40
Power [w]	6000

The Depot design parameters are as follows:

Dry Mass [kg]	1326
Fuel for 24 Clients [kg]	480
Fuel for Servicer [kg]	160

As mentioned in Subsection 2.2.1.3, an average dry mass of a communication satellite is 815 kg. Assuming the satellite's fuel supply is not necessarily completely depleted by the time of refueling, we shall take the average satellite mass to be 900 kg. One of the most common propulsion types for stationkeeping of geostationary communication satellites is the Arcjet propulsion system, which uses hydrazine as propellant and typically provides Isp values of approximately 600 sec [34]. The average yearly fuel demand for stationkeeping of geostationary satellites (both for East-West and North-South stationkeeping) is 60 m/s [34]. Therefore, a supplement of a mere 20 kg of hydrazine to a client allows life extension of more than 2 years (approximately 800 days). For client satellites using more efficient propulsion systems, such as Hall Effect Thrusters, that use Xenon as propellant and provide on average an Isp of 1700 sec, 20 kg of propellant could extend mission lifetime in more than 6 years (2260 days), which is more than 40% of the original client's full operational lifetime, assuming a lifetime of 15 years for a communication satellite.

2.3 Scenario 3: LEO – GEO

This scenario includes a transfer of a servicer from LEO to GEO and the subsequent servicing of satellites in GEO with an optional subsequent return to LEO. The rationale for this scenario is to investigate an OOS mission where a payload would be launched to LEO (e.g. to the ISS) and the servicer will “shuttle” between LEO and GEO to transfer

the payload to GEO and potentially return to LEO to pick up more supply (fuel, hardware etc). The payload in this case might be for instance an entire communication satellite that the servicer would transport to GEO, thus allowing for a much cheaper launch to LEO instead of directly to GEO or GTO. Alternatively, the payload could also be certain hardware components such as batteries, antennas etc., which should be transported to GEO in order to be replaced in a communication satellite.

2.3.1 Mission Architecture

The calculation of a low-thrust transfer from LEO to GEO is done here for a simplified scenario of coplanar equatorial LEO-GEO transfer. This simplifying assumption poses an impractical restriction on the mission since the injection orbit would have to have inclination zero. This is possible only with a sea-launch, which is, as of yet, not as common as land launches. A more realistic scenario would have to include inclination reduction during the transfer, but such a scenario is left to a future study. The initial (LEO) and final (GEO) orbital parameters taken for this scenario are summarized in Tab. 2-7:

Tab. 2-7: LEO-GEO Transfer. Data taken from [20]

	a [km]	i [deg]	e	Ω [deg]	ω [deg]	ν [deg]
LEO	7,000	0.0	0.01	0	0	0
GEO	42,000	0.0	0.01	N/D	N/D	N/D

Once the servicer reaches the GEO orbit, the investigation of the multiple-target OOS is similar to that which is described in Section 2.2. For this scenario it is assumed that the servicer is supposed to transport hardware components from LEO to GEO. In GEO, the servicer attends 10 satellites, replacing one hardware component on each client. It is assumed that each hardware component weighs 20 kg. After servicing the last client, the servicer returns to LEO, in order to collect further supplies. The clients selection process is done similarly to Subsection 2.2.2.

2.3.2 Servicer Design

The servicer in this scenario is assigned a similar task to the one described in Subsection 2.2.2, namely deliver payload to satellites in GEO. The major difference here is, of course, the depot orbit, which is now located at an altitude of approximately 620 km. therefore, the transfer time and required propellant mass for the transition from the depot orbit to the first client would be much higher than the GEO-GEO case. In addition, in this scenario 10 satellites are assumed to be serviced during one sortie, as oppose to 6 in the GEO-GEO refueling scenario. Hence, the launch mass of the servicer in this case has to be larger:

Isp [sec]	1700
Thrust [mN]	440
Total Mass [kg]	2670
Power [W]	6000

3 Applied Tools

In this chapter, a detailed account is given of the tools that were used for the investigation of the scenarios described in Chapter 2. For the investigation of the first scenario (LEO-LEO) a low-thrust trajectory optimization program called InTrance was utilized. Section 3.1 provides general information about InTrance and about the optimization method implemented in it. In the second (GTO-GEO) and third (LEO-GEO) scenarios an additional low-thrust trajectory analysis tool was developed with Matlab for this work. Section 3.2 provides description of the development of this tool.

3.1 Trajectory Analysis Using InTrance

In 2004, B. Dachwald published his work on a program called InTrance, which stands for Intelligent Trajectory optimization using neurocontroller evolution [37]. InTrance was originally designed to be a preliminary analysis tool for optimization of deep space heliocentric transfer trajectories using low-thrust propulsion. Later, in 2015, A. Ohndorf extended Dachwald's work to include also planetocentric and multiphase (multi-target) transfer trajectory optimization [20]. Ohndorf's extension is what allows InTrance to be used in this work for the optimization of geocentric transfer trajectories as part of an on-orbit servicing mission. However, the program does not include a model for atmospheric drag at the moment, which is a dominant disturbance in LEO. Therefore, the program cannot provide reasonably accurate results for LEO trajectory optimization. Still, the analysis of LEO transfers carried out here using InTrance could be admissible as a preliminary analysis during the conceptual phase of an OOS mission design.

3.1.1 Trajectory Optimization

Optimization of transfer trajectories, using high thrust chemical propulsion is a relatively straightforward task, since the thrust phases required for such transfers are very short compared to the full transfer time. Thus, these thrust arcs can be approximated as impulsive maneuvers that change the spacecraft's velocity instantaneously while its position remains fixed. In contrast, low thrust transfer trajectories require thrust arcs that last a significant fraction of the entire transfer arc and can no longer be considered impulsive maneuvers. Consequently, the thrust force and the associated control vector become continuous functions of time of infinite dimension, which can only be computed numerically as discrete approximation of the problem [37].

Traditionally, low-thrust continuous transfer trajectories have been optimized using Local Trajectory Optimization Methods (LTOMs), such as non-linear programming (NLP) optimization, neighboring extremal methods or gradient methods. Common to all LTOMs is their requirement for some initial guess (i.g.) to initialize the algorithm. This initial guess usually requires expert knowledge of astrodynamics, since the final solution would eventually converge, as the name suggests, to a LOCAL optimum, which would typically be in the vicinity of the initial guess [20].

In contrast, Global Optimization Trajectory Methods (GTOMs) are usually heuristic methods that attempt to find a global optimal solution to a problem by searching the entire search space which is independent of the initial guess. GTOMs include, among other methods, Dynamic Programming, Simulated Annealing, Multiple Shooting and

Genetic Programming. In addition to their independence of the initial guess, GTOMs are also capable of running autonomously without the continuous supervision of an expert in astrodynamics and optimization theory (e.g. through machine learning).

Tab. 3-1 compares LTOMs and GTOMs. A green cell represents a relative advantage with respect to the other method, whereas a red cell represents a disadvantage. A white cell represents an indifferent attribute.

Tab. 3-1: LTOMs - GTOMs comparison based on [20] and [38]

Criterion	LTOMs	GTOMs
Initial guess dependence	Final solution close to i.g. Requires experts knowledge	Final solution independent of i.g.
Convergence Behavior	Convergence to local optimum close to i.g., Often not robust	Can find global optimum irrespective of i.g., robust
Expert knowledge / supervision	Required for i.g. and fine-tuning of simulation parameters	No expert supervision required after proper problem formulation
Computational effort	Considerable storage and CPU run-time requirements for multi-modal problems. Suitable for use with small search-spaces	No relative benefits over LTOMs for small search-spaces. Advantage by larger multi-modal search-spaces
Optimization of initial conditions	Not part of the optimization process. Responsibility of expert	Can be optimized as part of the trajectory optimization
Accuracy/Fidelity	High	Low - Medium
Determinism	Mathematical and deterministic methods. High confidence in results	Heuristic nondeterministic methods. Several runs of same problem may be needed to gain confidence in results

For a more detailed account of the relative advantages and disadvantages of LTOMs and GTOMs the reader is referred to [20] and [38].

3.1.1.1 Artificial Neural Networks

Artificial Neural Networks (ANNs) are used as control methods that derive on the behavior of natural neural networks. An ANN takes input data, and transfers it through a network transfer function to acquire the output. The ANN consists of processing units called neurons organized in interconnected layers that can exchange information among themselves. This process is illustrated schematically in Fig. 3-1. The first layer is always the input layer, which includes the neurons that receive the input from the environment. The last layer is the output layer. Between the input and output layers there can be any number of intermediate hidden layers that consist of any number of neurons. Fig. 3-1 illustrates an ANN with 3 input neurons, a hidden layer with 2 neurons and one output neuron. A training algorithm trains the network function by adjusting its function parameters to obtain the required output. The neurons of an ANN

are defined by a transfer function that maps the input data going into the neuron to an output value going out of it. In addition, each neuron is assigned a weight factor w , which multiplies the output value of the neuron. The ANN can be trained by using an optimization algorithm as the training algorithm (such as, for instance, evolutionary algorithms), or using known true input and output data to run through the network. The training process adjusts the network function parameters (e.g. transfer function parameters, weight factors etc.) to minimize the error between the ANN's output and the known true output.

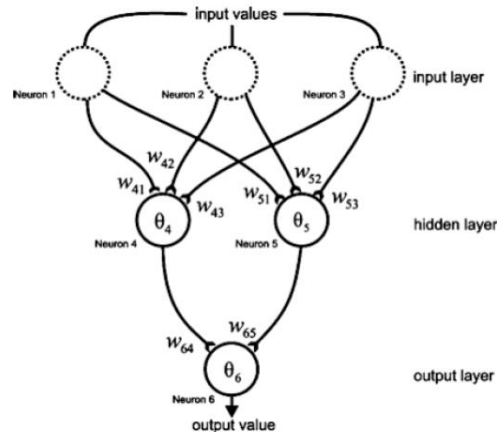


Fig. 3-1: Layered artificial neural network. Adapted from [37].

3.1.1.2 Evolutionary Algorithms

Evolutionary Algorithms (EA) are an optimization method inspired from the natural process of evolution. They utilize evolutionary operators to improve the average quality of a population of input data sets, also called individuals, through iterations (called generations) until the quality of the population (also called fitness) meets some predefined criterion. In general, EAs consist of 4 phases, each of which defined by an evolutionary operator:

1. Selection – Individuals from the population are selected to reproduce offspring with a probability relative to their fitness value. The fitness is a measure of an individual's capability to reproduce and create fit offspring.
2. Crossover/recombination – The selected individuals undergo crossover, in which their “genetic material” is split and then recombined in a specific manner, which results in new offspring.
3. Mutation – The newly created offspring undergo mutation, with some predefined probability. This stage is crucial in order to retain the population diversity and prevent premature convergence to a local optimum, rather than a global optimum.
4. Evaluation – The new offspring are evaluated, given some fitness value and put back into the original population, in preparation for the next generation.

The actual implementation of each operator (selection, crossover etc.) in an EA varies. For instance, the selection operator could be implemented as a “roulette wheel selection” where each individual is allocated a probability to be selected for reproduction, which is proportional to its fitness. Alternatively, the selection can be carried out as a “tournament selection”, where a tournament is run between several

randomly selected individuals. The individual with the highest fitness wins the tournament and is selected for reproduction [39]. Each implementation has its own advantages and disadvantages and it is left for the programmer to decide which implementation best suits his/her specific problem. A schematic EA cycle (generation) is illustrated in Fig. 3-2. Typically, the EA runs until a predefined maximum number of generations is reached, or the relative improvement of the averaged fitness of the population between two consecutive generations falls below a predefined value. In the end of a successful simulation, all the individuals of the population will be clustered close to the global optimum.

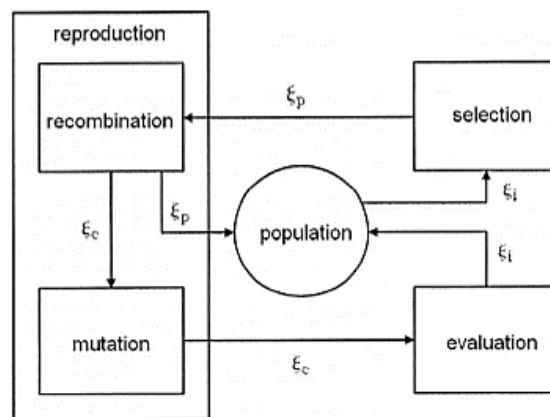


Fig. 3-2: General Evolutionary Algorithm structure. Adapted from [20]

3.1.2 Spacecraft Steering Using Evolutionary Neurocontrollers

InTrance is classified as a GTOM, implementing an artificial neural network, as a type of machine-learning method for finding the spacecraft's control history, and an evolutionary algorithm for training and optimizing the ANN. This entire entity, consisting of the ANN for finding the S/C control history and EA for optimizing the ANN, is named an Evolutionary Neurocontroller (ENC).

In InTrance, the EA holds a population of individuals, or chromosomes - ξ , each of which made up of the ANN's network function parameter vector - π . This vector holds parameters that completely define the ANN's behavior, e.g. transfer function parameters and all the neurons' weight factors (see Fig. 3-3). Hence, the network function parameter vector affects the ANN's output, namely the S/C thrust direction and magnitude, and therefore, also the resulting trajectory.

Fig. 3-4 delineates the general functionality layout of InTrance. The inner loop consists of the neurocontroller (NC), which is initialized with the spacecraft's and target's state vectors as well as the network function parameters vector. The NC's output is the S/C thrust vector (direction and magnitude) as function of the input S/C and target state vectors, or the difference between them. The resulting thrust vector is then inserted together with the S/C current state vector into the equations of motion which are integrated numerically to acquire the S/C new state vector. The new state vector is then checked against some termination criterion (e.g. if the distance to the target is smaller than some predefined value or if the number of iterations exceeded some value etc.). Once the termination condition is met, the fitness of the entire trajectory is evaluated by the EA, and the trajectory (i.e. the network function parameter vector) is put back into the population of trajectories.

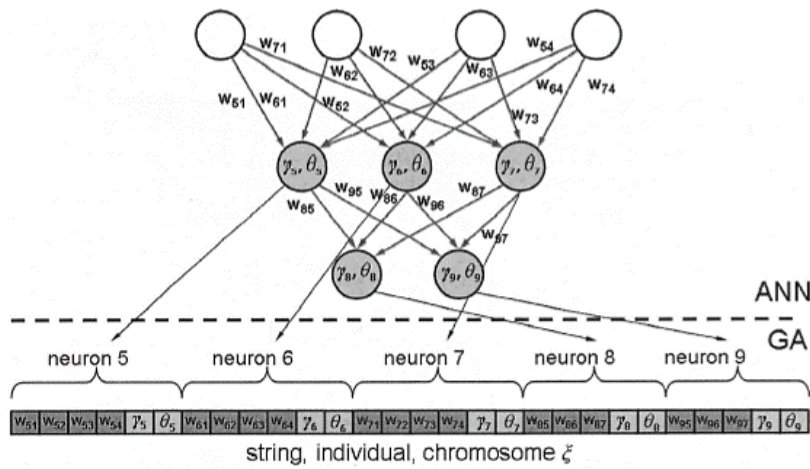


Fig. 3-3: An EA individual consisting of ANN parameters. w_{ij} – neurons’ weight factors, γ_i and θ_i – neurons’ transfer function parameters. Adapted from [20].

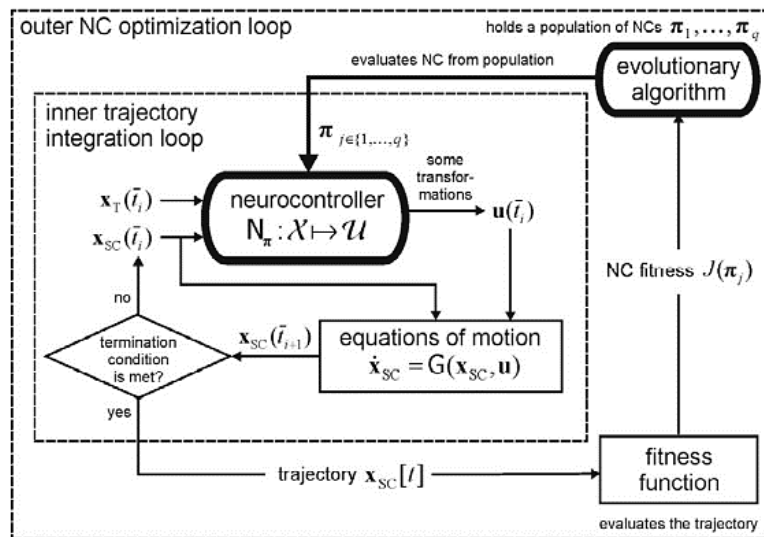


Fig. 3-4: InTrance Functionality Layout. Adapted from [37]

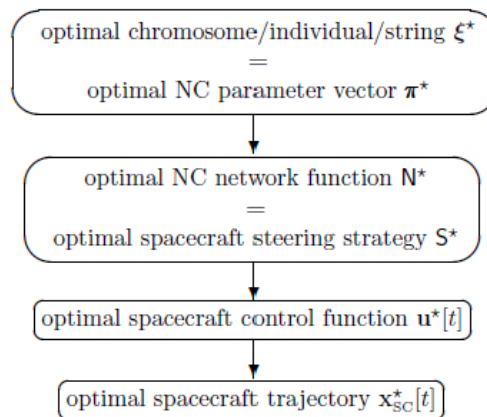


Fig. 3-5: Finding optimal trajectory from an EA individual using a neurocontroller. Adapted from [37]

Then, in the outer loop the EA advances the population through the evolutionary operators to derive a new generation of individuals. Individuals from the new population are then forwarded again into the NC (the inner loop). This iterative process continues until some predefined optimality condition for the entire trajectory is met, or the number of generations exceeds a predefined value.

The entire ENC process of finding an optimal trajectory from an individual (or chromosome) holding an ANN's parameter vector is illustrated in Fig. 3-5.

3.1.3 Extension to a Multiphase Non-Heliocentric Framework

The two major modifications that Ohndorf introduced to InTrance were the support of non-heliocentric low-thrust transfers and the inclusion of a multiphase framework [20].

3.1.3.1 Non-Heliocentric Transfers

In its original version InTrance was limited to calculations of heliocentric deep-space transfers. This meant that certain external perturbations which are irrelevant to deep-space missions, such as third body perturbations or J2 effects have been neglected. Also, certain assumptions have been made, for instance, that all trajectories are approximately equatorial and coplanar transfers, since all planets in the solar system are constrained to within 7 degrees of the ecliptic plane.

While these assumptions and restrictions are acceptable for most deep-space missions they may become unreasonable in the context of planetocentric orbits. Therefore, Ohndorf's extension added to InTrance consideration of such perturbations as J2 effect, third-body as well as orbital eclipse periods to account for the part of the orbit when the S/C is shaded by the central gravitational body. This last consideration is important for the use of SEP, especially in LEO orbits, since during eclipse periods the thruster's power generation sub-system is disabled.

3.1.3.2 Multiphase Transfers

Multiphase transfers refer to transfer trajectories comprised of multiple flight legs. These flight legs can be either thrust arcs or coast arcs, in which no thrust is applied. The break-down to flight legs, or mission phases, is done by the trajectory designer according to mission objectives. For instance, if a deep-space mission includes an asteroid fly-by, one mission phase could be the transfer from Earth to the asteroid, and a second mission phase could be the transfer from the asteroid to a third celestial body. However, if the transfer between Earth and the asteroid includes both thrust arcs and coast arcs, each of these could be considered as an additional mission phase. In the context of Earth-bound transfer trajectories for OOS, a mission phase would refer to a transfer of the servicer from its initial orbit (i.e. injection orbit, Depot orbit, current client's orbit) to the target's orbit.

In the multiphase framework in InTrance, each phase is simulated as a C++ simulation object. Fig. 3-6 illustrates schematically a multiphase mission consisting of 3 mission phases. The information of all the mission phases is encoded on the same candidate solution (i.e. chromosome) ξ . This information includes launch and arrival date, initial and final state and spacecraft or propellant mass of each phase. The initial and final conditions may be given as ranges instead of fixed values to facilitate optimization.

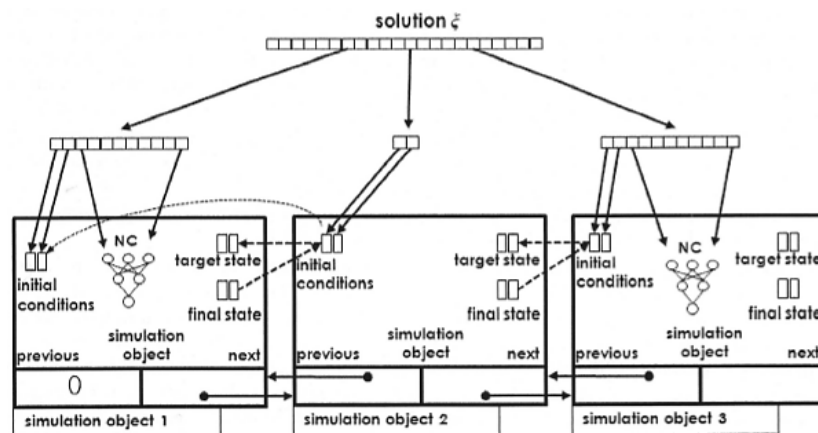


Fig. 3-6: InTrance Multiphase Framework. Adapted from [20]

While this feature allows exploring a larger design space of each phase and optimizing transition condition between phases, it also means that continuity between consecutive phases is not necessarily guaranteed. Therefore, a mechanism for guaranteeing such continuity conditions between phases is required. In Fig. 3-6 the first and last mission phases describe thrust arcs, as they include an NC which modifies the thrust vector, whereas the second phase corresponds to a coast arc. The figure highlights the bilateral interconnectivity of consecutive phases as the final state of phase i is taken as the initial state of phase $i+1$, while the initial state of phase $i+1$ is fed backwards to the final state of phase i . The optimization process done on the entire chromosome ξ ensures that the difference between the final state of phase i and initial state $i+1$ will be minimized. When this difference falls under a user-defined value, the transition is considered to be continuous and physically valid.

The added capability of InTrance to optimize individual mission phases could also facilitate the optimization of certain spacecraft design parameters, such as structure mass, propellant mass, fuel tanks mass and power supply systems.

In the prospect of OOS mission design the multiphase feature of InTrance could be beneficial by allowing the optimization of spacecraft mass and transition conditions between phases. For instance, if a maximum time limit is given for an entire multi-target OOS mission, a certain dwell time of the servicer between transitions might help minimizing fuel consumption, if this dwell time results in a more favorable constellation between the servicer and the next target, as long as the maximal entire mission time constraint is not exceeded. The multiphase feature of InTrance could help identifying such transit conditions. However, since this work is not concerned with the actual optimization of a specific mission, but rather with the identification of feasible scenarios the multiphase feature was not applied to the simulation in this work. Instead, every phase was simulated separately with manual adjustment of the transition conditions to guarantee continuity. For further discussion of the multiphase framework the reader is referred to [20].

3.2 Coplanar Low-Thrust Multi-Target Analysis Tool (Matlab)

3.2.1 General Description

One deficiency of InTrance, that has been encountered during the simulation of Scenario 1 was its inability to compute so-called “vector-rendezvous” maneuvers, in which ALL of the orbital elements of two spacecraft should be matched, including the true anomaly.

For the LEO-LEO scenario vector-rendezvous maneuvers were not of great importance, since the phasing maneuver required to match the true anomaly within the orbit takes typically only a small fraction of the entire transfer time between the two orbits. However, phasing maneuvers do become central for the GTO-GEO and LEO-GEO scenarios, since here all of the orbital elements of the client satellites and the servicer, after it reaches GEO, are the same, except for the true anomaly. Fortunately, there exists an analytical optimal solution for a low-thrust transfer between two coplanar spacecraft. This analytical solution is given by Equation (3-1) in terms of minimal transfer time between two coplanar circular orbits [26].

$$t_f = \frac{m_0}{\dot{m}_p} \left[1 - \exp\left(\frac{v_{out} - v_{in}}{v_*}\right) \right] \quad (3-1)$$

where, m_0 is the servicer’s mass in [kg], \dot{m}_p is the propellant mass flow rate in [kg/sec], v_{out} and v_{in} are the circular orbital velocity of the outer and inner orbits in [m/sec], respectively, and v_* is the thruster’s effective exhaust velocity in [m/sec]. Therefore, using InTrance was not necessary for the simulation of Scenarios 2 and 3, but instead a Matlab tool was developed, making use of Equation (3-1).

3.2.2 Assumptions and Restrictions

- Initial and final orbits have the same inclination.
- The S/C has a constant thrust, $F = const$
- The S/C has a constant mass flow rate, $\dot{m}_p = const$
- Thrust is applied continuously in the direction of orbital motion.
- No external perturbations act on the S/C.

3.2.3 Functional Description

Phasing, or relocation, of a S/C in a given orbit can be done in one of two ways; the S/C can be transferred to a higher/lower orbit where it will remain, drifting w.r.t the original orbit until the phasing angle reaches the value, at which the S/C could return to its original orbit with a zero phase angle. This transfer will be referred to as a “loiter transfer” in this work. Alternatively, another type of low-thrust transfer, which will be referred to as a “direct transfer”, is described in the work done by King et al in [33] (cf. Subsection 2.1.4). First, the change in phase angle resulting from the transfer of the S/C to a different orbit is calculated by,

$$\Delta\theta = \int_0^{t_f} (\dot{\theta}_0 - \dot{\theta}) dt \quad (3-2)$$

where, t_f is the transfer time in [sec] given by Equation (3-1), $\dot{\theta}_0$ is the constant mean motion of the initial orbit in [rad/sec] and $\dot{\theta}$ is the instantaneous mean motion in [rad/sec]. Then, the loiter time of the S/C in the target orbit could be calculated from,

$$t_{loiter} = \frac{\theta_{loiter}}{\dot{\theta}_0 - \dot{\theta}_f} \quad (3-3)$$

where, θ_{loiter} is the remaining angular difference in [rad] to be closed in the drifting orbit calculated from $\theta_{loiter} = \Delta\theta_{req} - 2\Delta\theta$, where $\Delta\theta_{req}$ is the required phasing angle in [rad]. $\dot{\theta}_f$ is the mean motion at the final orbit in [rad/sec].

In order to expedite the transfer and avoid the drifting time, the S/C could be transferred to an orbit at which the loiter time would be equal to zero, meaning that the S/C would spend half the transfer time moving to that orbit and half the time returning to the initial orbit. This is an iterative process, in which the altitude of the final orbit is incrementally changed in each iteration until an altitude is reached, in which t_{loiter} is sufficiently small (say, smaller than 10^{-6} sec).

Target Selection:

In order to select to which target the servicer should transfer, the transfer time between the initial orbit and final orbit is calculated with Equation (3-1). This could be relevant, for instance, in Subsection 2.2.1 (satellite removal from GEO) for selecting to which client to transfer when the servicer is at a specific AN in the graveyard orbit, or in the other direction, when the servicer is at a specific client location in GEO and has to decide to which AN in GYO the client should be brought.

After the transfer time of the servicer from its original orbit to its target orbit has been calculated, the exact arrival longitude of the servicer in its target orbit can be computed by integrating the servicer’s longitudinal drift rate (which is a function of altitude) throughout the transfer.

Once the servicer’s longitudinal position in the target orbit is established, selecting the target satellite to be rendezvoused with is achieved by looking for the satellite that is closest in longitude to that of the servicer. Fig. 3-7 shows this process schematically for an exemplary transfer from an initial orbit above GEO (e.g. GYO in subsection 2.2.1 or Depot orbit in Subsection 2.2.2) to the GEO orbit:

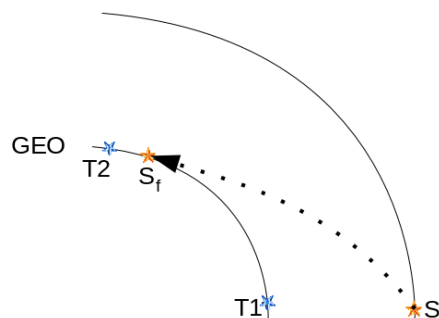


Fig. 3-7: Target rendezvous selection

The servicer starts at the initial orbit in point S_i . During the transfer, as it lowers its altitude towards the GEO, both its longitude and its longitudinal drift-rate change continuously. Upon arriving at the GEO orbit, at point S_r , the servicer finds itself closer to target T2 than target T1, and therefore, in this case, target T2 will be the selected target to be rendezvoused with.

Next, to adjust the servicer's exact longitudinal position to match that of the selected target client satellite two options exist, either a direct transfer or a loiter transfer.

However, let's assume without loss of generality that the servicer is already coming from a higher orbit. In case a loiter transfer is required since the target satellite is ahead of the servicer (which can be calculated before the maneuver actually takes place) then instead of reaching the GEO orbit and then correcting the longitudinal gap by going again upwards, the servicer could wait for the required time in the higher orbit, such that when it comes down to GEO it will already have the same longitude as the intended client. This is of course analogous in the other direction, in case the servicer should move **from** GEO **to** a higher orbit and the target satellite is **behind** the servicer.

Transfer between Clients

For sub-scenario 2.2: GEO refueling (Subsection 2.2.2) the only difference is, that when transferring between clients both the initial and final orbits are the same, namely GEO. That means that saving up fuel by waiting in the initial orbit, which is possible for transfer from/to GEO to/from a different orbit is no longer possible here. Therefore, depending on the relative location of the next client w.r.t the current client being served (i.e. ahead or behind current client w.r.t direction of motion) a maneuver for either increasing the semi-major axis or decreasing it will have to be performed.

Since the clients for each sortie are randomly sampled from a true database of operational satellites in GEO, it cannot be assumed that they are evenly distributed around the GEO belt, and therefore, before each transfer the next client would have to be selected by comparing the angular difference between the current client and both the next closest client ahead of the current client and the next closest client behind the current one. The client with the smallest longitudinal difference would be selected as the next one to be serviced.

3.2.4 Program Modules

Based on the two types of phasing transfers described in the previous subsection (i.e. loiter transfer and direct transfer) different coplanar low-thrust transfer scenarios can be simulated. Presented below are three modules of the tool that were configured to simulate the 2nd and 3rd scenarios described in Sections 2.2 and 0, respectively. File names and code snippets are written in `Courier New` font. File names refer to Matlab code scripts, functions and text files that can be found in the supplemental material.

3.2.4.1 Multi-Target GTO-GEO Satellite Removal Module

Subsection 2.2.1 described a mission for the removal of decommissioned satellites from GEO to a graveyard orbit. For the purpose of the investigation of this mission the Matlab tool has been configured to compute the total mission time and total required propellant mass for the given scenario.

Main function: `GEO_transfer.m`

Input Files and Configuration:

Following input parameters should be provided to the program:

- Spacecraft configuration file named `spacecraft.txt` and including (see Appendix B):
 - Specific impulse in seconds (I_{sp})
 - Input power in W (Power)
 - Servicer mass in kg (servicer)
 - Client mass in kg (clinet)
 - Propellant mass in kg (mp)
 - Thruster efficiency (η)
- Number of Assembly Nodes (n_{AN} – to be adjusted in the code)
- Number of Client satellites (n_{CL} – to be adjusted in the code)
- Servicing duration in days (s_T – to be adjusted in the code)

The last three configuration parameters should be adjusted in the main function in the designated place at the beginning of the code.

Module Structure:

Fig. 3-8 shows schematically the algorithmic logic of the multi-target GTO-GEO satellite removal module. After initialization of the simulation parameters the program can flow in one of two directions depending on the direction of the transfer. The transfer direction is obviously alternating, since the servicer is intended to bring a client from GEO to GYO and then return directly back to GEO for the next client. Therefore, in case the servicer is transferring from GEO to GYO, first an additional mass of the client satellite is assumed for the transfer. Otherwise, for the GYO-GEO direction, the servicer is assumed to rid of the client satellite in one of the ANs, hence only the servicer's mass is assumed for the transfer. Next, both flow directions go through the same steps of selection of the next target to rendezvous with, as described in Subsection 3.2.3. Once the next target has been selected, the type of maneuver is identified and the required maneuver time and propellant mass is calculated. The transfer is assumed to once the calculated propellant mass has been removed from the servicer's mass. The program ends when all the clients have been serviced and brought to GYO.

An additional and optional outer loop for analysis can be added for post-simulation analysis (main function: `GYO_transfer_OPT.m`). Here, the amount of time dedicated for servicing can be increased in order to search for better results. Note, that the additional time allocated for servicing is not intended for actual operations of the servicer on its target, but this is just additional time that the servicer would spend drifting in the vicinity of its target, after completing its servicing operations. At first glance, this might sound counter-intuitive since adding more time for servicing should increase the total mission time. However, since this is a dynamic problem, increasing the servicing time could result in a more favorable constellation between the servicer and its targets leading to an overall shorter mission time and potentially even less propellant mass consumption (see Chapter 4).

The outer loop has also an optimization capability for identifying optimal servicing duration in terms of total mission time and propellant mass. To this end the following optimality condition is applied:

$$J = w_{m_p} \frac{m_p^n}{\max\{m_p^n\}} + w_{t_m} \frac{t_m^n}{\max\{t_m^n\}} + w_{t_{srv}} \frac{t_{srv}^n}{\max\{t_{srv}^n\}} \quad (3-4)$$

where, J is the objective function to be minimized, w_{m_p} , w_{t_m} and $w_{t_{srv}}$ are weight factors for the propellant mass, total mission time and servicing time, respectively. m_p^n is the total propellant mass of the nth simulation run, t_m^n is the total mission time of the nth simulation run and t_{srv}^n is the servicing time in the nth simulation run. The minimal value of J corresponds to the optimal servicing time. The weight factors could be adjusted to account for different mission objectives and the impact of total propellant mass on the mission compared to the impact of total mission time.

Output Files:

The inner calculation loop generates information relating to the last transfer that has been carried out by the servicer(see Appendix C1). The data is saved to an output file, named `output_AAacBBn.txt`, where AA is the total number of the clients in the simulation and BB is the total number of assemble nodes. This file contains following information:

- Simulation initial configuration
 - Servicing duration in days
 - Number of clients and their respective locations
 - Number of ANs and their respective locations
- Transfer information
 - Transfer number
 - Servicer initial orbit and location in current transfer
 - Chosen target for current transfer
 - Transfer type: Direct or Loiter
 - Servicer final longitudinal position at target orbit (after transfer and before servicing)
 - Maneuver time:
 - For direct transfers this is the time needed for adjusting the servicer's longitude to match that of the target
 - For loiter transfer this is the loiter time
 - Transfer time = Maneuver time + transfer time between the two orbits + servicing time
 - Mission Elapsed Time (MET)
 - Propellant mass used for current transfer
 - Propellant mass used since beginning of mission
- Total mission time for all transfers
- Total used propellant mass for all transfers

If the Analysis/Optimization loop is also utilized the following output data is generated:

- A graph showing total mission time and total required propellant mass as function of servicing time with the optimal value for servicing time
- A graph of the objective function J as function of the servicing time and the optimal value of the servicing time

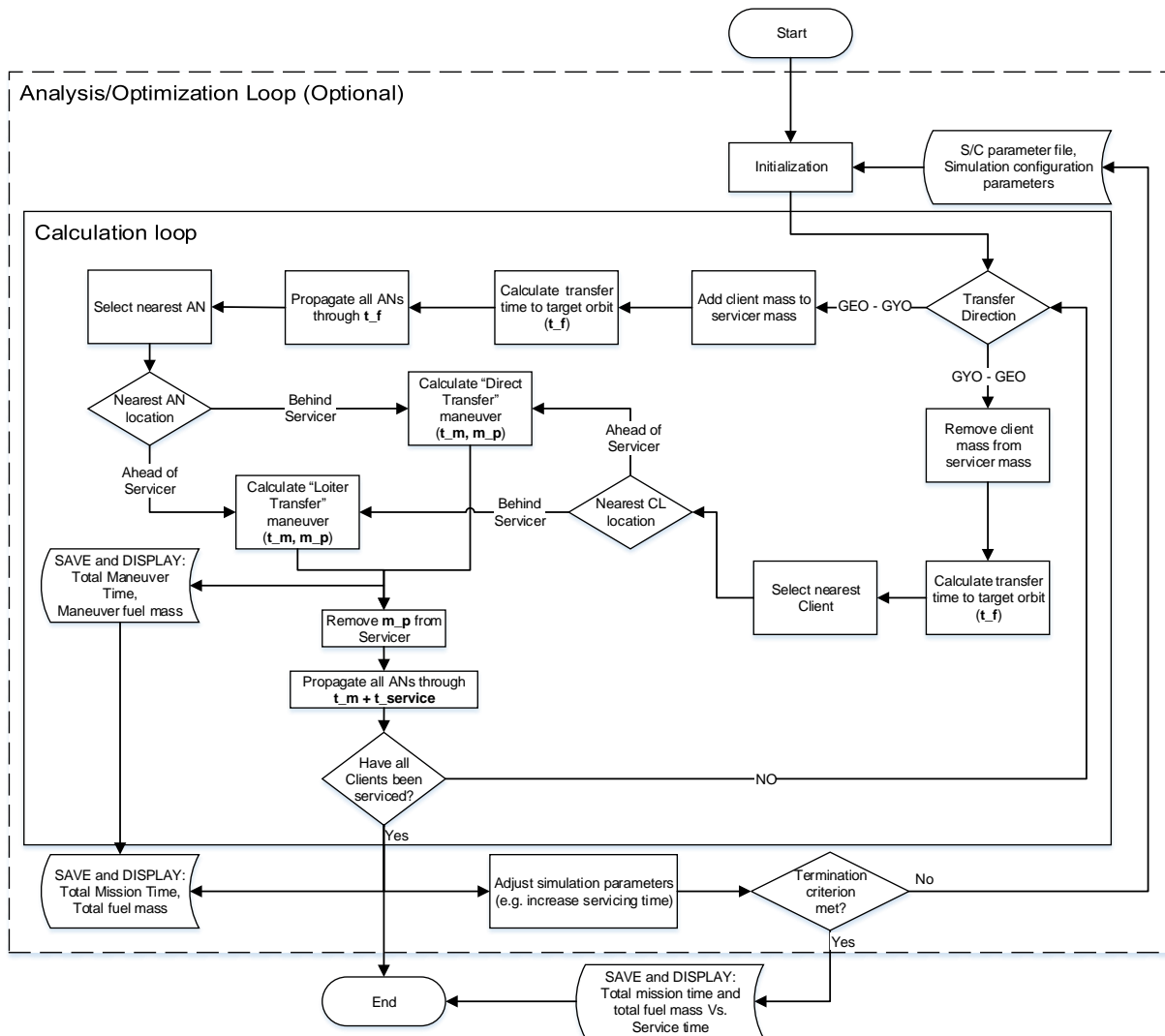


Fig. 3-8: GEO satellite removal program structure

3.2.4.2 Multi-Target GTO-GEO Satellite Refueling Module

This module investigates the GEO refueling sub-scenario described in Subsection 2.2.2.

Main function: `GEO_refueling.m`

Input Files and Configuration:

Following input parameters should be provided to the program:

- Spacecraft configuration file named `spacecraft.txt` and including (see Appendix B):
 - Specific impulse in seconds (I_{sp})
 - Input power in W (Power)
 - Servicer dry mass in kg (servicer)
 - Propellant mass for one client in kg (client)
 - Propellant mass for servicer in kg (m_p)
 - Thruster efficiency (η_{ta})

- Refined GEO satellite database file named `GEO_SAT_DB.xlsx`
- Number of Client satellites (`nCL` – to be adjusted in the code)
- Depot station longitudinal location in deg (`DL` – to be adjusted in the code)
- Servicing duration in days (`sT` – to be adjusted in the code)
- Number of simulation runs (`runs` – to be adjusted in the code)

The last four configuration parameters should be adjusted in-code in the main function in the designated place at the beginning of the code.

Module Structure:

Fig. 3-9 shows schematically the algorithmic logic of the multi-target GTO-GEO satellite refueling module. The program assumes the mission begins at the Depot station's orbit where both the servicer and the Depot are located. After initialization of the simulation parameters using the S/C input file, the client satellite database and the user defined in-code parameters, the calculation loop begins. The servicer removes fuel from Depot enough to refuel 6 client satellites. Next, the first client to be serviced is selected according to the process described in Subsection 3.2.3. and the transfer to that client is calculated. The service of the first client is assumed to be complete after the servicer has reached the client's location in GEO and has transferred fuel to that client. Following that, the servicer again selects the next client to be serviced and transfers to that client. This loop continues until all 6 clients of that sortie have been refueled. The blue arrows in Fig. 3-9 represent the GEO-GEO transfer loop between clients. After all clients have been serviced, the servicer needs to replenish its fuel supply for additional clients as well as its own fuel supply. To that end, first the Depot location is propagated throughout the entire time the servicer has spent on the sortie to find the Depot current location in its orbit. Then, the type of maneuver to the Depot orbit is selected accordingly. Finally, the transfer time and propellant mass of that transfer is calculated, the masses of fuel for both 6 additional clients and the servicer itself are transferred from the Depot to the servicer, and the next sortie begins. After all sorties have been carried out, and the Depot reservoir of clients' fuel has been depleted the mission ends.

An additional and optional outer loop for analysis can be added for post-simulation analysis. This loop enables multiple runs of the simulation to be carried out successively, saving each simulation output to a different file. Since the client satellites are randomly sampled from a database, each run will use a different set of clients, leading to different results. In addition, the values of total mission time of all runs are saved to a separate `t_tot_sum.csv` file and the total used propellant mass of the entire mission of all runs are saved to a separate `mp_sum.csv` file. This allows post-simulation analysis of this sub-scenario. An in-code parameter (called `runs`) controls the number of simulation runs will be carried out. By setting this parameter to 1 the outer analysis loop can be switched off.

Output Files:

The inner calculation loop generates information relating to the last transfer that has been carried out in the current sortie (see Appendix C2). The data is saved to an output file, named `outputXX.txt`, where `XX` is a serial number of the current simulation run.

This file contains following information:

- Simulation initial configuration:
 - Servicing duration in days
 - Depot station initial total mass in kg
- Sortie information:
 - Sortie number
 - Client locations for current sortie
 - Transfers information:
 - Information relating to the first transfer from Depot station to first client in GEO:
 - Depot location at beginning of transfer
 - Depot mass at beginning of transfer (after servicer have been equipped with fuel for 6 clients)
 - Initial servicer mass
 - Chosen first client in GEO (identifier number and longitude)
 - Maneuver type
 - Maneuver transfer time
 - MET
 - Used propellant for maneuver
 - Transfers between clients:
 - Current client (identifier number and longitude)
 - Chosen next client (identifier number and longitude)
 - Maneuver transfer time
 - Maneuver direction; either Clockwise (CW) which is taken as positive direction or Counterclockwise (CCW) which is taken as negative direction.
 - Duration of spiraling upwards/downwards
 - Duration of spiraling downwards/upwards
 - MET
 - Used propellant for maneuver
- Total mission time of all transfers
- Total used propellant mass for all transfers
- Final Depot mass

If the Analysis loop is also utilized the following output data is additionally generated:

- A `t_tot_sum.csv` file, including all total mission times (in days) of all simulation runs.
- An `mp_sum.csv` file, including all total required propellant masses of all runs.

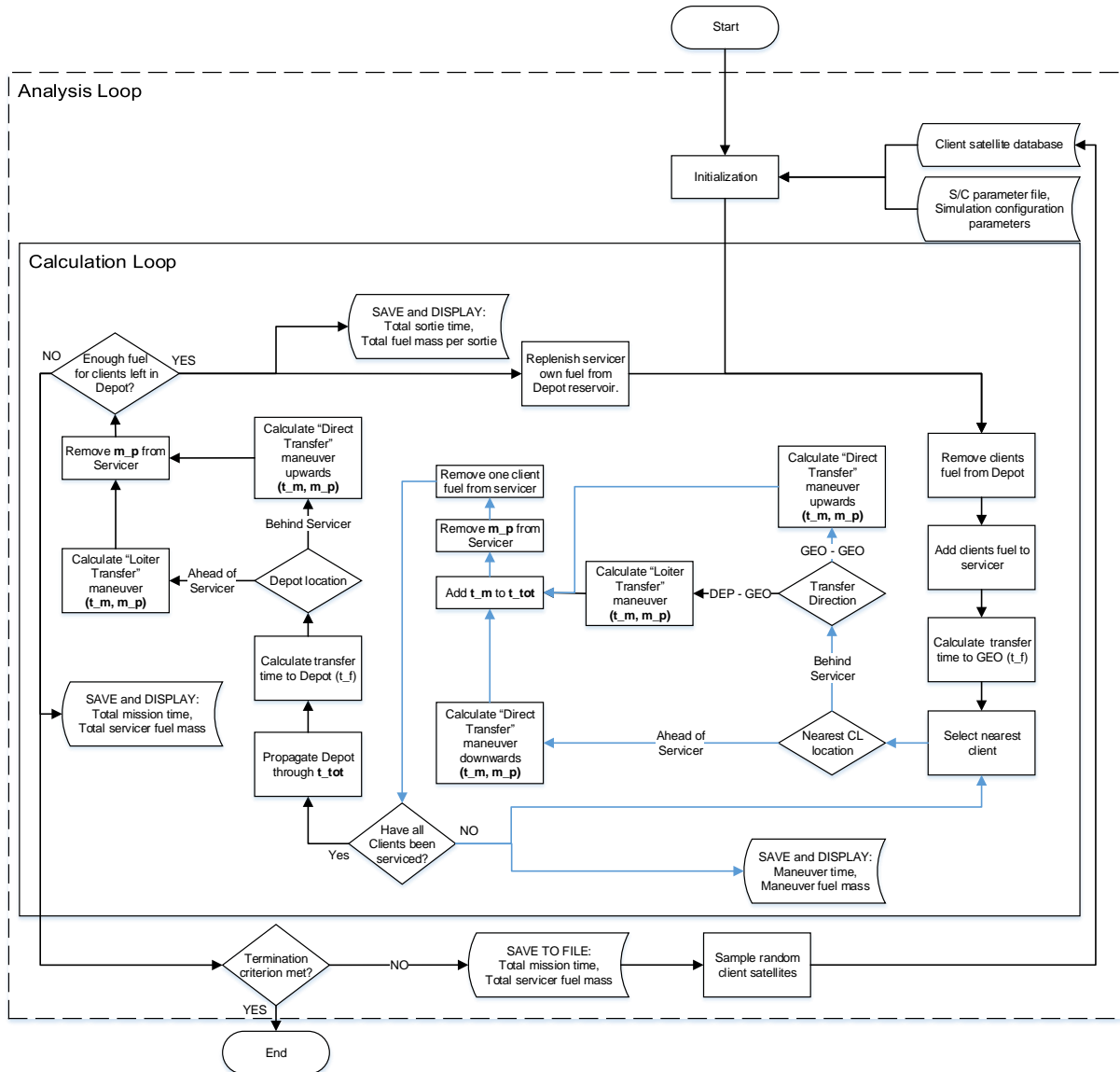


Fig. 3-9: GEO satellite refueling program structure

3.2.4.3 Multi-Target LEO-GEO Satellite Repair Module

This module investigates the LEO-GEO satellite repair scenario described in subsection 2.3. It is designed similar to the GEO refueling module described in the previous subsection. The only difference is in the implementation of this module which is described in Section 4.3.

3.2.5 Program Validation

In order to validate the code and verify its functionality an external open-source program for space mission analysis has been used. The program, which is called General Mission Analysis Tool (GMAT), was developed by a team of NASA, private industry, and public and private contributors [40]. The validation process involved configuring a mission simulation in GMAT with similar design parameters to those that were used in the Matlab tool. The results acquired from GMAT were then compared

to the Matlab results both quantitatively and qualitatively. The following scenario, corresponding to sub-scenario 2.1 (cf. Subsection 2.2.1), has been simulated both in the Matlab tool and in GMAT:

Number of assembly nodes: 16, evenly distributed
 Number of clients: 10, evenly distributed
 Spacecraft design: as described in Subsection 2.2.1.
 External perturbations: None
 Propellant mass: 57kg (included in the servicer total mass of 2000 kg)

First, the simulation has been run in Matlab and the details and characteristics of each transfer have been calculated. A snippet of the output file for the 3rd – 5th transfers are given below:

```

=====
Transfer 3:

Servicer initial orbit: GEO
Servicer initial location: 324.000 deg
Chosen target: AN #3 ( 45.000 deg)(320.810 deg)
Transfer type: direct
Direct transfer 1/2 transfer time: 91169.013 sec
Servicer final orbit: Graveyard
Servicer final location: 316.654 deg
Maneuver time: 2.110 days (182338.027 sec)
Transfer time: 10.045 days (867853.194 sec)
MET: 28.970 days (2503020.615 sec)
Transfer propellant mass: 6.946 kg
Used propellant mass: 18.183 kg
=====
=====
=====
Transfer 4:

Servicer initial orbit: Graveyard
Servicer initial location: 276.127 deg
Chosen target: CL #9 (288.000 deg)
Transfer type: direct
Direct transfer 1/2 transfer time: 120937.152 sec
Servicer final orbit: GEO
Servicer final location: 288.000 deg
Maneuver time: 2.799 days (241874.304 sec)
Transfer time: 10.460 days (903727.156 sec)
MET: 39.430 days (3406747.771 sec)
Transfer propellant mass: 7.893 kg
Used propellant mass: 26.077 kg
=====
=====
=====
Transfer 5:

Servicer initial orbit: GEO
Servicer initial location: 288.000 deg
Chosen target: AN #6 (112.500 deg)(297.096 deg)
    
```

```

Transfer type: loiter
Servicer final orbit: Graveyard
Servicer final location: 292.962 deg
Maneuver time:    1.847 days (159576.711 sec)
Transfer time:    9.776 days (844664.678 sec)
MET:    49.206 days (4251412.448 sec)
Transfer propellant mass:    2.120 kg
Used propellant mass:    28.197 kg
=====
=====

```

As can be seen, transfers 3 and 4 are of type Direct transfer, whereas transfer 5 is a loiter transfer. Each transfer block gives information about the current servicer's location (orbit and longitude) and the chosen next target.

Next, the information from the Matlab simulation was configured in GMAT accordingly. Fig. 3-10 shows the corresponding GMAT configuration of the aforementioned simulation, where the transfers given in the output snippet above are marked by red frames.

A direct transfer is marked by the transfer number followed by "(D)". The transfer begins by propagating the servicer from its initial orbit to its final orbit (GEO-GYO in Transfer #3 or GYO-GEO in Transfer #4). The termination condition of this mission segment is given as the SMA of the target orbit. Next, the relocation of the servicer to the exact longitude of the target is configured. To this end, the servicer is first propagated in one direction, either upwards as in Transfer #3 or downwards as in Transfer #4 depending on the corresponding origin orbit. The termination condition for this mission segment is given as a flight time equal to the value of "Direct transfer 1/2 transfer time" as calculated in Matlab. Once the termination condition is met the thrust direction is reversed and the servicer is propelled in the opposite direction, with the same termination condition of flight time equal to 1/2 the transfer time of the direct transfer. Spiraling outwards in one direction and then inwards in the other direction in equal times should bring the servicer to the required end longitude in the target orbit.

A loiter transfer is marked by the transfer number followed by "(L)". The transfer begins by propagating the servicer to a drift orbit 50 km above the initial orbit, if the initial orbit is GEO and 50 km below GYO if the initial orbit is GYO. The termination condition of this mission segment is given as the SMA of the drift orbit. Next, the required loiter time, as calculated in Matlab, is given as a flight-time termination condition of the following mission segment. Lastly, the servicer is propagated from the drift orbit to its target orbit, and the target orbit SMA is given as the termination condition. By transferring the servicer to a drift orbit and letting it wait there for a certain loiter time, and then bringing it to its target orbit should bring the servicer to the exact required longitude in the target orbit.

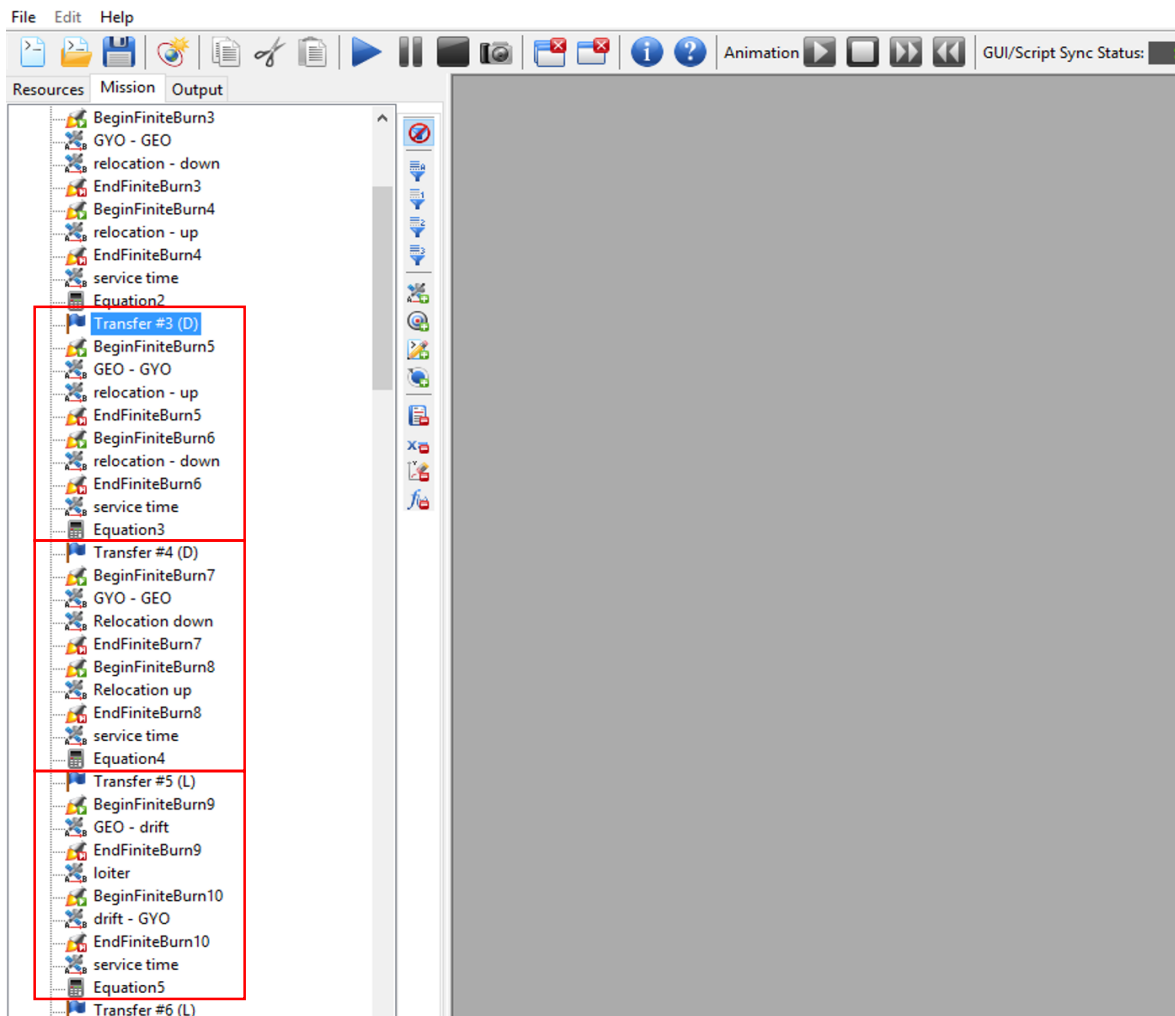


Fig. 3-10: GMAT mission configuration

In each transfer, after the servicer reaches its designated target, an additional mission segment is added to account for the servicing time. A transfers finally ends with the update of the servicer mass indicated in Fig. 3-10 by the line “EquationX” after “service time”. The servicer mass is increased by the mass of one client satellite if the transfer ends in GEO, and it is decreased by the mass of one client if the transfer ends in GYO.

Consequently, the accuracy of the Matlab results was compared to the results from GMAT in terms of the total propellant mass consumption, end longitude of each transfer and the total transfer time.

Fig. 3-11 shows the results of the GMAT simulation for servicer longitude as function of mission elapsed time in seconds. The servicer longitude is displayed as the red line. The horizontal lines are the constant longitudes of the 10 clients and the inclined lines are the drifting longitudes of the assembly nodes. The x-marks in the plot represent the beginning of a transfer. Fig. 3-11 illustrates how the servicer alternately transfers between ANs and clients. This alternation as well as the type of transfer are further emphasized in Fig. 3-12. The servicer is again designated by the red line, GYO is the green line and GEO is marked as the blue line. The direct transfers are identified in the figure as the “spikey” transfers, in which the servicer has to increase its altitude above GYO or decrease it beneath GEO, depending on the transfer direction. The loiter

transfers are identified as the transfers, in which the servicer remains for a certain duration in an intermediate altitude between GEO and GYO.

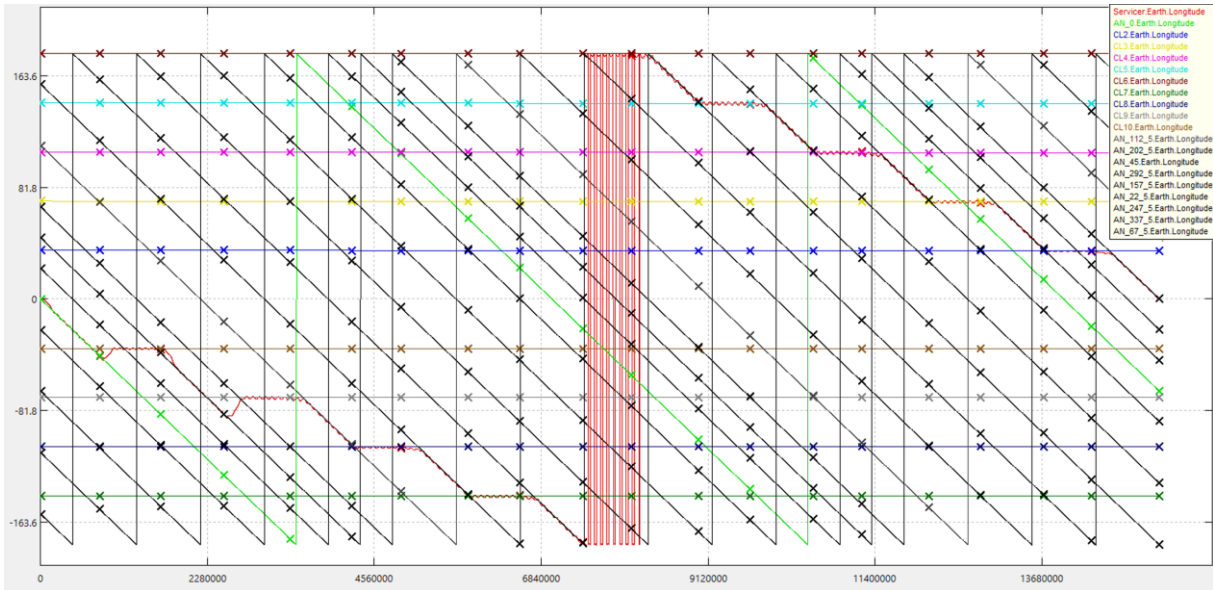


Fig. 3-11: GMAT results: Servicer longitude in deg vs. MET in sec

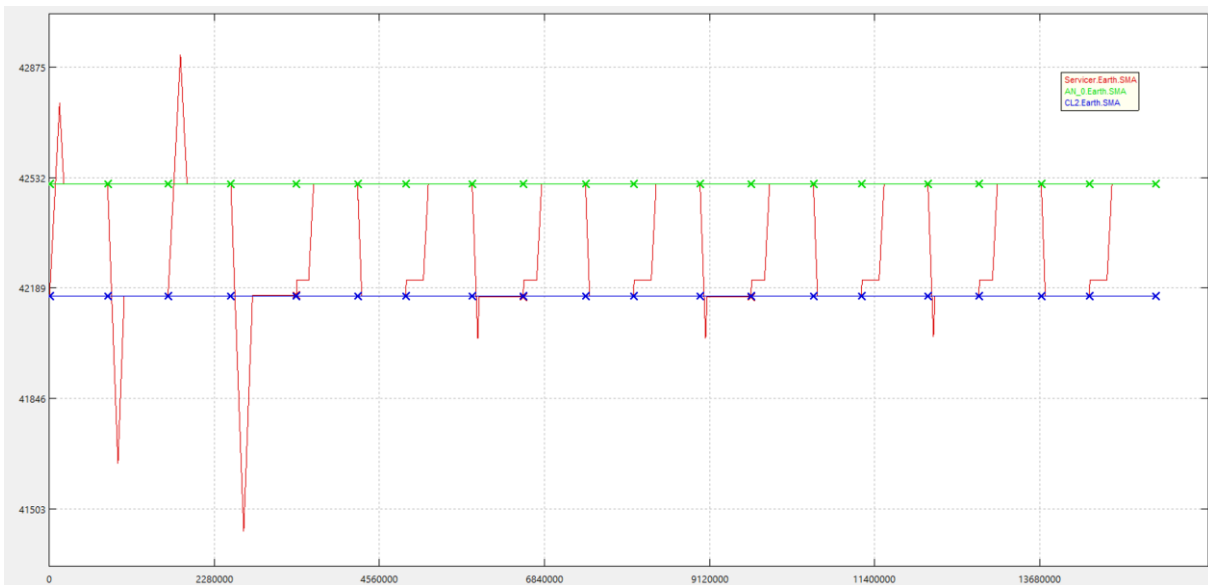


Fig. 3-12: GMAT results: Servicer altitude in km vs. MET in sec



Tab. 3-2 gives the end longitude of the servicer in each transfer, i.e. the longitude of the servicer in the target orbit after inclusion of the servicing time. The table compares results acquired in Matlab to those obtained from GMAT. The averaged absolute difference in longitude between GMAT and the Matlab tool is approximately 0.7° .

Tab. 3-2: Longitude accuracy validation

Transfer	Matlab	GMAT	Absolute Difference
1	318.773°	318.202°	0.571°
2	324°	323.48°	0.52°
3	276.127°	275.77°	0.357°
4	288°	288.215°	0.215°
5	253.607°	252.442°	1.165°
6	252°	251.102°	0.898°
7	217.057°	217.286°	0.229°
8	216°	216.349°	0.349°
9	181.488°	181.938°	0.45°
10	180°	178.551°	1.449°
11	145.058°	144.958°	0.1°
12	144°	142.936°	1.064°
13	109.487°	109.084°	0.403°
14	108°	108.191°	0.191°
15	73.062°	71.618°	1.444°
16	72°	70.68°	1.32°
17	37.483°	36.055°	1.428°
18	36°	35.2°	0.8°
19	1.06°	0.805°	0.255°

Fig. 3-13 depicts fuel mass consumption of the servicer throughout the scenario. In the left figure, propellant mass consumption is illustrated as function of mission elapsed time. In the right figure the servicer total mass is shown in green and the servicer dry mass in red. The right figure also illustrates the added mass to the servicer after it docks with a client and transfers it to GYO, and the decrease in mass after it deposits the client in one of the assembly nodes. The total propellant mass consumed for the entire mission according to GMAT was 56.658 kg, whereas the Matlab calculation resulted in 56.668 kg, a relative difference of less than 0.02%.

In terms of total mission time, the GMAT simulation resulted in 176.7808 days, while the Matlab calculation gave a value of 176.787 days for the entire mission – an accuracy of more than 99.996%.

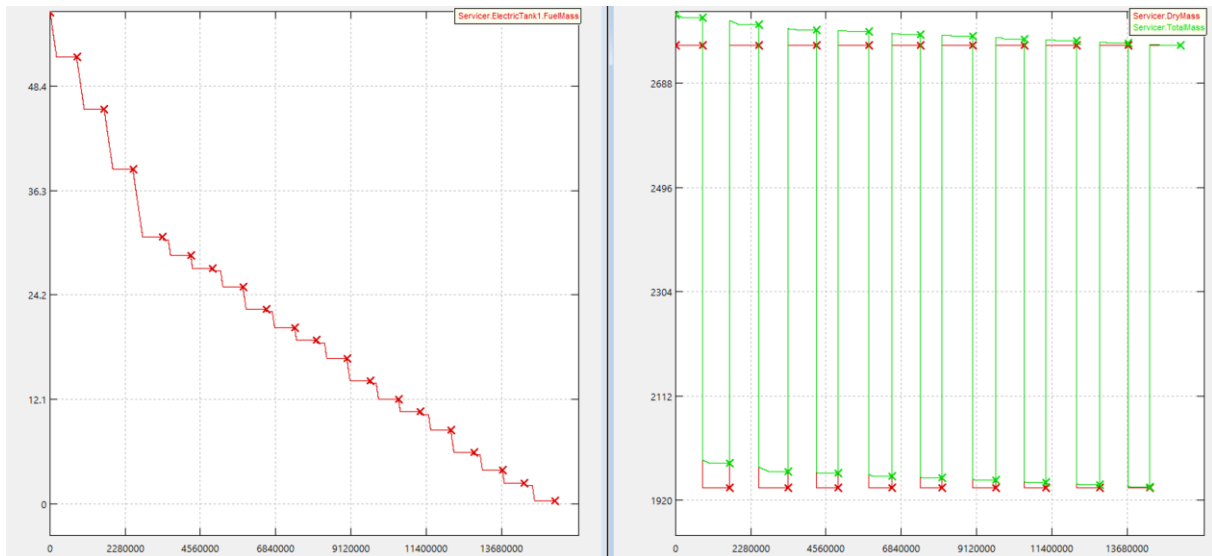


Fig. 3-13: GMAT results: Propellant mass consumption in kg vs MET in sec. Left – Propellant mass. Right – Servicer dry mass in red and total mass in green.

Similar validation tests were also carried out for sub-scenario 2.2 and similar results in terms of the accuracy of the Matlab code were found. This could be expected since there is no substantial difference between sub-scenario 2.1 and sub-scenario 2.2 in terms of the coding of the transfers. The difference is only in the application of the same transfers (i.e. direct transfers or loiter transfers) to different mission architectures including different number of clients. However, the major source of potential inaccuracies, which is the coding of the transfers themselves remains the same. Due to the similarity between Scenario 2 and Scenario 3, in terms of the design of the Matlab tool, no additional validation of Scenario 3 was needed.

Therefore, with the results presented above the Matlab tool is assumed validated.

4 Results and Discussion

This chapter presents the implementation of the scenarios described in Chapter 2, the results of the corresponding simulations and a consequent discussion of these results.

4.1 Scenario 1: LEO – LEO

Scenario 1 was entirely simulated with InTrance. As described in Section 2.1, this scenario begins with the servicer transferring from its injection orbit to the orbit of the first target. Then, it sequentially transfers between the rest of the targets. Each transfer is simulated in a separate simulation block. The first transfer is given the initial conditions of the mission. Then, the initial conditions of the simulation block of transfer $i+1$ are manually adjusted to match the final conditions of transfer i .

Each simulation block in InTrance includes, among other, the spacecraft configuration file, EA parameters file, NC parameter file and a simulation file including all of the simulation and environmental parameters and boundary conditions.

All simulations in InTrance are initiated with a so-called “coldstart” file which delivers a rudimentary first solution. The solution chromosome (which actually describes the entire transfer trajectory) can be later input to a second “warmstart” run that would result in a more accurate solution. Since at first, the search space for the global solution is very large and in order to reduce computation time, the coldstart-run typically uses a low-precision integration method like RUNGE-KUTTA-FEHLBERG 4(5) and a relatively lenient final condition for the relative distance and relative velocity of the servicer to the target [20]. In the warmstart-runs, once the search space has been localized and restricted to the vicinity of a potential global solution, more computationally expensive integrators and final conditions can be used in order to increase the ultimate solution’s accuracy.

In the results given below of the various transfers of scenario 1, the total computation run-time includes the run-time of both the coldstart runs and the subsequent warmstart runs, until the required relative distance accuracy and relative velocity accuracy have been reached.

4.1.1 Transfer 1: From Injection Orbit to Client #5

The first transfer of the mission is also the longest one, as it includes an increase of more than 400 km in altitude, a reduction of more than 3 deg in inclination as well as an increase in eccentricity from 0.001 to 0.004. Fig. 4-1 to Fig. 4-3 show this transfer from three different views. In Fig. 4-3 the initial and final orbit are indicated by red arrows. This figure clearly illustrates how the servicer starts from a lower and more inclined orbit and raises its altitude while reducing its inclination through many revolutions around the Earth. computed. Finally, using the output of the acquired solution, which gives the SMA, eccentricity and inclination angle of the servicer in each time step along the trajectory, the local RAAN drift rate is calculated in each time step, and the accumulated RAAN angle drift is found. Subtracting the accumulated RAAN drift from the final location of the Target’s RAAN angle gives the injection RAAN angle of the servicer.

Tab. 4-1 shows the orbital elements of both the servicer and the target at the beginning

and end of the transfer. The first line is computed. Finally, using the output of the acquired solution, which gives the SMA, eccentricity and inclination angle of the servicer in each time step along the trajectory, the local RAAN drift rate is calculated in each time step, and the accumulated RAAN angle drift is found. Subtracting the accumulated RAAN drift from the final location of the Target's RAAN angle gives the injection RAAN angle of the servicer.

Tab. 4-1 is identical to Tab. 2-2 and as explained in Subsection 2.2.1.1 the value for the servicer's initial RAAN angle is computed retroactively to match the target's RAAN angle by the end of the transfer. For the computation itself the J2 effect was not considered in order to expedite the computation, which can also be clearly seen in Fig. 4-1, Fig. 4-2 and Fig. 4-3. Once the total transfer time (without nodal drift consideration) has been calculated, the amount of nodal regression of the target during that time could be computed. Finally, using the output of the acquired solution, which gives the SMA, eccentricity and inclination angle of the servicer in each time step along the trajectory, the local RAAN drift rate is calculated in each time step, and the accumulated RAAN angle drift is found. Subtracting the accumulated RAAN drift from the final location of the Target's RAAN angle gives the injection RAAN angle of the servicer.

Tab. 4-1: Transfer 1 initial and final states

	a [km]	i [deg]	e	Ω [deg]	ω [deg]	ν [deg]
Servicer Initial state	6,878	87.3	0.001	54.29	0	0
Final state	7308	82.94	0.004	-30.89	N/A	N/A

Note, that since InTrance cannot calculate geocentric vector rendezvous transfers (cf. 3.2) the true anomaly angle (ν) is completely left out of the simulation. Instead, an additional dedicated time for phasing and servicing is added to the calculated transfer time. The row is computed. Finally, using the output of the acquired solution, which gives the SMA, eccentricity and inclination angle of the servicer in each time step along the trajectory, the local RAAN drift rate is calculated in each time step, and the accumulated RAAN angle drift is found. Subtracting the accumulated RAAN drift from the final location of the Target's RAAN angle gives the injection RAAN angle of the servicer.

Tab. 4-1 that corresponds to the Final state of the servicer includes 7 days for phasing and servicing. In addition, since the orbits are nearly circular, the argument of perigee (ω) is not considered here.

Transfer 1 final simulation results are as follows:

- Relative distance accuracy < 5 m
- Relative velocity accuracy < 8 m/s
- Total transfer time: 148 days (155 days including 7 days servicing time)
- Total propellant mass: 62.659 kg
- No. of Revolutions: 2173
- Total computation run-time: 284 hrs

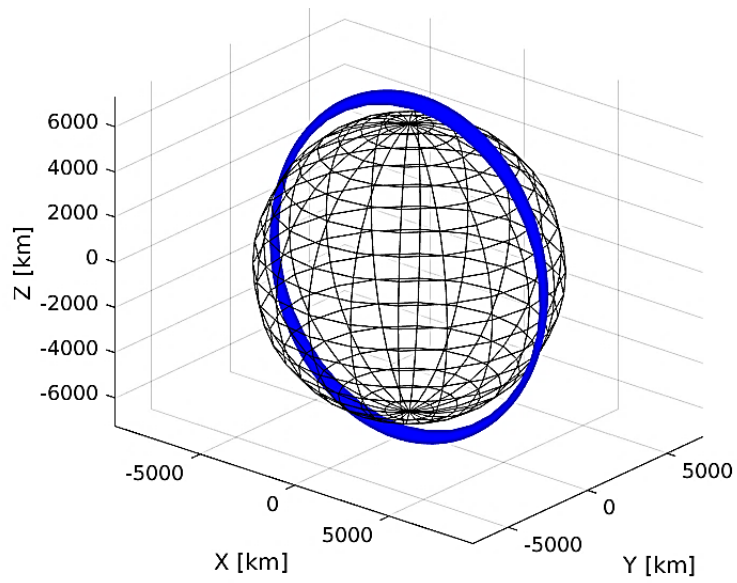


Fig. 4-1: Transfer 1 isometric projection

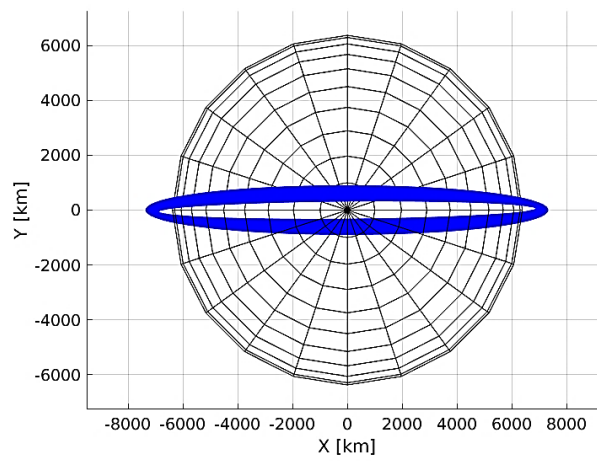


Fig. 4-2: Transfer 1 polar view

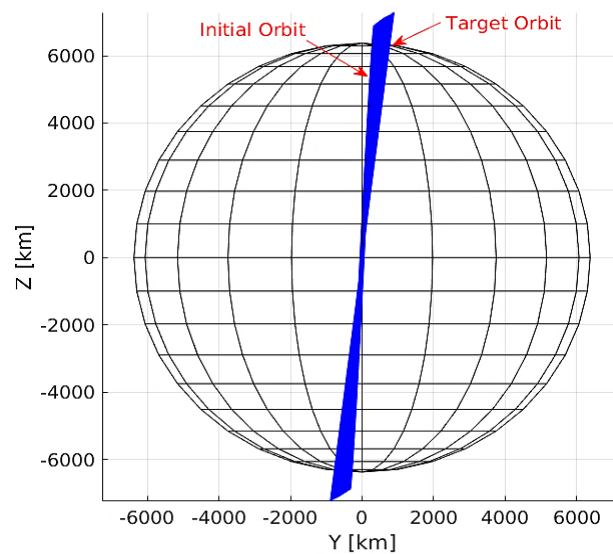


Fig. 4-3: Transfer 1 equatorial view

4.1.2 Transfer 2: From Client #5 to Client #1

Tab. 4-2 summarizes the orbital elements of both the servicer and the target at the beginning and end of transfer 2.

Tab. 4-2: Transfer 2 initial and final states

	a [km]	i [deg]	e	Ω [deg]	ω [deg]	ν [deg]
Servicer Initial state	7308	82.94	0.004	-30.89	N/A	N/A
Target Initial state	7349	82.94	0.003	-30.66	N/A	N/A
Final state	7349	82.94	0.003	-41.85	N/A	N/A

This transfer begins at the location of the first target (client #5) at the time after the servicer has finished servicing it. Unlike the first transfer, in this and all the subsequent transfers, the initial RAAN angle cannot be chosen freely in order to exactly match the target's RAAN angle at the time of rendezvous. Instead, it is determined by the servicer's RAAN angle at the time it has finished servicing the previous client. Therefore, the difference in RAAN angle must be corrected by the propulsion system. In this transfer, this correction amounts to 0.23 deg eastwards change in RAAN angle.

Fig. 4-4 depicts the first transfer in blue and the subsequent second transfer in red. It is evident from this figure that the second transfer (as well as all the subsequent transfers) is much shorter than the first one and requires fewer revolutions. The slight increase in altitude with constant inclination can also be seen in this figure. For clarity, Fig. 4-5 and Fig. 4-6 show a frontal view and a side view of the second transfer only, respectively.

Transfer 2 final simulation results are as follows:

- Relative distance accuracy < 1 m
- Relative velocity accuracy < 5 m/s
- Total transfer time: 8 days (15 days including 7 days servicing time)
- Total propellant mass: 3.82 kg
- No. of Revolutions: 111
- Total computation run-time: 453 hrs

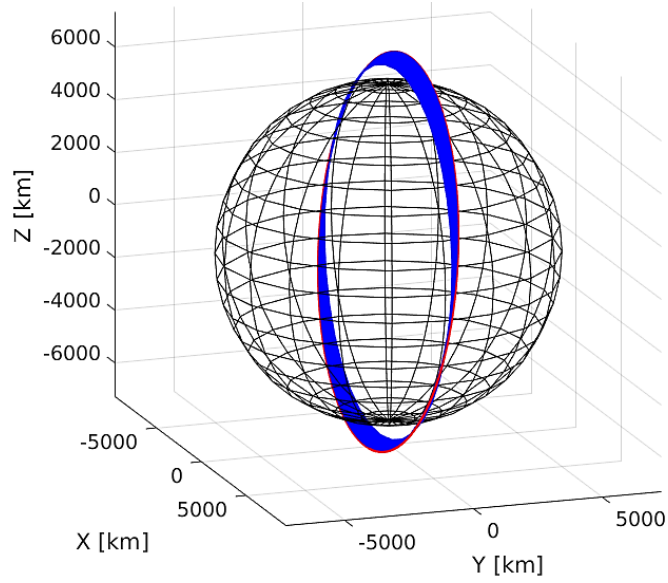


Fig. 4-4: Transfers 1 (blue) and 2 (red) isometric projection

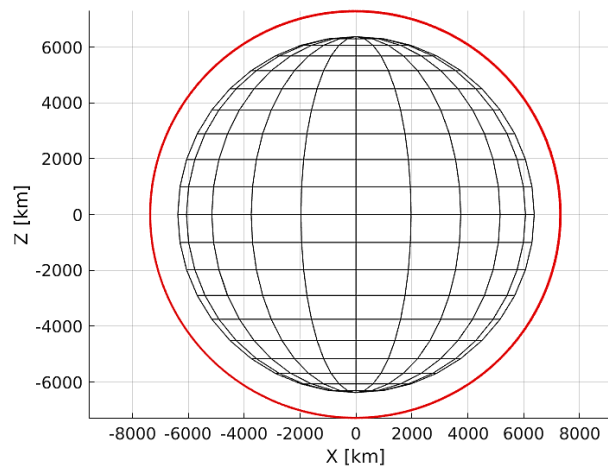


Fig. 4-5: Transfer 2 front view

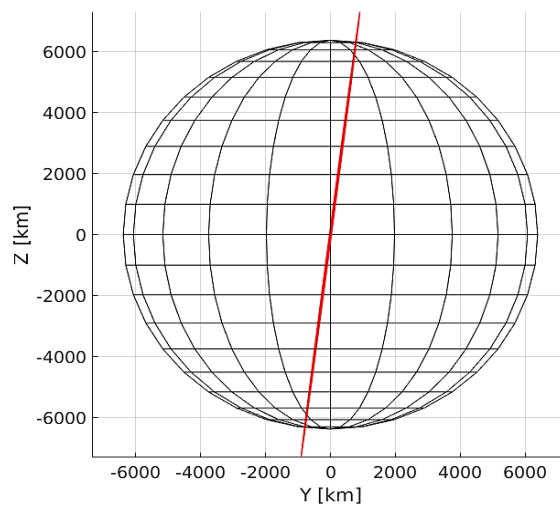


Fig. 4-6: Transfer 2 side view

4.1.3 Transfer 3: From Client #1 to Client #3

Tab. 4-3 summarizes the orbital elements of both the servicer and the target at the beginning and end of transfer 3.

Tab. 4-3: Transfer 3 initial and final states

	a [km]	i [deg]	e	Ω [deg]	ω [deg]	ν [deg]
Servicer initial state	7349	82.94	0.003	-41.85	N/A	N/A
Target initial state	7353	82.93	0.003	-41.21	N/A	N/A
Final state	7353	82.93	0.003	-68.05	N/A	N/A

Transfer 3 final simulation results are as follows:

- Relative distance accuracy < 5 m
- Relative velocity accuracy < 5 m/s
- Total transfer time: 29 days (36 days including 7 days servicing time)
- Total propellant mass: 7.59 kg
- No. of Revolutions: 444
- Total computation run-time: 644 hrs

In this transfer, the servicer gains only 4 km in altitude, but also has to reduce 0.01 deg in inclination and traverse 0.64 deg in RAAN angle, which are more fuel and time expensive maneuvers. This is evident from the longer transfer time and larger propellant mass consumption and number of revolutions around Earth of this transfer in comparison to the previous one.

Fig. 4-7 depicts the second transfer in red and the subsequent third transfer in green. For clarity, Fig. 4-8 and Fig. 4-9 show a frontal view and a side view of the second transfer only, respectively.

The larger RAAN angle change of this transfer compared to the previous one becomes evident by comparing Fig. 4-9 to Fig. 4-6. The side view projection in both figures shows the transfer as a “thicker” line at the equator, which corresponds to the servicer’s RAAN angle traversing an angular distance eastward.

Observing Fig. 4-9 w.r.t Fig. 4-6, it can be qualitatively appreciated that the third transfer is “thicker” in the equator compared to the second one. This, again, relates to the larger eastwards movement of the RAAN angle of Transfer 3 w.r.t Transfer 2.

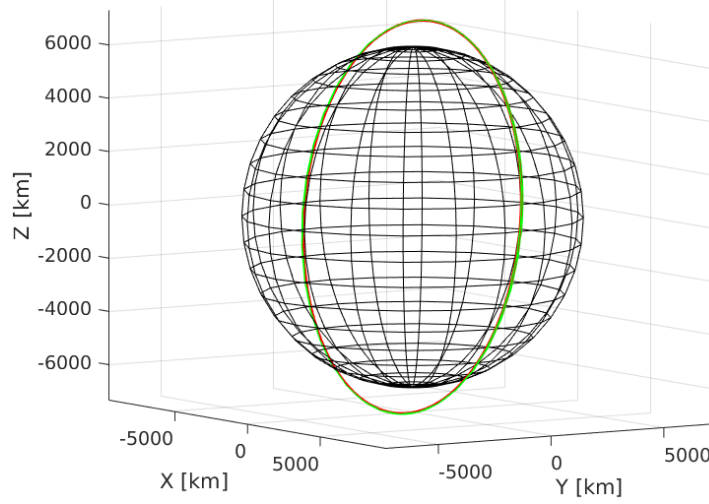


Fig. 4-7: Transfers 2 (red) and 3 (green) isometric projection

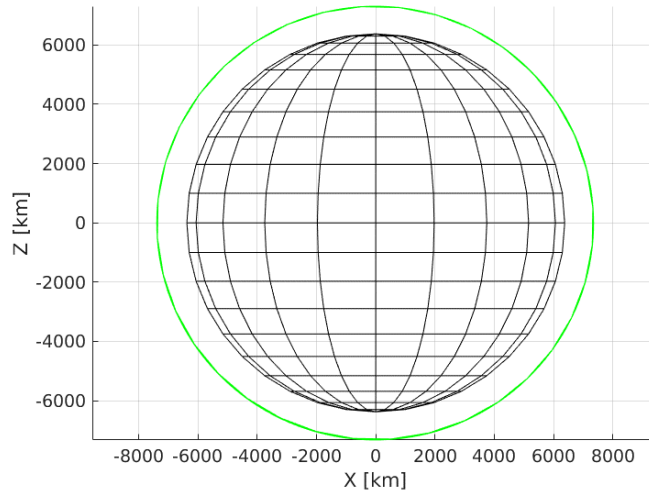


Fig. 4-8: Transfer 3 front view

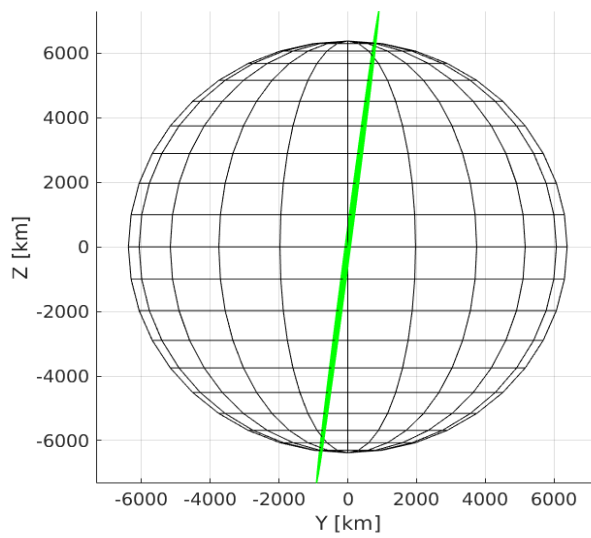


Fig. 4-9: Transfer 3 side view

4.1.4 Transfer 4: From Client #3 to Client #4

Tab. 4-4 summarizes the orbital elements of both the servicer and the target at the beginning and end of transfer 4.

Tab. 4-4: Transfer 4 initial and final states

	a [km]	i [deg]	e	Ω [deg]	ω [deg]	ν [deg]
Servicer initial state	7353	82.93	0.003	-68.05	N/A	N/A
Target initial state	7356	82.94	0.003	-67.7	N/A	N/A
Final state	7356	82.94	0.003	-90.74	N/A	N/A

Transfer 4 final simulation results are as follows:

- Relative distance accuracy < 10 m
- Relative velocity accuracy < 5 m/s
- Total transfer time: 24 days (31 days including 7 days servicing time)
- Total propellant mass: 3.116 kg
- No. of Revolutions: 271
- Total computation run-time: 522 hrs

The required RAAN angle change for this transfer amounts to 0.35 deg eastwards. This is larger than RAAN angle change of the second transfer and smaller than that of the third transfer. In addition, a decrease of 0.01 degrees in inclination and an increase of 3 km in altitude are incorporated into this transfers. This results in a total transfer time and propellant mass consumption of this transfer, which are intermediate to the ones of Transfer 2 and 3.

Fig. 4-10 depicts the second transfer in red and the subsequent third transfer in green. For clarity, Fig. 4-11 and Fig. 4-12 show a frontal view and a side view of the second transfer only, respectively.

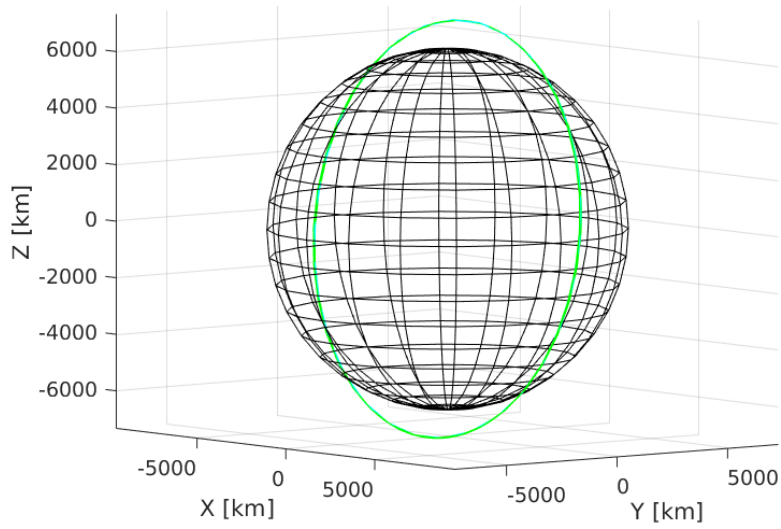


Fig. 4-10: Transfers 3 (green) and 4 (cyan) isometric projection

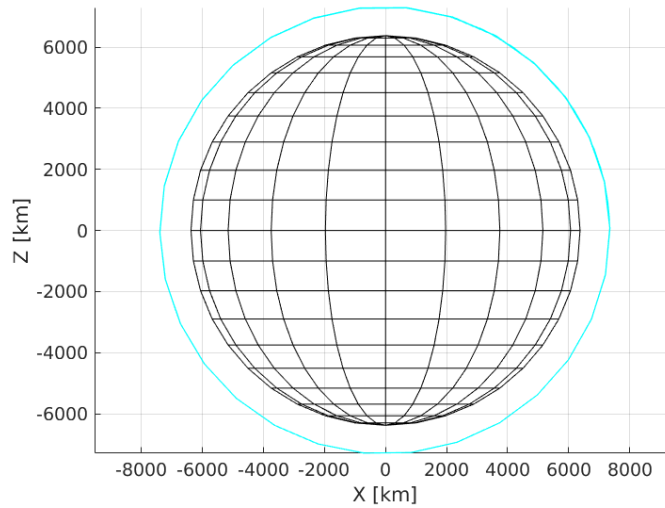


Fig. 4-11: Transfer 4 front view

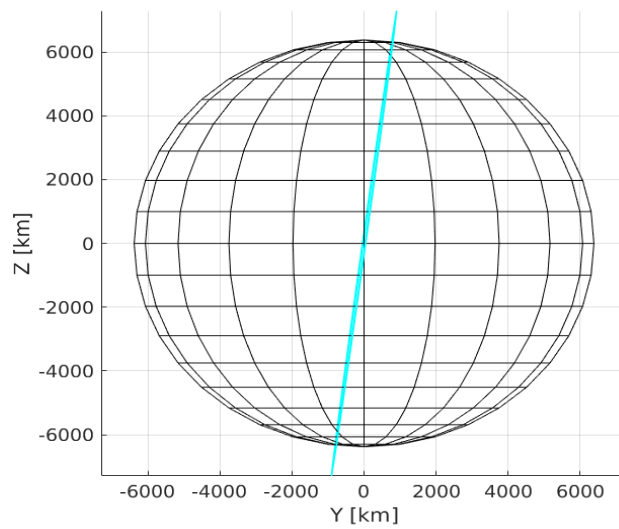


Fig. 4-12: Transfer 4 side view

4.1.5 Transfer 5: From Client #4 to Client #2

Tab. 4-5 summarizes the orbital elements of both the servicer and the target at the beginning and end of transfer 5.

Tab. 4-5: Transfer 5 initial and final states

	a [km]	i [deg]	e	Ω [deg]	ω [deg]	ν [deg]
Servicer initial state	7356	82.94	0.003	-90.74	N/A	N/A
Target Initial state	7362	82.92	0.002	-88.88	N/A	N/A
Final state	7362	82.92	0.002	-144.59	N/A	N/A

Transfer 3 final simulation results are as follows:

- Relative distance accuracy < 50 m
- Relative velocity accuracy < 7 m/s
- Total transfer time: 68 days (75 days including 7 days servicing time)
- Total propellant mass: 18.214 kg
- No. of Revolutions: 936
- Total computation run-time: 621 hrs

The last transfer is the longest one after Transfer 1. This could be attributed to the relatively large RAAN angle change of 1.86 deg eastwards. In

Fig. 4-13 depicts the second transfer in red and the subsequent third transfer in green. For clarity, Fig. 4-14 and Fig. 4-15 show a frontal view and a side view of the second transfer only, respectively. From observation of Fig. 4-15 the large RAAN angle change of this transfer can be appreciated.

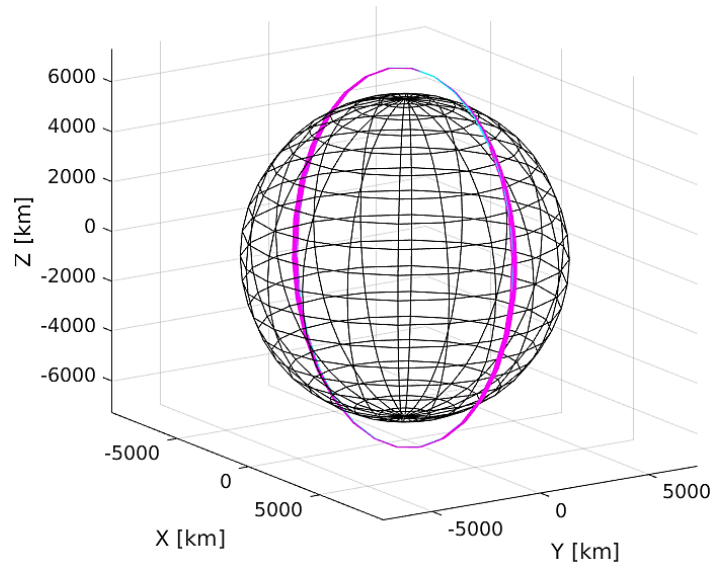


Fig. 4-13: Transfers 4 (cyan) and 5 (magenta) isometric projection

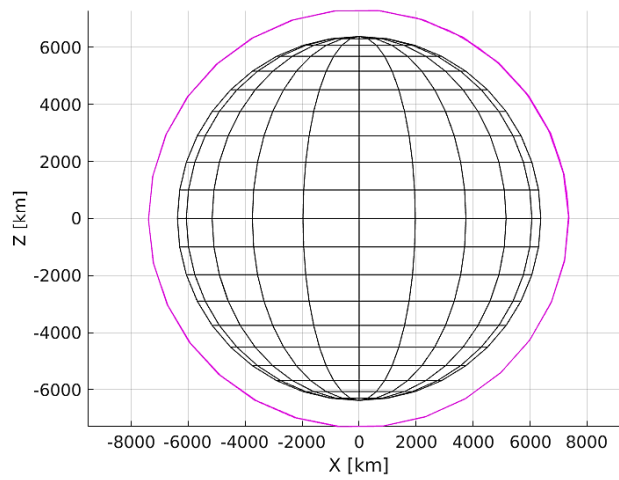


Fig. 4-14: Transfer 5 front view

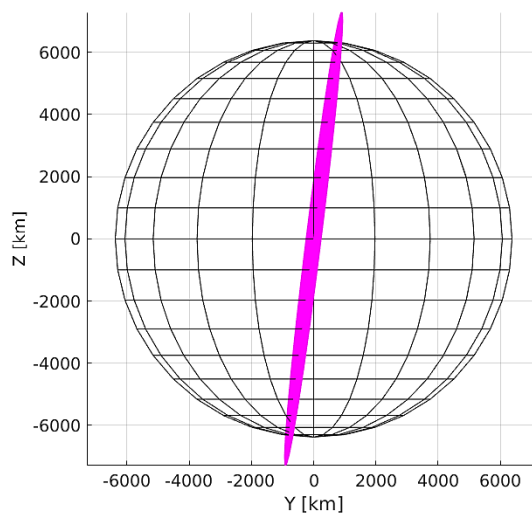


Fig. 4-15: Transfer 5 side view

4.1.6 Discussion

Tab. 4-6 summarizes and compares the simulation results of all the previously discussed transfers in terms of the evaluation metrics listed in Section 1.4.

Tab. 4-6: Scenario 1 simulation results

Transfer	Transfer time [days]	Propellant mass [kg]	Revolution count	Computation time [hours]
1	155	62.659	2173	284
2	15	3.82	111	453
3	36	7.59	444	644
4	31	3.116	271	522
5	75	18.214	936	621
Total	312	95.399	3935	2524

In the description of Scenario 1 in Section 2.1, the scenario's objective was defined as the removal of 5 high-risk targets from a crowded LEO orbit within 1 year. From Tab. 4-6 we can see that the selected 5 high-risk targets have all been attended and serviced in 312 days, which leaves almost a 2 months margin to the 1 year total mission time requirement. In [13–16] S. Peters investigated a similar mission, upon which guidelines the targets for this work were chosen and the general mission architecture was based (cf. Subsection 1.2.4). In her work, Peters asserted that for the entire mission 190 kg of Hydrazine propellant were required to rendezvous with and service 5 targets. The servicer plus one deorbit kit in Peter's work weighed approximately 1500 kg. The number of transfers in Peter's work was double the number of transfers in this work, since there, the servicer had to move to a parking orbit after servicing each client in order to pick up a new deorbit kit, while in this work all of the deorbit kits were assumed to be held in the servicer. However, the transfer trajectory design in Peter's work assumed the servicer and targets all lie in the same orbital plane, which avoided employing fuel-expensive out-of-plane maneuvers. In addition, the servicer was assumed to be launched directly to the parking orbit, which was close to the target's orbit. In this work, the simplifying assumption of only coplanar transfers was discarded, and, in addition, a more realistic injection orbit was chosen based on available launcher systems. This resulted in a larger, albeit more realistic figure for the required propellant mass. Still, even with the consideration of more realistic fuel-expensive transfer trajectories and with a heavier spacecraft (2000 kg vs. 1500 kg) the total required propellant mass found in this work amount to almost half of that found in Peter's work. Hence, the results found in this work for total mission time and total required propellant mass facilitate arguments favoring low-thrust propulsion over conventional chemical propulsion for OOS mission in the LEO region.

However, the last column in Tab. 4-6 deserves a closer examination. The averaged computation time of an individual transfer is calculated from Tab. 4-6 to be approximately 500 hours which is almost 21 days. For the entire mission approximately 3.5 months' worth of computation time were required. While this extensive demand on

computation time may be tolerable in the prospect of an academic study such as this one, it becomes utterly impractical when it has to be done as part of an industrial mission conceptual study, in which promptness is traded-off against accuracy of the solution.

Therefore, the results obtained from the simulation of this scenario confirm the feasibility of low-thrust propulsion for certain ADR mission types in the LEO region, specifically missions in which the targets are clustered and require only small out-of-plane changes. However, such low-thrust LEO OOS missions require many revolutions of the S/C around Earth which translates to an extremely heavy workload on the computer. Therefore, more experience in using global optimization tools for the optimization of LEO trajectories and the advancement of such tools are vital for expediting the simulation run-time to the point where it may become admissible to use GTOM tools in the framework of a conceptual study of a specific mission.

4.2 Scenario 2: GTO – GEO – GEO/GYO

In this scenario, the first transfer of the servicer from GTO to GEO was computed with InTrance, since most GTO orbits are inclined, meaning that the servicer has to change several orbital elements simultaneously, namely SMA, eccentricity and inclination. The Matlab tool developed for this thesis can deal only with coplanar circular orbits. Therefore, InTrance was used for calculating the transfer from GTO to GEO and the Matlab tool was then used for the calculations of the transfers between clients in GEO.

Since the major part of the simulation of this scenario is done with the Matlab tool, the required computational run-time for this scenario is determined primarily by the GTO-GEO transfer, simulated with InTrance. The computation run-time of the rest of the scenario, which was done with Matlab corresponds to a small fraction of the GTO-GEO transfer computation time.

4.2.1 Transfer GTO to GEO

The initial and final orbital elements that were given as input into the InTrance simulation of the GTO to GEO transfer are shown in the first two rows in Tab. 4-7.

The final simulation results of the GTO to GEO transfer are listed below:

- Relative distance accuracy < 5 m
- Relative velocity accuracy < 7 m/s
- Total transfer time: 129 days
- Total propellant mass: 296 kg
- No. of Revolutions: 202
- Total computation run-time: 454 hrs

Fig. 4-16 to Fig. 4-18 show the transfer from different viewpoints. In all figures, the initial GTO orbit is colored in magenta and the final GEO orbit is colored in red. Fig. 4-17 shows clearly the eccentricity change of the servicer during the transfer, while Fig. 4-18 makes particularly evident the change in inclination and altitude.

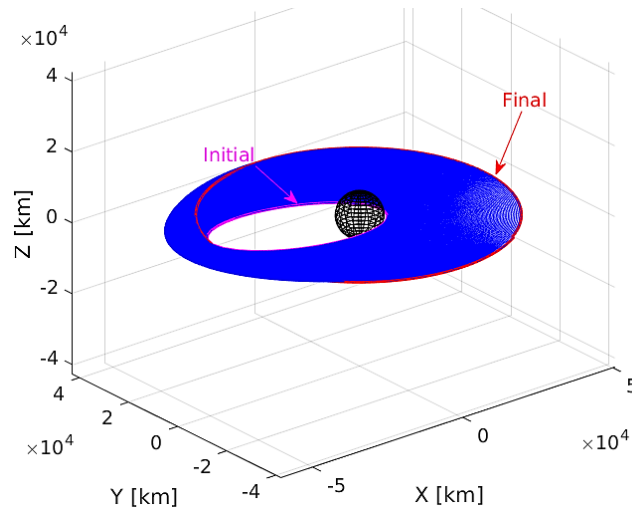


Fig. 4-16: GTO to GEO transfer isometric view

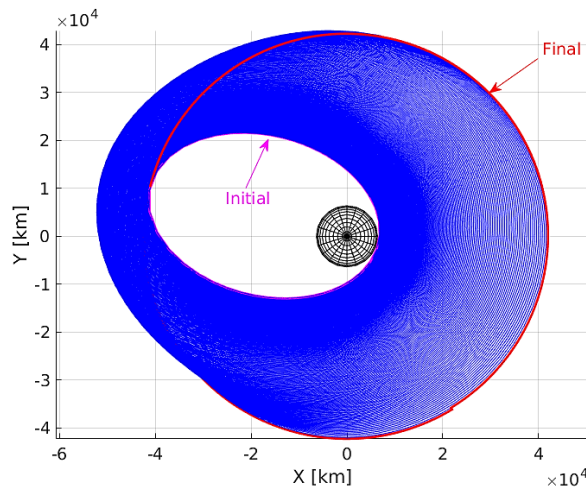


Fig. 4-17: GTO to GEO polar view

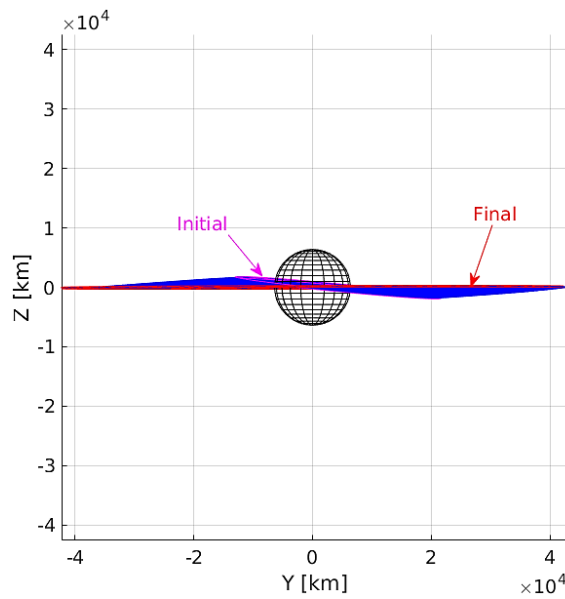


Fig. 4-18: GTO to GEO equatorial view

4.2.2 Validation with GESOP

As shortly mentioned in sub-section 2.2.1.6 and as evident also from Tab. 4-7, the InTrance simulation can only calculate an Earth-bound transfer trajectory emanating from a well-defined orbital location (i.e. all orbital elements are given) to a free target orbit, in which the true anomaly is not pre-defined. Therefore, the resulting transfer time and consumed propellant mass do not take into account the phasing maneuvers required for bringing the servicer location to a specific location in the target orbit. To check how significant this phasing maneuver actually is w.r.t the entire transfer maneuver, the commercial trajectory optimization software GESOP has been used. The S/C design that was used in the GESOP simulation is as follows:

Total mass: 2300 kg

Thrust: 440 mN

Specific Impulse: 1700 s.

The first simulation, considered a GTO to GEO transfer with free target's true anomaly constraint. The initial and final orbital elements given in this simulation run are the same as the ones shown in the first two rows in Tab. 4-7 and the actual results from this simulation are given in the third row.

Tab. 4-7: GTO to GEO initial and final states

	a [km]	i [deg]	e	Ω [deg]	ω [deg]	ν [deg]
Initial state	24422.4	6	0.728	167.7	178.1	8.26
Final state	42164.1	0	0	N/A	N/A	N/A
Final state GESOP	42164.137	0.00	0.00	0.14	2.61	3.42 ³

The final servicer longitude in the target orbit from this GESOP simulation run was found to be 38.67°E, the total transfer time was 125.56 days and the total propellant mass resulted in 283.56 kg. The results from GESOP, both in terms of total transfer time and total propellant mass are better than the ones obtained from InTrance by approximately 2.5%.

In the second GESOP simulation run, an additional end constraint for the end longitude of the servicer was set to 200°E (-160°W). With this simulation run, the effect of the phasing maneuver on the total transfer time and propellant mass was investigated. It was found that with this added longitude constraint, the total transfer time was 125.82 days and the total propellant mass was 284.16 kg. These results correspond to an increase of less than 0.25% of the results of the first run, with no end longitude constraint. This validates the assumption that the additional time and propellant mass required for the phasing of the S/C in GEO is a very small fraction of the entire flight time and propellant mass required for the transfer itself from GTO to GEO.

³ This value in GESOP is given as Mean anomaly and not True anomaly

4.2.3 Sub-scenario 2.1

Once the servicer has reached the GEO orbit the simulation of the mission carries on with the Matlab tool described in Subsection 3.2.4.1.

As discussed in Subsection 2.2.1, the mission assumes 10 clients to be serviced, distributed evenly around the GEO belt, and 16 assembly nodes evenly distributed in an orbit 350 km above GEO. The S/C design parameters are as described in Subsection 2.2.1.6.

The results of the Matlab simulation are given in Tab. 4-8. Each row corresponds to one transfer where first two columns describe the type and location of the current target being attended, i.e. whether it is a client being attached to the servicer or an assembly node being docked to. The 2nd and 3rd column describe the end target of the transfer and its location at the beginning of the transfer. The last two columns give the total transfer time and propellant mass required for the transfer, including the servicing time.

Tab. 4-8: Sub-scenario 2.1 Matlab results

	Current target	Long. [deg]	Next target	Long. [deg]	Transfer time [days]	Propellant mass [kg]
<i>Transfer 1</i>	Client 1	0.0	AN 1	0.0	9.27	5.173
<i>Transfer 2</i>	AN 1	318.7	Client 10	324.0	9.66	6.064
<i>Transfer 3</i>	Client 10	324.0	AN 3	320.81	10.04	6.946
<i>Transfer 4</i>	AN 3	276.127	Client 9	288.0	10.46	7.893
<i>Transfer 5</i>	Client 9	288.0	AN 6	297.096	9.776	2.12
<i>Transfer 6</i>	AN 6	253.607	Client 8	252.0	7.695	1.5
<i>Transfer 7</i>	Client 8	252.0	AN 8	264.377	10.637	2.117
<i>Transfer 8</i>	AN 8	217.057	Client 7	216.0	8.143	2.607
<i>Transfer 9</i>	Client 7	216.0	AN 10	225.835	9.97	2.114
<i>Transfer 10</i>	AN 10	181.488	Client 6	180.0	7.662	1.493
<i>Transfer 11</i>	Client 6	180.0	AN 12	192.402	10.643	2.11
<i>Transfer 12</i>	AN 12	145.058	Client 5	144.0	8.134	2.588
<i>Transfer 13</i>	Client 5	144.0	AN 14	153.872	9.978	2.107
<i>Transfer 14</i>	AN 14	109.487	Client 4	108.0	7.661	1.486
<i>Transfer 15</i>	Client 4	108.0	AN 16	120.407	10.643	2.105
<i>Transfer 16</i>	AN 16	73.062	Client 3	72.0	8.124	2.565
<i>Transfer 17</i>	Client 3	72.0	AN 2	81.921	9.989	2.101
<i>Transfer 18</i>	AN 2	37.483	Client 2	36.0	7.659	1.48
<i>Transfer 19</i>	Client 2	36.0	AN 4	48.413	10.643	2.098
Total					176.787	56.668

Note, that when the end target of a transfer is an AN, then in the following row the longitude of the current target will be different than the longitude of the end target in the previous row, although they are the same target (compare, for instance, column 3 and 4 of Transfer 1 with column 1 and 2 of Transfer 2). The reason is, that the 4th column in the table refer to the longitude of the target at the **beginning** of the transfer, and this longitude changes during the transfer and servicing of the target. Of course, this does not happen when the next target is a client in GEO, since by definition satellites in GEO maintain constant longitude throughout their operational lifetime.

The mission described in this sub-scenario, was based on Notional Mission 1 of the NASA OOS Report in [1], and the total mission time was limited to 5 years. From the results presented in Tab. 4-8 and in Subsection 4.2.1, the total mission time including both the transfer from GTO to GEO and the removal of 10 satellites from GEO to GYO is approximately 305 days, which is less than a year. The total amount of required propellant mass for the entire mission is 347 kg, 83% of which are just for the GTO to GEO transfer and the rest is for the removal of the client satellites.

As explained in the description of the Matlab module used for this sub-scenario in Subsection 3.2.4.1, there exists a possibility to optimize the entire mission by adjusting the time dedicated for servicing. The results of this optimization process are depicted in Fig. 4-19. The vertical axes display the mission evaluation metrics – total propellant mass in blue and total mission duration in orange. The horizontal axis corresponds for the servicing time. In the case depicted in this figure, the minimal servicing duration of 7 days turns out to be also the optimal servicing time in terms of the objective function, as displayed in Fig. 4-20. There, we see that the objective function, which searches for the optimal (minimal) solution in terms of both total mission time and total propellant mass, with more weight given to minimal propellant mass (cf. Subsection 3.2.4.1) reaches the minimum at the minimal value for servicing duration (7 days). However, this doesn't necessarily mean this is always the case. The result of the optimization depend on how many ANs are in use, how many clients are to be serviced, and how much weight each factor in the optimization equation (3-4) is given.

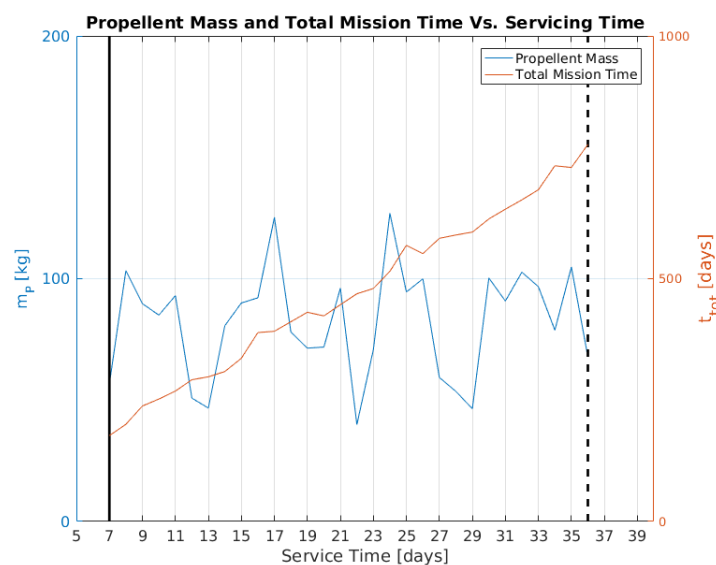


Fig. 4-19: Total mission time and total propellant mass as function of servicing time

An interesting observation from Fig. 4-19 is, that counter to intuition, longer servicing duration does not always mean longer total mission time. For example, a servicing duration of 25 days corresponds to a total mission time of approximately 568 days. By adding one additional day for servicing, the total mission time actually decreases in 17 days to 551 days. This happens, since the added duration for servicing (in which the servicer does not actually service, but just drifts in the vicinity of the target) results in a more favorable constellation between the servicer and clients which, in turn, results in an overall shorter mission. In certain configurations of the total number of ANs, clients and objective function definition, this could result in a global minimum of the objective function at a value of the servicing duration which is actually higher than the required minimum of 7 days.

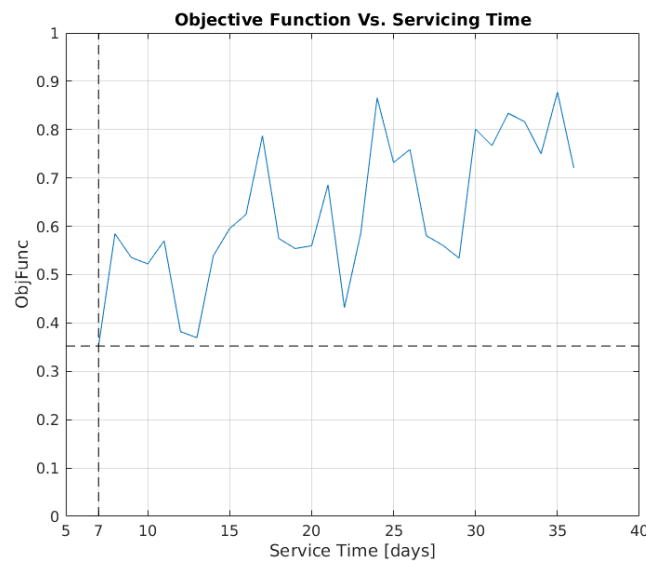


Fig. 4-20: Objective function Vs. servicing time

The computation run-time that was required for the entire simulation of this sub-scenario was found to be approximately 5.3 seconds for a single simulation run (using `GYO_transfer.m`) and approximately 111 seconds for an optimization run (using `GYO_transfer_OPT.m`) considering service time between 7 days and 37 days with 1 day intervals.

4.2.4 Sub-scenario 2.2

An exemplary output file of a simulation run of this sub-scenario is provided in Appendix C2. A single simulation run calculates the amount of time and propellant mass required for an entire mission consisting of visiting 24 clients in 4 sorties. To get a figure for the average total mission time and required average total propellant mass, 150 simulation runs were carried out, where in each one different client satellites were randomly sampled from the refined list. The results of the 150 simulations for the total propellant mass are shown in the histogram in Fig. 4-21.

The average value from the 150 runs was found to be $\bar{m}_p \cong 95 \text{ kg}$. Including a 30% margin this resulted in a total propellant mass of 125 kg which will be loaded as payload into the Depot station. The average total servicing time for attending 24 clients was calculated at $t_{tot} = 615 \text{ days} \cong 1.7 \text{ years}$. A histogram of the total servicing time is shown in Fig. 4-22.

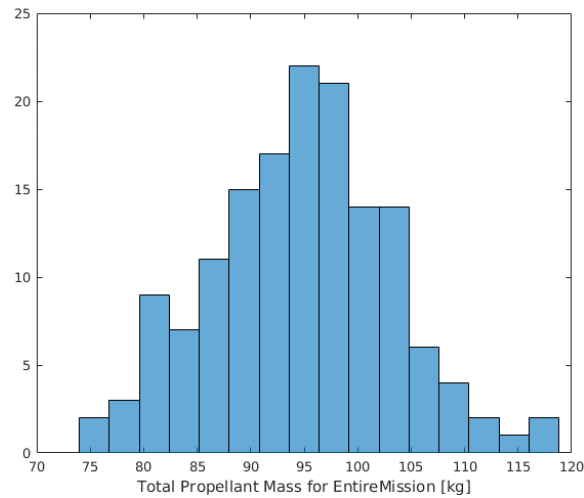


Fig. 4-21: Histogram of servicer's total required propellant mass from 150 simulation runs

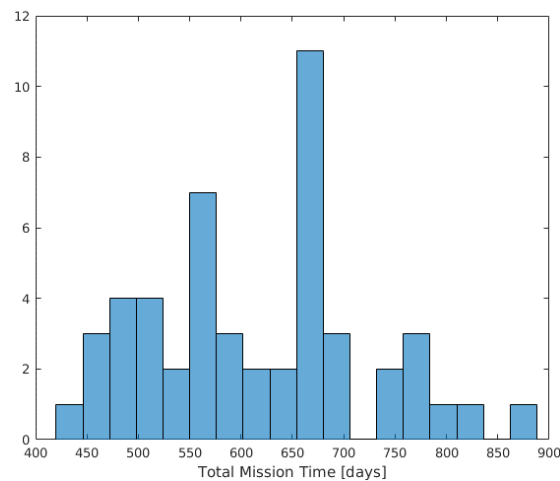


Fig. 4-22: Histogram of total servicing time from 150 simulation runs

The NASA scenario envisioned a mission lifetime of 10 years, which includes the launching and commissioning phase of the satellite and depot station, the servicing of 26 GEO satellites and the eventual removal of both the servicer and the depot to a graveyard orbit after the end of the mission. They have also assumed the client satellites are evenly distributed around the GEO belt. Both in the NASA report and in this thesis the mission was assumed to be continuous, i.e. the servicer is always in operation – either refueling, transferring or resupplying at the depot. There are no idle moments, in which the servicer awaits a mission.

The results obtained in this study in terms of propellant mass are obviously quite low, and it will be inappropriate to compare them to the NASA reference scenario which used chemical propulsion. What is interesting to note is the total mission life time. In this study, the average total mission time was found to be 744, which takes into account 615 days as averaged total servicing time and 129 days for the transit from GTO to GEO. If the worst case scenario from Fig. 4-22 is considered, then 930 days are taken for the servicing time, and the entire mission time is calculated at 1059 days, which are almost 3 years. These results are surprisingly low compared to the total 10-year mission time, considering that the client satellites in this work were sampled randomly

from a real list of operational satellites and were not distributed evenly around GEO as in the NASA report. The explanation for the relatively low total mission time could be attributed to the fact, that due to the high efficiency of the EP system, relatively fuel-expensive maneuvers could be performed for the transfers between clients, which could expedite the transfers. Such maneuvers would be deemed impractical with a chemical propulsion because they would require an unreasonable amount of propellant. In comparison, in the NASA reference scenario, the servicer would save fuel by always raising its altitude to a drift orbit (127 km above GEO) and would wait there for the longitudinal difference to the next client to diminish. These drifting arcs are quite time consuming and are avoided in this study.

Computation run-time per simulation of this sub-scenario was found to be roughly 8 seconds and roughly 25 minutes were required for computing 150 runs.

4.3 Scenario 3: LEO – GEO

This module of Matlab is identical to the GEO satellite refueling module described in Subsection 3.2.4.2. To use it for this scenario the Depot orbit parameters were set according to Tab. 2-7, i.e. an equatorial circular orbit at an altitude of 625 km. The number of clients was set to 10 and the number of sorties was set to 1. The results of the simulation are given in Tab. 4-9.

Tab. 4-9: Scenario 3 Matlab results

	Current target	Long. [deg]	Next target	Long. [deg]	Transfer time [days]	Fuel mass [kg]
<i>Tour start</i>	Depot	0.0	Client 5	276.0	613.962	365.08
<i>Transfer 1</i>	Client 5	276.0	Client 6	281.2	9.696	1.641
<i>Transfer 2</i>	Client 6	281.2	Client 7	315.0	13.827	4.156
<i>Transfer 3</i>	Client 7	315.0	Client 8	335.5	12.292	3.222
<i>Transfer 4</i>	Client 8	335.5	Client 9	345.0	10.587	2.183
<i>Transfer 5</i>	Client 9	345.0	Client 10	352.7	10.214	1.956
<i>Transfer 6</i>	Client 10	352.7	Client 1	42.5	15.111	4.938
<i>Transfer 7</i>	Client 1	42.5	Client 2	47.0	9.431	1.48
<i>Transfer 8</i>	Client 2	47.0	Client 3	119.5	16.673	5.888
<i>Transfer 9</i>	Client 3	119.5	Client 4	140.7	12.211	3.172
<i>Return to Depot</i>	Client 4	140.7	Depot	90.388	476.801	283.899
Total					1200.805	677.615

As could be expected, this scenario results in a much longer total mission time than the sub-scenarios of Scenario 2 due to the very long transit time between LEO and GEO. This transfer duration could become even longer if a more realistic Depot orbit is considered with an inclination different than 0.

5 Conclusions and Future Work

Today, humanity relies on satellites in more ways than most people realize. From the obvious GPS navigation system helping us find our way in a foreign country and land our planes more safely and TV communication-satellites providing us entertainment from around the globe, to Earth observation satellites providing data for weather predictions, or communication satellites which are essential for encrypted bank transactions and credit card validations. With today's reliance on satellite technology it would be safe to say that a day without satellites will result in a social, economic and military chaos. Therefore, the importance of safeguarding the future of space systems and accessibility to space cannot be overstated. For this to happen, two major challenges must be overcome. First, the space debris environment, especially in Low Earth Orbit and in the Geostationary Orbit must be stabilized. Second, access to space must become more affordable. The concept of on-orbit servicing provides a viable solution to deal with both these challenges. Through active debris removal of high risk "space junk" from congested orbits OOS can directly help stabilizing the space debris environment. Through repairing and refueling of satellites in orbit, the number of new launches and new satellites in orbit can drop significantly, thereby contributing also to the sustainability of the ever-growing space debris environment. In addition, servicing a spacecraft in-orbit can extend the operational lifetime of the spacecraft which can relax reliability and redundancy requirements during the mission design process, which in turn can be translated into cheaper and more affordable missions.

To date, however, studies on OOS have concentrated mainly on perfecting autonomous rendezvous and docking maneuvers of a servicer attending a single target, which can be either cooperative or non-cooperative. Considerable progress has been made in recent years towards accomplishing this feat. Therefore, in this thesis the next phase of OOS mission design has been addressed, namely the optimization of OOS missions by using high-efficiency low-thrust solar electric propulsion and extending the OOS mission from a single target to multiple targets.

The investigation done here, laid the foundations for a more extensive future analysis of multi-target low-thrust OOS mission. Three scenarios have been studied here, which are representative of probable future OOS missions. First, a LEO scenario has been set up, in which 5 high-risk massive rocket bodies had to be removed from orbit. The chosen targets were clustered in a polar orbit, in an altitude range between 900 km and 1000 km. This scenario included a servicer transferring from an injection orbit at 500 km to the target's orbit and then sequentially transferring from one target to the next. After rendezvousing with a client, the servicer had attached a deorbit kit, which was responsible for autonomously deorbiting the target, and then moved on to the next client. All of the transfers were simulated using InTrance, a low-thrust trajectory optimization program using artificial neural network with evolutionary algorithms to find globally (near) optimal low-thrust transfer trajectories. According to widely accepted guidelines for stabilization of the LEO space debris environment at least 5 high-risk debris objects should be removed from congested orbits each year. The results obtained from the simulations revealed that meeting this 5 objects per year limit is feasible using solar electric propulsion with lower propellant mass consumption compared to chemical propulsion. However, the simulation of the entire mission using InTrance took more than 2500 hours to accomplish. This extremely long duration can be attributed to the inherent high computational effort associated with global

optimization methods, that have to explore a very large search space of solutions. But is also likely that the relatively little experience and documentation available for InTrance resulted in suboptimal configuration of the simulations which lengthened the simulations' run-time. More experience and more extensive know-how in using InTrance could help in the future to better define and set up simulations that would converge faster.

The second scenario focused on servicing satellites in GEO, which is one of the most lucrative regions in space due to its high commercial value and limited usable satellite slots. The two major factors restricting the use of communication satellite in GEO are operational slots occupied by decommissioned satellites and fuel depletion in an otherwise healthy and functional satellite. The former, prevents launching a new satellite until the occupied slot is made available and the latter renders a functioning satellite inoperable. OOS could remedy both issues by either removing or refueling satellites in GEO. Both these solutions have been investigated in two separate sub-scenarios. For the simulation of these missions a Matlab tool has been developed that computed required propellant mass and mission time for coplanar circular multi-target OOS missions. The use of InTrance for these scenarios was limited only to the initial transfer of the servicer from its injection GTO orbit to GEO. Further use of InTrance not necessary since transfers between satellites in GEO are always (nearly) coplanar, for which optimal analytical low-thrust trajectory solutions already exist. These analytical solutions have been implemented in the Matlab tool. The results of these scenarios have been compared to similar studies found in the literature, where chemical propulsion has been used. It was found that in both sub-scenarios the total mission time was well under the predefined maximum mission time limit and the total required propellant mass was much lower than that calculated in the reference missions. This is of course attributed for the high efficiency of the SEP, which not only reduces the mass of the required propellant, but also allows for faster, and more fuel expensive maneuvers, which would have otherwise been deemed impractical.

Lastly, a third scenario has been simulated in which a servicer would transport hardware components from LEO to GEO, service 10 clients in GEO and then return to LEO. For this scenario it was found that the entire mission would take more than 670 kg of propellant and more than 3 years to accomplish, with 90% of which required just for the transfers to and from GEO. It is hard to evaluate of the feasibility of such a mission since no other studies have been found in the literature to which the results could be compared. The justification for such a scenario is that by using the services of such a "taxiing" spacecraft, hardware could be sent with cheaper launchers to LEO instead of GTO or GEO and then be transported by the servicer to their designated target in GEO. Instead of carrying as payload many spare parts for multiple targets in GEO, the servicer could be used to transport a whole spacecraft to its location in GEO.

The required computation run-time for Scenario 2, which is predominantly determined by the InTrance simulation of the GTO-GEO transfer, amounts to about 455 hours for both sub-scenarios, since in both of them the Matlab simulation accounts for tiny fraction of the InTrance computation run-time. This computation run-time translates to roughly 19 days. In comparison to the very long computation duration required for Scenario 1, the computation duration of Scenario 2 appears to be more acceptable in the frame of a mission's conceptual study phase. The third scenario, which in this thesis involved only the use of the Matlab tool required computation time in the order of several seconds.

While the scenarios investigated here and the results presented are not general in nature, as they correspond to the design of a specific mission and a specific spacecraft, they do prove that multi-target OOS missions using low-thrust propulsion are feasible and could be beneficial both in terms of fuel mass consumption and total mission time. More importantly, this study develops both the framework and the tools for investigating other multi-target OOS scenarios in the future as required.

Being an inaugural work, many assumptions and simplification had to be made in order to limit the scope of this thesis. In future work, special attention should be given to the problem of optimizing the sequence of targets to be serviced. In this work, the order in which targets have been serviced have been optimized locally, yet this is a dynamic problem that requires solving a dynamic traveling salesman problem in order to find a globally optimal sequence. An optimal sequence can further reduce the required propellant mass and/or total mission time of such scenarios, rendering such missions even more profitable.

Further work can also be done in enhancing InTrance to support LEO multiphase transfers. First, vector rendezvous of two bodies in LEO should be included in the program in order to be able to simulate rendezvous and docking of spacecraft in low-Earth orbits. Second, orbit perturbations due to atmospheric drag can be implemented in the program, which will increase the fidelity of the resulting solution.

Another improvement to the work done here could be the optimization of the transition between phases using InTrance. In the first scenario, each transfer has been simulated separately by manually adjusting a transfer's initial conditions to match the final conditions of the previous transfer. However, a great feature of the extended version of InTrance is its ability to optimize transition conditions as part of the optimization process. Since the goal of this thesis was not optimizing a specific scenario, but rather examining whether a scenario is feasible or not, this feature was not used in this work. However, for a future work, this feature could facilitate obtaining more optimal results of investigated scenarios.

The third scenario which have been relatively briefly examined in this thesis deserves a more comprehensive investigation. With improvements in modern low-thrust propulsion technologies, tug services for entire satellites from LEO to GEO could potentially help cutting down launch costs. A more thorough investigation of this scenario, including an economic trade-study comparing the results of such a scenario to dedicated launch costs could shed more light on the feasibility of this scenario.

6 References

- [1] *On-orbit Satellite Servicing Study: Project Report*. National Aeronautics and Space Administration. Goddard Space Flight Center, 2010.
- [2] Wikipedia, *List of International Space Station spacewalks - Wikipedia, the free encyclopedia*. [Online] Available: <https://en.wikipedia.org/w/index.php?oldid=711498945>. Accessed on: Apr. 05 2016.
- [3] DARPA, *Orbital Express*. [Online] Available: <http://archive.darpa.mil/orbitalexpress/index.html>. Accessed on: Apr. 05 2016.
- [4] Wikipedia, *Space Infrastructure Servicing - Wikipedia, the free encyclopedia*. [Online] Available: <https://en.wikipedia.org/w/index.php?oldid=667949126>. Accessed on: Apr. 21 2016.
- [5] J. N. Pelton, *New Solutions for the Space Debris Problem*. Cham [u.a.]: Springer International Publishing, 2015.
- [6] O. Schwarz, *DEOS - SpaceTech GmbH*. [Online] Available: <http://www.spacetechnology.com/products/missions-satellites/deos>. Accessed on: Apr. 21 2016.
- [7] ViviSat, *Services - Vivisat*. [Online] Available: http://www.vivisat.com/?page_id=10. Accessed on: Apr. 05 2016.
- [8] C. Henry, *ViviSat Launching First MEV for In-Orbit Servicing in 2018 - Via Satellite* -. [Online] Available: http://www.satellitetoday.com/technology/2016/03/24/vivisat-launching-first-mev-for-in-orbit-servicing-in-2018/?hq_e=el&hq_m=3227788&hq_l=1&hq_v=205e1834a2. Accessed on: Apr. 05 2016.
- [9] ESA, “e.deorbit Implementation Plan,” http://blogs.esa.int/cleanspace/files/2016/02/e.deorbit-Implementation-Plan-Issue_1_2015.pdf.
- [10] ASTROSCALE. [Online] Available: <http://astroscale.com/services>. Accessed on: Apr. 05 2016.
- [11] O. Nobu, S. Yuki, and P. Moreels, *Private Space Company Space-Based Solutions to the Growing Threat Coming From Orbital Debris*. 66th International Astronautical Congress, Jerusalem, Israel, 2015.

- [12] *effective-space*. [Online] Available: <http://www.effective-space.com/>. Accessed on: Apr. 05 2016.
- [13] S. Peters, R. Förstner, M. Weigel, and H. Fiedler, "Reference Scenario and Target Identification for Autonomous Active Space Debris Removal Methods," Sixth European Conference on Space Debris, ESA, Darmstadt, 2013.
- [14] S. Peters, R. Förstner, and H. Fiedler, "AUTONOMY FOR ACTIVE SPACE DEBRIS REMOVAL: RESEARCH ISSUES AND APPROACHES,"
- [15] S. Peters, H. Fiedler, and R. Förstner, *ADReS-A: Autonomy Requirements for Active Debris Removal*. 66th International Astronautical Congress, Jerusalem, Israel, 2015.
- [16] S. Peters, H. Fiedler, and R. Förstner, *ADReS-A: Mission architecture for the removal of SL-8 rocket bodies*. Aerospace Conference, IEEE: IEEE, 2015.
- [17] C. Bombardelli, J. Herrera-Montojo, and J. L. Gonzalo, "Multiple Removal of Spent Rocket Upper Stages with an Ion Beam Shepherd," in *ESA Special Publication*, 2013, p. 90.
- [18] R. Bevilacqua and M. Romano, "Rendezvous maneuvers of multiple spacecraft using differential drag under J2 perturbation," *Journal of Guidance, Control, and Dynamics*, vol. 31, no. 6, pp. 1595–1607, 2008.
- [19] B. Chamot and M. Richard, "Mission and system architecture design for active removal of rocket bodies in low earth orbit," *Master's thesis, Massachusetts Institute of Technology, US*, 2012.
- [20] A. Ohndorf, "Multiphase Low-Thrust Trajectory Optimization Using Evolutionary Neurocontrol," *Doctor thesis - Technische Universiteit Delft*, 2015.
- [21] J.-C. Liou, "An active debris removal parametric study for LEO environment remediation," *Advances in Space Research*, vol. 47, no. 11, pp. 1865–1876, 2011.
- [22] S. Peters, R. Förstner, and H. Fiedler, "AUTONOMY FOR ACTIVE SPACE DEBRIS REMOVAL: RESEARCH ISSUES AND APPROACHES,"
- [23] ESA Space Debris Mitigation WG, "ESSB-HB-U-002," [http://www.iadc-online.org/References/Docu/ESSB-HB-U-002-Issue1\(19February2015\).pdf](http://www.iadc-online.org/References/Docu/ESSB-HB-U-002-Issue1(19February2015).pdf).

- [24] JFCC SPACE/J3, *Space-Track.Org*. [Online] Available: <https://www.space-track.org/>. Accessed on: Nov. 26 2015.
- [25] *ISCK documents: Dnepr, S. L.S, user's guide, Issue 2, Nov. 2001*. [Online] Available: http://www.kosmotras.ru/en/docs_mkk/. Accessed on: Nov. 30 2015.
- [26] U. Walter, *Astronautics: the physics of space flight*. John Wiley & Sons, 2012.
- [27] K. Kumar *et al*, *Agora: Mission to demonstrate technologies to actively remove Ariane rocket bodies*. 66th International Astronautical Congress, Jerusalem, Israel, 2015.
- [28] R. Kawashima, "International activities of UNISEC and Proposal of UNISEC-Global," http://www.unisec-global.org/pdf/UNISEC-Global_kawashima_v8.1.pdf.
- [29] *D-Orbit | Smart commissioning and decommissioning systems to optimize spacecraft operations*. [Online] Available: <http://www.deorbitaldevices.com/>. Accessed on: Apr. 16 2016.
- [30] "D3 Technical Sheet," <http://www.deorbitaldevices.com/wp-content/themes/d-orbit/pdf/d3-technical-sheet.pdf>.
- [31] G. P. Sutton and O. Biblarz, *Rocket propulsion elements*. John Wiley & Sons, 2010.
- [32] Orbital ATK, "UltraFlex™ Solar Array Systems," https://www.orbitalatk.com/space-systems/space-components/solar-arrays/docs/FS007_15_OA_3862%20UltraFlex.pdf.
- [33] S. T. King, M. L. R. Walker, and C. A. Kluever, "Small Satellite LEO Maneuvers with Low-Power Electric Propulsion," vol. 44th AIAA/ASME/SAE/ASEE Joint Propulsion Conference & Exhibit, 2008.
- [34] J.R. Wertz and W.J. Larson, Eds, *Space mission analysis and design: [SMAD III]*, 3rd ed. Torrance, Calif.: Microcosm Press, 2010.
- [35] Astos Solutions, *GESOP*. [Online] Available: <https://www.astos.de/products/gesop>. Accessed on: May 16 2016.
- [36] Satellite Signals Ltd, *List of satellites in geostationary orbit*. [Online] Available: <http://www.satsig.net/sslist.htm>. Accessed on: Apr. 19 2016.
- [37] B. Dachwald, "Low-thrust trajectory optimization and interplanetary mission analysis using evolutionary neurocontrol," *Doctor thesis*–

Universität der Bundeswehr München Fakultät für Luft und Raumfahrttechnik Institut für Raumfahrttechnik, 2004.

- [38] K. Alemany and R. D. Braun, "Survey of global optimization methods for low-thrust, multiple asteroid tour missions," 2007.
- [39] D. E. Golberg, "Genetic algorithms in search, optimization, and machine learning," *Addison wesley*, vol. 1989, 1989.
- [40] GMAT, *GMAT Wiki Home*. [Online] Available: <http://gmatcentral.org/display/GW/GMAT+Wiki+Home>. Accessed on: Apr. 30 2016.

Appendices

A. Refined List of Current Satellites in GEO

* List refined from [36]. Last updated on: 20th November 2015

	Sat ID	Common Name	Long. [°]	Inc. [°]		Sat ID	Common Name	Long. [°]	Inc [°]
1	12061B	YAMAL 300K	-177	0.1	136	11074A	AMOS-5	17	0
2	09008A	NSS-9	-176.9	0	137	07016A	ASTRA 1L	19.2	0
3	00081B	AMC-8 (GE-8)	-139	0	138	11049B	ARABSAT-5C	20	0.1
4	10008A	GOES 15	-135.4	0.2	139	12062B	EUTELSAT 21B	21.6	0.1
5	04003A	AMC-10 (GE-10)	-135	0	140	10021A	ASTRA 3B	23.5	0.1
6	05041A	GALAXY 15 (G-15)	-133	0	141	07056B	SKYNET 5B	25.1	0.1
7	04017A	AMC-11 (GE-11)	-131	0	142	13044A	EUTELSAT 25B	25.5	0
8	96054A	AMC-1 (GE-1)	-129.1	0.4	143	10025A	BADR-5	26	0
9	03013B	GALAXY 12 (G-12)	-129	0	144	98050A	ASTRA 2A	28	0.1
10	08063A	CIEL-2	-128.8	0	145	14089A	ASTRA 2G	28.2	0
11	03044A	GALAXY 13 (HORIZONS-1)	-127	0	146	13056A	ASTRA 2E	28.5	0.1
12	05030A	GALAXY 14 (G-14)	-125	0	147	05005A	XTAR-EUR	29	0.1
13	08038B	AMC-21	-124.9	0	148	10032B	ARABSAT-5A	30.5	0.1
14	08024A	GALAXY 18 (G-18)	-123	0	149	12043B	HYLAS 2	31.1	0
15	03034A	GALAXY 23 (G-23)	-121	0	150	00054A	ASTRA 2B	31.4	1
16	04016A	DIRECTV 7S	-119.1	0	151	14011B	ASTRA 5B	31.5	0
17	10010A	ECHOSTAR 14	-118.9	0	152	11016A	INTELSAT NEW DAWN	32.8	0
18	02006A	ECHOSTAR 7	-118.8	0	153	01011A	EUTELSAT 33C	33.1	0.1
19	07009A	ANIK F3	-118.7	0	154	09065A	EUTELSAT 36B	35.9	0.1
20	13012A	EUTELSAT 117 WEST A	-116.8	0	155	00028A	EUTELSAT 36A	36.1	0.1
21	13058A	SIRIUS FM-6	-116.1	0	156	14006B	ATHENA-FIDUS	37.8	0
22	06049A	XM-4 (BLUES)	-115.2	0	157	11042A	PAKSAT-1R	38	0.1
23	11059A	VIASAT-1	-115.1	0	158	03020A	HELLAS-SAT 2	39	0
24	12075B	MEXSAT 3	-114.8	0	159	15012A	EXPRESS-AM7	40	0
25	06020A	EUTELSAT 113 WEST A	-113	0	160	14007A	TURKSAT 4A	42	0
26	06054A	WILDBLUE-1	-111.2	0	161	11077A	NIGCOMSAT 1R	42.5	0.1
27	04027A	ANIK F2	-111.1	0	162	96021A	ASTRA 1F	44.3	0
28	06003A	ECHOSTAR 10	-110.2	0	163	02062A	NIMIQ 2	44.5	0.8
29	02023A	DIRECTV 5 (TEMPO 1)	-110.1	0	164	00068A	INTELSAT 12 (IS-12)	45	0
30	08035A	ECHOSTAR 11	-110	0	165	13006B	AZERSPACE 1	46	0
31	00076A	ANIK F1	-107.3	0	166	05041B	SYRACUSE 3A	47	0
32	12035A	ECHOSTAR 17	-107.1	0	167	01019A	INTELSAT 10 (IS-10)	47.5	0.3
33	04041A	AMC-15	-105	0	168	12016A	YAHSAT 1B	47.6	0
34	06054B	AMC-18	-104.9	0	169	08065B	EUTELSAT 48D	48.1	0.1
35	09033A	GOES 14	-104.6	0.2	170	03053A	YAMAL 202	49.1	0
36	11035A	SES-3	-103	0	171	15060A	TURKSAT 4B	50.1	0



37	05015A	SPACEWAY 1	-102.9	0	172	15023A	TURKMENALEM52E/MONACOSA	52	0
38	07032A	DIRECTV 10	-102.8	0	173	11016B	YAHSAT 1A	52.5	0
39	01052A	DIRECTV 4S	-101.2	0	174	12075A	SKYNET 5D	52.7	0.1
40	06043A	DIRECTV 9S	-101.1	0	175	14064A	EXPRESS-AM6	53	0
41	10016A	SES-1	-101	0	176	12070A	YAMAL 402	54.9	0
42	05019A	DIRECTV 8	-100.9	0	177	14078A	GSAT-16	55	0.1
43	14078B	DIRECTV 14	-99.3	0	178	11022A	GSAT-8	55.1	0
44	08013A	DIRECTV 11	-99.2	0	179	14010A	EXPRESS-AT1	56	0
45	05046B	SPACEWAY 2	-99.1	0	180	09058A	NSS-12	57	0
46	06023A	GALAXY 16 (G-16)	-99	0	181	14023B	KAZSAT 3	58.5	0
47	08045A	GALAXY 19 (G-19)	-97	0	182	02007A	INTELSAT 904 (IS-904)	60	0
48	09034A	SIRIUS FM-5	-96	0	183	01025A	ASTRA 2C	60.3	0
49	14062A	INTELSAT 30 (IS-30)	-95.1	0	184	04007A	ABS-4 (MOBISAT-1)	61	0
50	02030A	GALAXY 3C (G-3C)	-95	0	185	01039A	INTELSAT 902 (IS-902)	62	0
51	07036A	SPACEWAY 3	-94.9	0	186	13073A	INMARSAT 5-F1	62.6	0
52	97026A	GALAXY 25 (G-25)	-93.1	0	187	09054B	COMSATBW-1	63	0.1
53	12026A	NIMIQ 6	-91.1	0	188	02041A	INTELSAT 906 (IS-906)	64.1	0
54	07016B	GALAXY 17 (G-17)	-91	0	189	13045A	AMOS-4	65	0
55	05022A	GALAXY 28 (G-28)	-89.1	0	190	10065B	INTELSAT 17 (IS-17)	66	0
56	13075A	TKSAT-1 (TUPAC KATARI)	-87.2	0.1	191	12043A	INTELSAT 20 (IS-20)	68.5	0
57	11049A	SES-2	-87	0	192	13062A	RADUGA-1M 3	70	0
58	10053A	XM-5	-85.2	0	193	12069A	EUTELSAT 70B	70.5	0.1
59	05008A	XM-3 (RHYTHM)	-85.1	0	194	12011A	INTELSAT 22 (IS-22)	72.1	0
60	04048A	AMC-16	-85	0	195	07037A	INSAT-4CR	74	0
61	00046A	BRASILSAT B4	-84	0.5	196	14006A	ABS-2	74.9	0
62	00007A	HISPASAT 1C	-83.8	0.1	197	12013A	APSTAR 7	76.5	0
63	03024A	AMC-9 (GE-12)	-83	0	198	06020B	THAICOM 5	78.5	0
64	08044A	NIMIQ 4	-82	0	199	11048A	COSMOS 2473	80	0
65	15054B	ARSAT 2	-81.1	0.1	200	03060A	EXPRESS-AM22 (SESAT 2)	80.1	0
66	15026B	SKY MEXICO-1	-78.8	0	201	13038B	INSAT-3D	82.1	0.1
67	08055A	VENESAT-1	-78	0	202	11034A	GSAT-12	83	0
68	95073A	ECHOSTAR 1	-77.2	0	203	07063B	HORIZONS-2	84.9	0
69	11054A	QUETZSAT 1	-77	0	204	10002A	RADUGA-1M 2	85	0
70	02039A	ECHOSTAR 8	-76.9	0	205	09067A	INTELSAT 15 (IS-15)	85.1	0
71	10006A	INTELSAT 16 (IS-16)	-76.2	0	206	11035B	KAZSAT-2	86.5	0
72	12062A	STAR ONE C3	-75	0.1	207	12067A	CHINASAT 12 (ZX 12)	87.5	0
73	09050A	NIMIQ 5	-72.7	0	208	11022B	ST-2	88	0
74	00067A	AMC-6 (GE-6)	-72	0	209	14082A	YAMAL 401	90	0.1
75	14062B	ARSAT 1	-71.8	0.1	210	09032A	MEASAT-3A	91.5	0
76	08018B	STAR ONE C2	-70	0	211	08028A	CHINASAT 9 (ZX 9)	92.2	0
77	01018A	XM-1 (ROLL)	-68.6	0	212	03013A	INSAT-3A	93.5	0



78	97050A	AMC-3 (GE-3)	-67	0	213	02057A	NSS-6	95	0
79	07056A	STAR ONE C1	-65	0	214	07007B	SKYNET 5A	95.2	0.1
80	11021A	TELSTAR 14R	-63	0	215	08003A	EXPRESS-AM33	96.5	0
81	97059A	ECHOSTAR 3	-61.8	1	216	13020A	CHINASAT 11 (ZX 11)	98	0
82	10034A	ECHOSTAR 15	-61.6	0	217	12028A	CHINASAT 2A (ZX 2A)	98.3	0.1
83	12065A	ECHOSTAR 16	-61.5	0	218	09042A	ASIASAT 5	100.5	0
84	03033A	ECHOSTAR 12 (RAINBOW 1)	-61.3	0	219	05023A	EXPRESS-AM3	103	0
85	13006A	AMAZONAS 3	-61	0	220	00016A	ASIASTAR	105	0.5
86	12045A	INTELSAT 21 (IS-21)	-58	0	221	14046A	ASIASAT 8	105.3	0
87	99071A	GALAXY 11 (G-11)	-55.6	0	222	11069A	ASIASAT 7	105.5	0
88	15039A	INTELSAT 34	-55.5	0	223	99042A	TELKOM 1	108	0
89	04031A	AMAZONAS 1	-55.4	0.6	224	00059A	NSS-11 (AAP-1)	108.2	0
90	15005A	INMARSAT 5-F2	-55	0	225	09027A	SES-7 (PROTOSTAR 2)	108.3	0.1
91	12057A	INTELSAT 23 (IS-23)	-53	0	226	07036B	BSAT-3A	109.9	0
92	00072A	INTELSAT 1R (IS-1R)	-50	0	227	00060A	N-SAT-110 (JCSAT-110)	110.1	0
93	98014A	NSS-806	-47.5	0.1	228	11026A	CHINASAT 10 (ZX 10)	110.5	0
94	09064A	INTELSAT 14 (IS-14)	-45	0	229	12002A	FENGYUN 2F	112.2	0.6
95	07044B	INTELSAT 11 (IS-11)	-43	0	230	06034A	KOREASAT 5 (MUGUNGWHA 5)	113	0
96	13026A	SES-6	-40.5	0	231	07031A	ZHONGXING-6B	115.6	0
97	09009A	TELSTAR 11N	-37.6	0	232	10070B	KOREASAT 6	116	0
98	05003A	NSS-10 (AMC-12)	-37.4	0	233	99046A	ABS-7	116.1	0
99	02016A	INTELSAT 903 (IS-903)	-34.5	0	234	05046A	TELKOM 2	118	0
100	10065A	HYLAS 1	-33.5	0	235	05028A	THAICOM 4	119.5	0
101	08034A	INTELSAT 25 (IS-25)	-31.5	0	236	14052A	ASIASAT 6	119.9	0
102	02044A	HISPASAT 1D	-30	0	237	03014A	ASIASAT 4	122.2	0
103	03007A	INTELSAT 907 (IS-907)	-27.5	0	238	12023A	JCSAT-13	123.8	0
104	02027A	INTELSAT 905 (IS-905)	-24.5	0	239	10042A	CHINASAT 6A (ZX 6A)	125	0
105	14058A	LUCH (OLYMP)	-24.4	0	240	09044A	JCSAT-RA (JCSAT-12)	127.9	0.1
106	12007A	SES-4	-22	0	241	06033A	JCSAT-3A	128	0
107	02019A	NSS-7	-20	0.7	242	10032A	COMS 1	128.2	0
108	01024A	INTELSAT 901 (IS-901)	-18	0	243	11047A	CHINASAT 1A (ZX 1A)	129.9	0
109	08030A	SKYNET 5C	-17.8	0.1	244	10064A	ZHONGXING-20A	130.1	0.1
110	99059A	TELSTAR 12 (ORION 2)	-15	0.1	245	12023B	VINASAT-2	131.9	0
111	01042A	EUTELSAT 8 WEST A	-12.7	0.1	246	08018A	VINASAT-1	132	0
112	02040A	EUTELSAT 12 WEST A	-12.5	0.1	247	06010A	JCSAT-5A	132.1	0
113	09007A	EXPRESS-AM44	-11	0	248	05012A	APSTAR 6	134	0
114	15039B	EUTELSAT 8 WEST B	-8	0.1	249	04024A	APSTAR 5 (TELSTAR 18)	138	0
115	11051A	EUTELSAT 7 WEST A	-7.3	0.1	250	14010B	EXPRESS-AT2	139.9	0
116	10037A	NILESAT 201	-7	0.1	251	13077A	EXPRESS-AM5	140.1	0
117	06033B	SYRACUSE 3B	-5.2	0	252	15054A	SKY MUSTER (NBN1A)	140.2	0
118	02035A	EUTELSAT 5 WEST A	-5	0	253	14060A	HIMAWARI 8	140.7	0



119	08022A	AMOS-3	-4	0	254	98033A	CHINASAT 5A (ZX 5A)	142	0
120	15010A	ABS-3A	-2.9	0	255	08007A	KIZUNA (WINDS)	143	0
121	04022A	INTELSAT 10-02	-1	0	256	08038A	SUPERBIRD-C2	144	0
122	09058B	THOR 6	-0.9	0	257	06004A	HIMAWARI-7 (MTSAT-2)	145	0
123	08006A	THOR 5	-0.7	0	258	07044A	OPTUS D2	152	0
124	12035B	METEOSAT-10 (MSG-3)	0	0.4	259	02015A	JCSAT-2A	154	0
125	10037B	RASCOM-QAF 1R	2.9	0	260	15046A	TJS-1	155	0.1
126	14030A	EUTELSAT 3B	3.1	0.1	261	03028B	OPTUS C1	156	0
127	07057A	ASTRA 4A (SIRIUS 4)	4.8	0	262	99053A	ABS-6	159	0.1
128	12036A	SES-5	5	0.1	263	06043B	OPTUS D1	160	0
129	04008A	EUTELSAT 7A	7	0.1	264	00012A	SUPERBIRD-B2	162	0
130	10069A	EUTELSAT KA-SAT 9A	9	0	265	14054A	OPTUS 10	164	0.1
131	09016A	EUTELSAT 10A	10	0.1	266	12030A	INTELSAT 19 (IS-19)	166	0
132	09008B	EUTELSAT HOT BIRD 13D	13	0	267	98065A	INTELSAT 8 (IS-8)	169	0
133	10021B	COMSATBW-2	13.2	0	268	05052A	EUTELSAT 172A (GE-23)	172	0.1
134	11057A	EUTELSAT 16A	16	0.1	269	15042A	INMARSAT 5-F3	179	0
135	12040A	TIANLIAN 1-03	16.7	0.1	270	11056A	INTELSAT 18 (IS-18)	180	0



B. Matlab Input Spacecraft Configuration File

Following is an exemplary spacecraft configuration file. The file must be named `spacecraft.txt` and be located in the same directory as the main function.

Spacecraft Configuration File:

```
Isp= 1700 sec
Power= 6000 W
servicer= 2000 kg
client= 815 kg
mp= 0 kg
etta= 0.612
```



C. Matlab Output Files

C1. GTO-GEO Satellite Removal Module

An exemplary output file for a simulation of 3 Assembly Nodes, 10 Clients and 8 days servicing time:

```

=====
Mission Initial Configuration:
-----
Service Time: 8 days

Client 1 initial location: 0.000 deg
Client 2 initial location: 36.000 deg
Client 3 initial location: 72.000 deg
Client 4 initial location: 108.000 deg
Client 5 initial location: 144.000 deg
Client 6 initial location: 180.000 deg
Client 7 initial location: 216.000 deg
Client 8 initial location: 252.000 deg
Client 9 initial location: 288.000 deg
Client 10 initial location: 324.000 deg

Assembly node 1 initial location: 0.000 deg
Assembly node 2 initial location: 120.000 deg
Assembly node 3 initial location: 240.000 deg
=====
Transfer 1:
Servicer initial orbit: GEO
Servicer initial location: 0.000 deg
Chosen target: AN #1 ( 0.000 deg)( 0.000 deg)
Transfer type: direct
Direct transfer 1/2 transfer time: 57439.998 sec
Servicer final orbit: Graveyard
Servicer final location: 355.828 deg
Maneuver time: 1.330 days (114879.996 sec)
Transfer time: 10.268 days (887118.667 sec)
MET: 10.268 days (887118.667 sec)
Transfer propellant mass: 5.173 kg
Used propellant mass: 5.173 kg
=====
Transfer 2:
Servicer initial orbit: Graveyard
Servicer initial location: 314.325 deg
Chosen target: CL #10 (324.000 deg)
Transfer type: direct
Direct transfer 1/2 transfer time: 110973.532 sec
Servicer final orbit: GEO
Servicer final location: 324.000 deg
Maneuver time: 2.569 days (221947.063 sec)
Transfer time: 11.234 days (970574.452 sec)
MET: 21.501 days (1857693.119 sec)
Transfer propellant mass: 7.377 kg
Used propellant mass: 12.550 kg
=====
Transfer 3:
Servicer initial orbit: GEO
Servicer initial location: 324.000 deg
Chosen target: AN #2 (120.000 deg)( 24.353 deg)
Transfer type: loiter
Servicer final orbit: Graveyard
Servicer final location: 20.199 deg
Maneuver time: 15.307 days (1322510.576 sec)
Transfer time: 24.241 days (2094387.944 sec)
MET: 45.742 days (3952081.062 sec)
Transfer propellant mass: 2.130 kg
Used propellant mass: 14.681 kg
=====
Transfer 4:
Servicer initial orbit: Graveyard
Servicer initial location: 276.519 deg
Chosen target: CL #9 (288.000 deg)
Transfer type: direct
Direct transfer 1/2 transfer time: 119271.316 sec
Servicer final orbit: GEO
Servicer final location: 288.000 deg
Maneuver time: 2.761 days (238542.633 sec)
Transfer time: 11.422 days (986896.321 sec)
MET: 57.164 days (4938977.383 sec)
Transfer propellant mass: 7.808 kg
Used propellant mass: 22.489 kg
=====
Transfer 5:
Servicer initial orbit: GEO
Servicer initial location: 288.000 deg
Chosen target: AN #3 (240.000 deg)(345.706 deg)
Transfer type: loiter
Servicer final orbit: Graveyard
Servicer final location: 341.567 deg
Maneuver time: 14.614 days (1262620.060 sec)
Transfer time: 23.544 days (2034211.319 sec)

```



```
MET: 80.708 days (6973188.702 sec)
Transfer propellant mass: 2.123 kg
Used propellant mass: 24.612 kg
=====
Transfer 6:
Servicer initial orbit: Graveyard
Servicer initial location: 240.970 deg
Chosen target: CL #8 (252.000 deg)
Transfer type: direct
Direct transfer 1/2 transfer time: 116851.476 sec
Servicer final orbit: GEO
Servicer final location: 252.000 deg
Maneuver time: 2.705 days (233702.951 sec)
Transfer time: 11.363 days (981770.749 sec)
MET: 92.071 days (7954959.451 sec)
Transfer propellant mass: 7.673 kg
Used propellant mass: 32.284 kg
=====
Transfer 7:
Servicer initial orbit: GEO
Servicer initial location: 252.000 deg
Chosen target: AN #1 ( 0.000 deg) (310.422 deg)
Transfer type: loiter
Servicer final orbit: Graveyard
Servicer final location: 306.297 deg
Maneuver time: 14.804 days (1279026.058 sec)
Transfer time: 23.731 days (2050335.323 sec)
MET: 115.802 days (10005294.774 sec)
Transfer propellant mass: 2.115 kg
Used propellant mass: 34.400 kg
=====
Transfer 8:
Servicer initial orbit: Graveyard
Servicer initial location: 204.856 deg
Chosen target: CL #7 (216.000 deg)
Transfer type: direct
Direct transfer 1/2 transfer time: 117057.854 sec
Servicer final orbit: GEO
Servicer final location: 216.000 deg
Maneuver time: 2.710 days (234115.707 sec)
Transfer time: 11.365 days (981901.725 sec)
MET: 127.167 days (10987196.499 sec)
Transfer propellant mass: 7.676 kg
Used propellant mass: 42.076 kg
=====
Transfer 9:
Servicer initial orbit: GEO
Servicer initial location: 216.000 deg
Chosen target: AN #2 (120.000 deg) (274.301 deg)
Transfer type: loiter
Servicer final orbit: Graveyard
Servicer final location: 270.191 deg
Maneuver time: 14.774 days (1276439.713 sec)
Transfer time: 23.698 days (2047467.099 sec)
MET: 150.864 days (13034663.598 sec)
Transfer propellant mass: 2.108 kg
Used propellant mass: 44.184 kg
=====
Transfer 10:
Servicer initial orbit: Graveyard
Servicer initial location: 168.882 deg
Chosen target: CL #6 (180.000 deg)
Transfer type: direct
Direct transfer 1/2 transfer time: 116609.374 sec
Servicer final orbit: GEO
Servicer final location: 180.000 deg
Maneuver time: 2.699 days (233218.749 sec)
Transfer time: 11.351 days (980723.102 sec)
MET: 162.215 days (14015386.700 sec)
Transfer propellant mass: 7.645 kg
Used propellant mass: 51.829 kg
=====
Transfer 11:
Servicer initial orbit: GEO
Servicer initial location: 180.000 deg
Chosen target: AN #3 (240.000 deg) (238.388 deg)
Transfer type: loiter
Servicer final orbit: Graveyard
Servicer final location: 234.292 deg
Maneuver time: 14.798 days (1278581.046 sec)
Transfer time: 23.719 days (2049327.663 sec)
MET: 185.934 days (16064714.363 sec)
Transfer propellant mass: 2.100 kg
Used propellant mass: 53.929 kg
=====
Transfer 12:
Servicer initial orbit: Graveyard
Servicer initial location: 132.874 deg
Chosen target: CL #5 (144.000 deg)
Transfer type: direct
Direct transfer 1/2 transfer time: 116324.026 sec
Servicer final orbit: GEO
Servicer final location: 144.000 deg
```



```
Maneuver time: 2.693 days (232648.052 sec)
Transfer time: 11.341 days (979871.850 sec)
MET: 197.275 days (17044586.212 sec)
Transfer propellant mass: 7.623 kg
Used propellant mass: 61.552 kg
=====
Transfer 13:
Servicer initial orbit: GEO
Servicer initial location: 144.000 deg
Chosen target: AN #1 ( 0.000 deg) (202.423 deg)
Transfer type: loiter
Servicer final orbit: Graveyard
Servicer final location: 198.342 deg
Maneuver time: 14.810 days (1279542.600 sec)
Transfer time: 23.727 days (2050009.308 sec)
MET: 221.002 days (19094595.520 sec)
Transfer propellant mass: 2.093 kg
Used propellant mass: 63.645 kg
=====
Transfer 14:
Servicer initial orbit: Graveyard
Servicer initial location: 96.874 deg
Chosen target: CL #4 (108.000 deg)
Transfer type: direct
Direct transfer 1/2 transfer time: 115998.746 sec
Servicer final orbit: GEO
Servicer final location: 108.000 deg
Maneuver time: 2.685 days (231997.492 sec)
Transfer time: 11.330 days (978941.593 sec)
MET: 232.333 days (20073537.113 sec)
Transfer propellant mass: 7.598 kg
Used propellant mass: 71.243 kg
=====
Transfer 15:
Servicer initial orbit: GEO
Servicer initial location: 108.000 deg
Chosen target: AN #2 (120.000 deg) (166.471 deg)
Transfer type: loiter
Servicer final orbit: Graveyard
Servicer final location: 162.404 deg
Maneuver time: 14.824 days (1280794.094 sec)
Transfer time: 23.738 days (2050981.813 sec)
MET: 256.071 days (22124518.926 sec)
Transfer propellant mass: 2.086 kg
Used propellant mass: 73.329 kg
=====
Transfer 16:
Servicer initial orbit: Graveyard
Servicer initial location: 60.872 deg
Chosen target: CL #3 ( 72.000 deg)
Transfer type: direct
Direct transfer 1/2 transfer time: 115683.948 sec
Servicer final orbit: GEO
Servicer final location: 72.000 deg
Maneuver time: 2.678 days (231367.895 sec)
Transfer time: 11.320 days (978033.220 sec)
MET: 267.391 days (23102552.146 sec)
Transfer propellant mass: 7.574 kg
Used propellant mass: 80.903 kg
=====
Transfer 17:
Servicer initial orbit: GEO
Servicer initial location: 72.000 deg
Chosen target: AN #3 (240.000 deg) (130.516 deg)
Transfer type: loiter
Servicer final orbit: Graveyard
Servicer final location: 126.463 deg
Maneuver time: 14.838 days (1281970.129 sec)
Transfer time: 23.749 days (2051879.763 sec)
MET: 291.139 days (25154431.909 sec)
Transfer propellant mass: 2.078 kg
Used propellant mass: 82.981 kg
=====
Transfer 18:
Servicer initial orbit: Graveyard
Servicer initial location: 24.870 deg
Chosen target: CL #2 ( 36.000 deg)
Transfer type: direct
Direct transfer 1/2 transfer time: 115367.125 sec
Servicer final orbit: GEO
Servicer final location: 36.000 deg
Maneuver time: 2.671 days (230734.250 sec)
Transfer time: 11.309 days (977121.699 sec)
MET: 302.449 days (26131553.608 sec)
Transfer propellant mass: 7.550 kg
Used propellant mass: 90.531 kg
=====
Transfer 19:
Servicer initial orbit: GEO
Servicer initial location: 36.000 deg
Chosen target: AN #1 ( 0.000 deg) ( 94.561 deg)
Transfer type: loiter
Servicer final orbit: Graveyard
```



```

Servicer final location: 90.523 deg
Maneuver time: 14.851 days (1283161.494 sec)
Transfer time: 23.759 days (2052793.945 sec)
MET: 326.208 days (28184347.553 sec)
Transfer propellant mass: 2.071 kg
Used propellant mass: 92.602 kg
=====

```

```

=====
Total transfer time: 326.208 days
Total propellant mass: 92.602 kg
=====

```

C2. GTO-GEO Satellite Refueling Module

An exemplary output file for a simulation of 3 Assembly Nodes, 10 Clients and 8 days servicing time:

```

=====
Mission Initial Configuration:
-----
Service Time: 7 days
Depot mass: 1951.000 kg
*****
Sortie #1
*****
Client 1 initial location: 28.000 deg
Client 2 initial location: 60.000 deg
Client 3 initial location: 139.900 deg
Client 4 initial location: 288.200 deg
Client 5 initial location: 299.000 deg
Client 6 initial location: 319.500 deg
=====
Tour Start
Depot start location: 0.000 deg
Depot mass: 1831.000 kg
Initial servicer mass: 2000.000 kg
First client = Client # 1 ( 28.000 deg)
Maneuver type: Relocation
Phase Up maneuver: 253384.173 sec
Phase Down maneuver: 253610.755 sec
Maneuver Transfer Time: 5.868 days (506994.927 sec)
MET: 13.261 days
Used propellant mass: 3.811 kg
=====
Transfer # 1
Served client = Client # 1 ( 28.000 deg)
Next client = Client # 2 ( 60.000 deg)
Maneuver Transfer Time: 6.206 days
Phasing Direction: CCW (+)
Phase 1 maneuver: 267988.052 sec
Phase 2 maneuver: 268244.591 sec
MET: 26.468 days
Used propellant mass: 7.590 kg
=====
Transfer # 2
Served client = Client # 2 ( 60.000 deg)
Next client = Client # 3 ( 139.900 deg)
Maneuver Transfer Time: 9.728 days
Phasing Direction: CCW (+)
Phase 1 maneuver: 419912.328 sec
Phase 2 maneuver: 420550.569 sec
MET: 43.195 days
Used propellant mass: 13.511 kg
=====
Transfer # 3
Served client = Client # 3 ( 139.900 deg)
Next client = Client # 4 ( 288.200 deg)
Maneuver Transfer Time: 13.137 days
Phasing Direction: CCW (+)
Phase 1 maneuver: 566929.866 sec
Phase 2 maneuver: 568110.237 sec
MET: 63.332 days
Used propellant mass: 21.508 kg
=====
Transfer # 4
Served client = Client # 4 ( 288.200 deg)
Next client = Client # 5 ( 299.000 deg)
Maneuver Transfer Time: 3.539 days
Phasing Direction: CCW (+)
Phase 1 maneuver: 152845.890 sec
Phase 2 maneuver: 152932.688 sec
MET: 73.871 days
Used propellant mass: 23.663 kg
=====
Transfer # 5
Served client = Client # 5 ( 299.000 deg)
Next client = Client # 6 ( 319.500 deg)
Maneuver Transfer Time: 4.843 days
Phasing Direction: CCW (+)
Phase 1 maneuver: 209155.987 sec

```



```

Phase 2 maneuver: 209320.513 sec
MET: 85.715 days
Used propellant mass: 26.611 kg
=====
Return to Depot
Last client = Client # 6 ( 319.500 deg)
Depot Location after resupply: 225.577 deg
Maneuver Transfer Time: 8.906 days
MET: 104.985 days
Maneuver type: Relocation
Phase Up maneuver: 385036.988 sec
Phase Down maneuver: 384473.405 sec
Used propellant mass: 32.255 kg
Final dry mass: 1880.000 kg
Final servicer mass: 1847.745 kg
=====
*****
Sortie #2
*****
Client 1 initial location: 37.800 deg
Client 2 initial location: 39.000 deg
Client 3 initial location: 116.000 deg
Client 4 initial location: 132.100 deg
Client 5 initial location: 143.000 deg
Client 6 initial location: 295.000 deg
=====
Tour Start
Depot start location: 225.577 deg
Depot mass: 1678.745 kg
Initial servicer mass: 2000.000 kg
First client = Client # 6 ( 295.000 deg)
Maneuver type: Relocation
Phase Up maneuver: 397069.681 sec
Phase Down maneuver: 397626.663 sec
Maneuver Transfer Time: 9.198 days (794696.344 sec)
MET: 121.577 days
Used propellant mass: 5.838 kg
=====
Transfer # 1
Served client = Client # 6 ( 295.000 deg)
Next client = Client # 1 ( 37.800 deg)
Maneuver Transfer Time: 11.087 days
Phasing Direction: CCW (+)
Phase 1 maneuver: 478557.587 sec
Phase 2 maneuver: 479377.736 sec
MET: 139.664 days
Used propellant mass: 12.588 kg
=====
Transfer # 2
Served client = Client # 1 ( 37.800 deg)
Next client = Client # 2 ( 39.000 deg)
Maneuver Transfer Time: 1.196 days
Phasing Direction: CCW (+)
Phase 1 maneuver: 51683.671 sec
Phase 2 maneuver: 51693.339 sec
MET: 147.860 days
Used propellant mass: 13.316 kg
=====
Transfer # 3
Served client = Client # 2 ( 39.000 deg)
Next client = Client # 3 ( 116.000 deg)
Maneuver Transfer Time: 9.487 days
Phasing Direction: CCW (+)
Phase 1 maneuver: 409527.261 sec
Phase 2 maneuver: 410142.407 sec
MET: 164.347 days
Used propellant mass: 19.091 kg
=====
Transfer # 4
Served client = Client # 3 ( 116.000 deg)
Next client = Client # 4 ( 132.100 deg)
Maneuver Transfer Time: 4.322 days
Phasing Direction: CCW (+)
Phase 1 maneuver: 186639.253 sec
Phase 2 maneuver: 186768.543 sec
MET: 175.669 days
Used propellant mass: 21.722 kg
=====
Transfer # 5
Served client = Client # 4 ( 132.100 deg)
Next client = Client # 5 ( 143.000 deg)
Maneuver Transfer Time: 3.536 days
Phasing Direction: CCW (+)
Phase 1 maneuver: 152728.584 sec
Phase 2 maneuver: 152816.183 sec
MET: 186.205 days
Used propellant mass: 23.875 kg
=====
Return to Depot
Last client = Client # 5 ( 143.000 deg)
Depot Location after resupply: 102.001 deg
Maneuver Transfer Time: 4.929 days
MET: 201.499 days

```



```

Maneuver type: Relocation
Phase Up maneuver: 212999.944 sec
Phase Down maneuver: 212827.729 sec
Used propellant mass: 27.097 kg
Final dry mass: 1880.000 kg
Final servicer mass: 1852.903 kg
=====
*****
Sortie #3
*****
Client 1 initial location: 20.000 deg
Client 2 initial location: 70.000 deg
Client 3 initial location: 127.900 deg
Client 4 initial location: 231.000 deg
Client 5 initial location: 257.000 deg
Client 6 initial location: 355.000 deg
=====
Tour Start
Depot start location: 102.001 deg
Depot mass: 1531.648 kg
Initial servicer mass: 2000.000 kg
First client = Client # 3 ( 127.900 deg)
Maneuver type: Relocation
Phase Up maneuver: 243813.319 sec
Phase Down maneuver: 244023.093 sec
Maneuver Transfer Time: 5.646 days (487836.412 sec)
MET: 214.538 days
Used propellant mass: 3.676 kg
=====
Transfer # 1
Served client = Client # 3 ( 127.900 deg)
Next client = Client # 2 ( 70.000 deg)
Maneuver Transfer Time: 8.410 days
Phasing Direction: CW (-)
Phase 1 maneuver: 363538.085 sec
Phase 2 maneuver: 363066.932 sec
MET: 229.948 days
Used propellant mass: 8.796 kg
=====
Transfer # 2
Served client = Client # 2 ( 70.000 deg)
Next client = Client # 1 ( 20.000 deg)
Maneuver Transfer Time: 7.763 days
Phasing Direction: CW (-)
Phase 1 maneuver: 335578.303 sec
Phase 2 maneuver: 335171.668 sec
MET: 244.711 days
Used propellant mass: 13.522 kg
=====
Transfer # 3
Served client = Client # 1 ( 20.000 deg)
Next client = Client # 6 ( 355.000 deg)
Maneuver Transfer Time: 5.449 days
Phasing Direction: CW (-)
Phase 1 maneuver: 235501.570 sec
Phase 2 maneuver: 235298.735 sec
MET: 257.160 days
Used propellant mass: 16.839 kg
=====
Transfer # 4
Served client = Client # 6 ( 355.000 deg)
Next client = Client # 5 ( 257.000 deg)
Maneuver Transfer Time: 10.750 days
Phasing Direction: CW (-)
Phase 1 maneuver: 464791.467 sec
Phase 2 maneuver: 463991.706 sec
MET: 274.910 days
Used propellant mass: 23.383 kg
=====
Transfer # 5
Served client = Client # 5 ( 257.000 deg)
Next client = Client # 4 ( 231.000 deg)
Maneuver Transfer Time: 5.485 days
Phasing Direction: CW (-)
Phase 1 maneuver: 237060.150 sec
Phase 2 maneuver: 236849.161 sec
MET: 287.395 days
Used propellant mass: 26.722 kg
=====
Return to Depot
Last client = Client # 4 ( 231.000 deg)
Depot Location after resupply: 203.984 deg
Maneuver Transfer Time: 105.253 days
MET: 403.013 days
Maneuver type: Loiter
Used propellant mass: 26.943 kg
Final dry mass: 1880.000 kg
Final servicer mass: 1853.057 kg
=====
*****
Sortie #4
*****
Client 1 initial location: 25.100 deg
Client 2 initial location: 90.000 deg

```



```

Client 3 initial location: 108.200 deg
Client 4 initial location: 263.000 deg
Client 5 initial location: 290.000 deg
Client 6 initial location: 352.700 deg
=====
Tour Start
Depot start location: 203.984 deg
Depot mass: 1384.705 kg
Initial servicer mass: 2000.000 kg
First client = Client # 4 ( 263.000 deg)
Maneuver type: Relocation
Phase Up maneuver: 366384.608 sec
Phase Down maneuver: 366858.727 sec
Maneuver Transfer Time: 8.487 days (733243.336 sec)
MET: 418.892 days
Used propellant mass: 5.406 kg
=====
Transfer # 1
Served client = Client # 4 ( 263.000 deg)
Next client = Client # 5 ( 290.000 deg)
Maneuver Transfer Time: 5.700 days
Phasing Direction: CCW (+)
Phase 1 maneuver: 246143.587 sec
Phase 2 maneuver: 246360.149 sec
MET: 431.593 days
Used propellant mass: 8.876 kg
=====
Transfer # 2
Served client = Client # 5 ( 290.000 deg)
Next client = Client # 6 ( 352.700 deg)
Maneuver Transfer Time: 8.620 days
Phasing Direction: CCW (+)
Phase 1 maneuver: 372126.497 sec
Phase 2 maneuver: 372627.898 sec
MET: 447.213 days
Used propellant mass: 14.123 kg
=====
Transfer # 3
Served client = Client # 6 ( 352.700 deg)
Next client = Client # 1 ( 25.100 deg)
Maneuver Transfer Time: 6.165 days
Phasing Direction: CCW (+)
Phase 1 maneuver: 266182.450 sec
Phase 2 maneuver: 266442.165 sec
MET: 460.377 days
Used propellant mass: 17.875 kg
=====
Transfer # 4
Served client = Client # 1 ( 25.100 deg)
Next client = Client # 2 ( 90.000 deg)
Maneuver Transfer Time: 8.658 days
Phasing Direction: CCW (+)
Phase 1 maneuver: 373750.380 sec
Phase 2 maneuver: 374269.238 sec
MET: 476.035 days
Used propellant mass: 23.146 kg
=====
Transfer # 5
Served client = Client # 2 ( 90.000 deg)
Next client = Client # 3 ( 108.200 deg)
Maneuver Transfer Time: 4.565 days
Phasing Direction: CCW (+)
Phase 1 maneuver: 197138.717 sec
Phase 2 maneuver: 197284.826 sec
MET: 487.600 days
Used propellant mass: 25.925 kg
=====
Return to Depot
Last client = Client # 3 ( 108.200 deg)
Depot Location after resupply: 77.607 deg
Maneuver Transfer Time: 3.750 days
MET: 501.714 days
Maneuver type: Relocation
Phase Up maneuver: 162033.056 sec
Phase Down maneuver: 161933.286 sec
Used propellant mass: 28.429 kg
Final dry mass: 1880.000 kg
Final servicer mass: 1851.571 kg
=====
Total transfer time: 501.714 days
Total propellant mass (used by servicer): 114.724 kg
Final depot mass: 1384.705 kg
=====

```

C3. LEO-GEO Satellite Repair Module

```

=====
Mission Initial Configuration:
-----
Service Time: 7 days
Depot station altitude: 7000 km
*****
Sortie #1
*****
Client 1 initial location: 42.500 deg
Client 2 initial location: 47.000 deg
Client 3 initial location: 119.500 deg
Client 4 initial location: 140.700 deg
Client 5 initial location: 276.000 deg
Client 6 initial location: 281.200 deg
Client 7 initial location: 315.000 deg
Client 8 initial location: 335.500 deg
Client 9 initial location: 345.000 deg
Client 10 initial location: 352.700 deg
=====
Tour Start
Depot start location: 0.000 deg
Initial servicer mass: 2670.000 kg
First client = Client # 5 ( 276.000 deg)
Maneuver type: Loiter
Maneuver Transfer Time: 7.235 days (625062.190 sec)
MET: 613.962 days
Used propellant mass: 365.080 kg
=====
Transfer # 1
Served client = Client # 5 ( 276.000 deg)
Next client = Client # 6 ( 281.200 deg)
Maneuver Transfer Time: 2.696 days
Phasing Direction: CCW (+)
Phase 1 maneuver: 116454.402 sec
Phase 2 maneuver: 116496.250 sec
MET: 623.659 days
Used propellant mass: 366.721 kg
=====
Transfer # 2
Served client = Client # 6 ( 281.200 deg)
Next client = Client # 7 ( 315.000 deg)
Maneuver Transfer Time: 6.827 days
Phasing Direction: CCW (+)
Phase 1 maneuver: 294796.839 sec
Phase 2 maneuver: 295067.874 sec
MET: 637.486 days
Used propellant mass: 370.877 kg
=====
Transfer # 3
Served client = Client # 7 ( 315.000 deg)
Next client = Client # 8 ( 335.500 deg)
Maneuver Transfer Time: 5.292 days
Phasing Direction: CCW (+)
Phase 1 maneuver: 228546.813 sec
Phase 2 maneuver: 228711.408 sec
MET: 649.778 days
Used propellant mass: 374.099 kg
=====
Transfer # 4
Served client = Client # 8 ( 335.500 deg)
Next client = Client # 9 ( 345.000 deg)
Maneuver Transfer Time: 3.587 days
Phasing Direction: CCW (+)
Phase 1 maneuver: 154921.350 sec
Phase 2 maneuver: 154997.737 sec
MET: 660.365 days
Used propellant mass: 376.282 kg
=====
Transfer # 5
Served client = Client # 9 ( 345.000 deg)
Next client = Client # 10 ( 352.700 deg)
Maneuver Transfer Time: 3.214 days
Phasing Direction: CCW (+)
Phase 1 maneuver: 138801.988 sec
Phase 2 maneuver: 138863.920 sec
MET: 670.579 days
Used propellant mass: 378.238 kg
=====

```




```
=====
Transfer # 6
Served client = Client # 10 ( 352.700 deg)
Next client = Client # 1 ( 42.500 deg)
Maneuver Transfer Time: 8.111 days
Phasing Direction: CCW (+)
Phase 1 maneuver: 350199.742 sec
Phase 2 maneuver: 350598.517 sec
MET: 685.690 days
Used propellant mass: 383.176 kg
=====
Transfer # 7
Served client = Client # 1 ( 42.500 deg)
Next client = Client # 2 ( 47.000 deg)
Maneuver Transfer Time: 2.431 days
Phasing Direction: CCW (+)
Phase 1 maneuver: 105014.587 sec
Phase 2 maneuver: 105050.804 sec
MET: 695.121 days
Used propellant mass: 384.656 kg
=====
Transfer # 8
Served client = Client # 2 ( 47.000 deg)
Next client = Client # 3 ( 119.500 deg)
Maneuver Transfer Time: 9.673 days
Phasing Direction: CCW (+)
Phase 1 maneuver: 417564.638 sec
Phase 2 maneuver: 418144.257 sec
MET: 711.794 days
Used propellant mass: 390.544 kg
=====
Transfer # 9
Served client = Client # 3 ( 119.500 deg)
Next client = Client # 4 ( 140.700 deg)
Maneuver Transfer Time: 5.211 days
Phasing Direction: CCW (+)
Phase 1 maneuver: 225016.626 sec
Phase 2 maneuver: 225186.802 sec
MET: 724.004 days
Used propellant mass: 393.716 kg
=====
Return to Depot
Last client = Client # 4 ( 140.700 deg)
Depot Location after resupply: 90.388 deg
Maneuver Transfer Time: 0.432 days
MET: 1200.805 days
Maneuver type: Loiter
Used propellant mass: 677.615 kg
Final dry mass: 2470.000 kg
Final servicer mass: 1792.385 kg
=====
Total transfer time: 1200.805 days
Total propellant mass (used by servicer): 677.615 kg
=====
```



D. InTrance Input Files

D1. Evolutionary Algorithm Parameter File – coldstart.eap

```
SEARCH_SPACE_HYPERCUBE_SIZE      = 1.0
HYPERCUBE_SHRINKING_FACTOR       = 0.7
POPULATION_SIZE                   = 50
POPULATION_SIZE_SSS              = 100
SEARCH_SCAN_EPOCHS               = 3
FITNESS_FUNCTION_TYPE            = J_ORB_ELEMENTS
CHROMOSOME_MUTATION_PROBABILITY  = 0.93
GEN_MUTATION_PROBABILITY         = 5.0e-3
SELECTION_PRESSURE_ON_TIME       = 0.0
HYPERCUBE_UPPER_LIMIT            = 1.0e-3
FBC_MET_FITNESS                  = 0.0
IL_POP_CONV_FBC_MET              = 5.0e-5
IL_POP_CONV_FBC_NOT_MET         = 5.0e-5
IL_EA_CONV_FBC_MET               = 1.0e-5
IL_EA_CONV_FBC_NOT_MET          = 1.0e-4
```

D2. Neurocontoroller Parameter File – ctrl.ncp

```
HIDDEN_LAYERS                    = 1
NEURONS_IN_HIDDEN_LAYER1        = 35
NC_OUTPUT                        = direct
TRANSFER_FUNCTION                 = sigmoid
```

E. Computer Specifications

The InTrance and Matlab simulations carried out in this thesis have been run on two different computer systems. The specifications of the respective computers are given below.

E1. InTrance Simulations

The InTrance simulations have been run on:

Computer Brand	Dell
Model	Latitude E6410 Notebook
Processor	Intel® Core i5-2300 (2.4 GHz)
Number of Cores	4
RAM	4 GB SO-DIMM DDR3
Graphics Coprocessor	Intel Integrated Graphics
Operating System	Windows 7 Enterprise; Service Pack 1
System Type	64-Bit
Hard Drive	160 GB 7200 RPM

E2. Matlab Simulations

The Matlab simulations have been run on:

Computer Brand	Lenovo
Model	Yoga
Processor	Intel® Core i7-4600U (2.10GHz, 4MB Cache)
Number of Cores	4
RAM	8GB / PC3-12800 1600MHz DDR3L
Graphics Coprocessor	Intel HD Graphics 4400
Operating System	Ubuntu 15.10
System Type	64-Bit
Hard Drive	256 GB Solid State Drive